Bedrock transport properties
Data evaluation and retardation model

Site descriptive modelling
SDM-Site Laxemar

Eva Selnert, Johan Byegård, Henrik Widestrand,
Seje Carlsten, Christin Döse, Geosigma AB

Eva-Lena Tullborg, Terralogica AB

June 2009

SKB

Bedrock transport properties
Data evaluation and retardation model

Site descriptive modelling
SDM-Site Laxemar

Eva Selnert, Johan Byegård, Henrik Widestrand,

Seje Carlsten, Christin Döse, Geosigma AB

Eva-Lena Tullborg, Terralogica AB

June 2009

Abstract

A descriptive model for the bedrock retardation properties is outlined and presented in this work as part of model version SDM-Site for Laxemar (built on data freeze for Laxemar 2.3, August 31, 2007). The model is based on the available data from the geology, hydrogeology, and hydrogeochemistry disciplines including the fracture mineral studies. The data from these areas are integrated with laboratory data from the porosity, diffusion and sorption experiments performed using site specific geological material. The outcome is described in retardation tables in which the retardation properties of different geological structures (i.e. rock types, fracture types and deformation zone units) are summarized. A classification of fracture types is presented (nine different fracture types) including statistics of their distribution among the open fractures. Important geological features of the deformation zones are identified (five different deformation zone units).

The results of the porosity measurements of unaltered rock samples (using the water saturation method) show that most samples are distributed in a porosity range from 0.1% to 0.5%. The rock types have average porosities from 0.2% for the more fine-grained rock types to 0.4% for the average- to coarse-grained or porphyritic rock types. It is indicated that alteration and micro fracturing leads to increased porosity. The identified deformation zone units have porosities in the range from 0.7% to 12%. However, the presence of these highly porous deformation zone units are associated to minor parts of the deformation zones. In addition to the presentation of porosity data according to the rock type concept, a sub-division in rock domains, fracture domains and hydraulic rock domains was done. None of the alternative sub-divisions decrease the variation in the results compared to the rock type concept. Furthermore the possible impact of sample location for a certain rock type was studied. No significant differences in porosity between the Laxemar and Simpevarp subareas are found for the major rock types.

Studies of the diffusive properties of the rock types yield formation factors (i.e. how much lower the diffusivity in the rock type is compared to the diffusivity in pure water) mainly in the range of $3 \cdot 10^{-5}$ to $5 \cdot 10^{-4}$. An expected dependence of the formation factor on the porosity is well verified; showing e.g. formation factors up to $8 \cdot 10^{-3}$ for the deformation zone unit cataclasite for porosities up to 6%. Laboratory values for the formation factor are found to be higher than the corresponding measurements performed in situ which indicates that stress release and sample disturbances during the drilling may cause an overestimation of the diffusivities determined in laboratory experiments.

According to the hydrogeochemical investigations, the groundwater compositions at Laxemar range from fresh at the surface via brackish to highly saline at about 1,500 m depth. In the laboratory experiments five different water types were used. Of these one was a fresh groundwater type and three were brackish-saline groundwater types (one brackish/marine and two were brackish/non-marine with different salinity). Brine type groundwater was identified as a possible extreme and was therefore included in the laboratory experiments. The selection of different groundwater types is of great importance for the batch sorption experiments where the groundwater composition is likely to influence the sorption; both from a surface/aqueous complexation perspective but also due to cation exchange competition.

An extensive series of batch sorption experiments using crushed rock material was performed in order to describe the radionuclide sorption interaction with the different geologic materials and the different groundwater types. Experiments using Cs, Sr and a trivalent actinide (Eu or Am) as tracer are presented; for a few materials the tracers Ra, Ni, Np and U were also added. For the major rock type in the focus area, Quartz monzodiorite, in combination with saline groundwater, the K_d values for Cs, Sr and Eu/Am are $2 \cdot 10^{-2}$, $3 \cdot 10^{-3}$ and $1 \cdot 10^{0}$ m³/kg, respectively. A general trend is that the material adjacent to the different fractures (altered wall rock) gives higher K_d compared to non-altered rock and that tracers presumed to adsorb with cation exchange mechanism (i.e. Cs, Sr and Ra) are more strongly adsorbed with decreasing ionic strength of the groundwater. The sorption measurements for Cs in saline groundwater of a small number of deformation zone unit samples indicate varying sorption strength compared to that of intact rock. The indications are weaker sorption for oxidized wall rock and increased sorption for fault rock/gouge.

Surface area measurements (BET) and cation exchange capacity (CEC) measurements were part of the sorption investigations. It is concluded that sorption strength, BET surface area and CEC are positively correlated although the relations are far from linear. High BET surface areas (e.g. as observed for fracture materials) cannot be directly interpreted to a corresponding sorption capacity.

Confirmation studies on intact drill core material using an electromigration sorption technique and diffusion/sorption experiments are presented and discussed.

The outcome of the report is the retardation model tables in which the different retardation properties of the different geological compartments (rock types, fracture types and deformation zone units) are summarized. Finally, the sample representation for the Laxemar local model area and the applicability of the retardation model within the Safety Assessment modelling is discussed.

Sammanfattning

I detta arbete identifieras och presenteras en beskrivande modell för bergets retardationsegenskaper som en del av modellversionen SDM-Site för Laxemar (byggd på datafrys 2.3 för Laxemar, 31 augusti, 2007). Modellen baseras på tillgängliga data från geologi-, hydrogeologi- och hydrogeokemiundersökningarna inklusive studier av sprickmineral. Data från dessa områden integreras med laboratoriedata från mätningar av porositet, diffusion och sorption på platsspecifika geologiska materialprover. Slutprodukten är retardationstabeller i vilka retardationsegenskaperna summeras för olika geologiska strukturer (bergarter, spricktyper och deformationszonenheter). En klassificering av nio olika spricktyper presenteras inklusive statistik för spricktypsfördelningen bland de öppna sprickorna. Betydelsefulla karakteristiska geologiska element i deformationszonerna identifieras (fem stycken).

Resultaten av porositetsmätningarna med vattenmättnadsmetoden för ej omvandlade prover visar att porositeten typiskt fördelas i ett område från 0.1% till 0.5%. Bergarterna har medel-porositeter från 0.2% för de mer finkorniga bergarterna till 0.4% för de medel- till grovkorniga eller porfyritiska bergarterna. Det indikeras att omvandling och förekomst av mikrosprickor leder till förhöjd porositet. Deformationszonenheterna har porositeter från 0.7% till 12%. Dock förekommer dessa porösa deformationszonenheter endast i mindre delar av deformationszonerna. I tillägg till presentation av porositetsdata enligt bergartskonceptet har en indelning i bergdomäner, sprickdomäner och hydrauliska bergdomäner gjorts. Ingen av de alternativa indelningsmetoderna minskade variabiliteten i porositetsresultaten jämfört med bergartskonceptet. Vidare studerades den möjliga påverkan av provtagningsplatsen för en bergarts porositet. Inga skillnader i porositet kunde påvisas mellan prover tagna i Laxemar- respektive Simpevarpsområdet.

Studier av bergarternas diffusionsegenskaper ger formationsfaktorer (dvs. hur mycket lägre diffusiviteten i bergarten är jämfört med diffusiviteten i rent vatten) huvudsakligen inom området $3 \cdot 10^{-5}$ to $5 \cdot 10^{-4}$. Ett förväntat beroende mellan formationsfaktor och porositet verifieras tydligt, t ex fås formationsfaktorer upp till $8 \cdot 10^{-3}$ för deformationszonenheten kataklasit med porositet upp till 6 %. Laboratoriemätningar av formationsfaktorn visade sig ge högre värden än motsvarande in situ-mätningar, vilket indikerar att tryckavlastning och störningar i proverna på grund av borrningen kan orsaka en överskattning av diffusiviteten i laboratoriemätningarna.

Enligt de hydrogeokemiska undersökningarna varierar grundvattnets sammansättning vid Laxemar från färskt vid ytan, via bräckt till kraftigt salt vid omkring 1 500 m djup. I laboratorieförsöken har fem olika vattentyper använts. En av dessa var av färskvattentyp och tre var av bräckt- till saltvattentyp (ett bräckt-marint och två bräckta-icke marina med olika salinitet). Grundvatten av typen mättad saltlösning identifierades som en möjlig extrem och inkluderades därför i laboratorieförsöken. Valet av olika typer av grundvatten är av stor betydelse för sorptionsexperimenten eftersom vattnets sammansättning påverkar sorptionen; både sett ur perspektivet yt-/vattenkomplexbildning och från en katjonbytesmodell.

En omfattande serie av satsvisa sorptionsexperiment med krossat bergmaterial har utförts för att beskriva radionukliders sorption (interaktion) med de olika geologiska materialen och grundvatten-typerna. Experiment med Cs, Sr och en trivalent aktinid (Eu eller Am) som spårämnen presenteras; för ett fåtal material tillkommer Ra, Ni, Np och U. För den mest frekventa bergarten i fokusområdet, kvartsmonzodiorit, i kombination med salint grundvatten, uppmättes följande K_d värden; Cs $2 \cdot 10^{-2}$ m³/kg, Sr $3 \cdot 10^{-3}$ m³/kg och Eu/Am $1 \cdot 10^0$ m³/kg. En generell trend är att material nära de olika sprickorna (omvandlat sidoberg) har högre K_d jämfört med icke omvandlat berg och att spårämnen som antas sorbera med en katjonbytesmekanism (t ex Cs, Sr och Ra) sorberar starkare när jonstyrkan i grundvattnet minskar. Sorptionsmätningarna av ett litet antal prover av deformationszonenheter indikerar en varierande sorptionsstyrka jämfört med intakt berg, från svagare sorption för oxiderat sidoberg till förhöjd sorption för material från skjuvzoner/gouge (kraftigt tektoniserat och delvist ej konsoliderat material).

Mätningar av specifik ytarea (BET) och katjonbyteskapacitet (CEC) utfördes som en del av sorptionsundersökningarna. Sorptionsstyrka, BET-yta och CEC är positivt korrelerade även om de inbördes

relationerna är långt ifrån linjära. Höga BET-ytor (som observeras för t ex sprickmaterial) kan inte direkt översättas till en motsvarande sorptionskapacitet.

Sorptionsavsnittet avslutas med att stödjande studier på intakt kärnmaterial med en elektromigration-sorptionsteknik och diffusion/sorptions-experiment presenteras och diskuteras.

Slutprodukten av rapporten är retardationstabellerna i vilka retardationsegenskaperna för de olika geologiska enheterna (bergarter, spricktyper och deformationszonsenheter) sammanfattas. Slutligen diskuteras provernas representerbarhet för Laxemar området och applicerbarheten av retardations-modellen inom säkerhetsanalysen.

Contents

1   Introduction

1.1   Background

The Swedish Nuclear Fuel and Waste Management Company (SKB) has conducted site investigations at two different locations, the Forsmark and Laxemar-Simpevarp areas, with the objective of siting a geological repository for spent nuclear fuel. The results from the investigations at the sites are used as a basic input to the site descriptive modelling.

A Site Descriptive Model (SDM) is an integrated description of the site and its regional setting, covering the current state of the geosphere and the biosphere as well as ongoing natural processes of importance for long-term safety. The SDM shall summarise the current state of knowledge of the site, and provide parameters and models to be used in further analyses within Safety Assessment, Repository Design and Environmental Impact Assessment. The present report is produced as a part of the model version SDM-Site for Laxemar (built on data freeze for Laxemar 2.3, August 31, 2007).

The process of site descriptive modelling of transport properties is described by /Berglund and Selroos 2004/. Essentially, the description consists of three parts:

- Description of rock mass and fractures/deformation zones, including relevant processes and conditions affecting radionuclide transport; the description should express the understanding of the site and therefore include the subdivision into rock/fracture domains.

- Retardation model: Identification and description of "typical" rock materials and fractures/deformation zones, including parametrisation.

- Transport properties model: Parametrisation of the 3D geological model and assessment of understanding, confidence and uncertainty.

The methods used within the transport programme produce primary data on the retardation parameters, i.e. the porosity, θ_m, the effective diffusivity, D_e, and the linear equilibrium sorption coefficient, K_d. The data for the Laxemar site-specific laboratory transport parameters are presented in /Selnert et al. 2009/. In the present report, these retardation parameters are evaluated, interpreted and presented in the form of a retardation model, all according to the strategy for laboratory measurements, data evaluation and development of retardation models described by /Widestrand et al. 2003/.

1.2   Conceptual model

1.2.1   Basic conceptual model

The conceptual model underlying the site descriptive transport modelling is based on a description of solute transport in discretely fractured rock. Specifically, the fractured medium is viewed as consisting of mobile zones, i.e. fractures and deformation zones where groundwater flow and advective transport take place, and immobile zones in rock mass, fractures and deformation zones where solutes can be retained, i.e. be removed, temporarily or permanently, from the mobile water /Berglund and Selroos 2004/. In the safety assessment framework that provides the basis for identification of retardation parameters in the site descriptive models, retardation is assumed to be caused by diffusion and linear equilibrium sorption. These processes are reversible and are here referred to as retardation processes.

The conceptualisation outlined above implies that radionuclide transport takes place along flow paths consisting of connected "sub paths" in fractures and deformation zones of different sizes. In this model, advection is the dominant process for moving the radionuclides in the transport direction, whereas the main role of diffusion is to remove the solutes from the mobile zone and transport them within the immobile zones, cf. Figure 1-1. An attempt to transfer such a generalized model into a descriptive model using available site specific geological data is given in Figure 1-2, where the TRUE Block Scale conceptual model for transport in a single fracture /Andersson et al. 2002/ is presented.
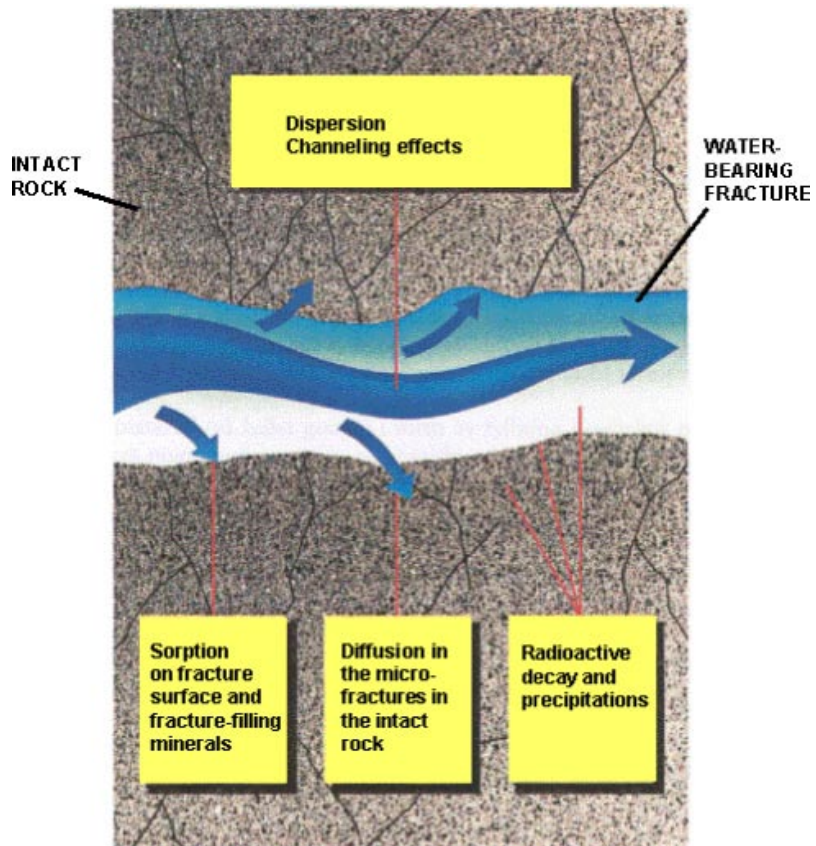
Figure 1-1. *Conceptualised drawing of transport processes applied for an example of a fracture in crystalline rock.*
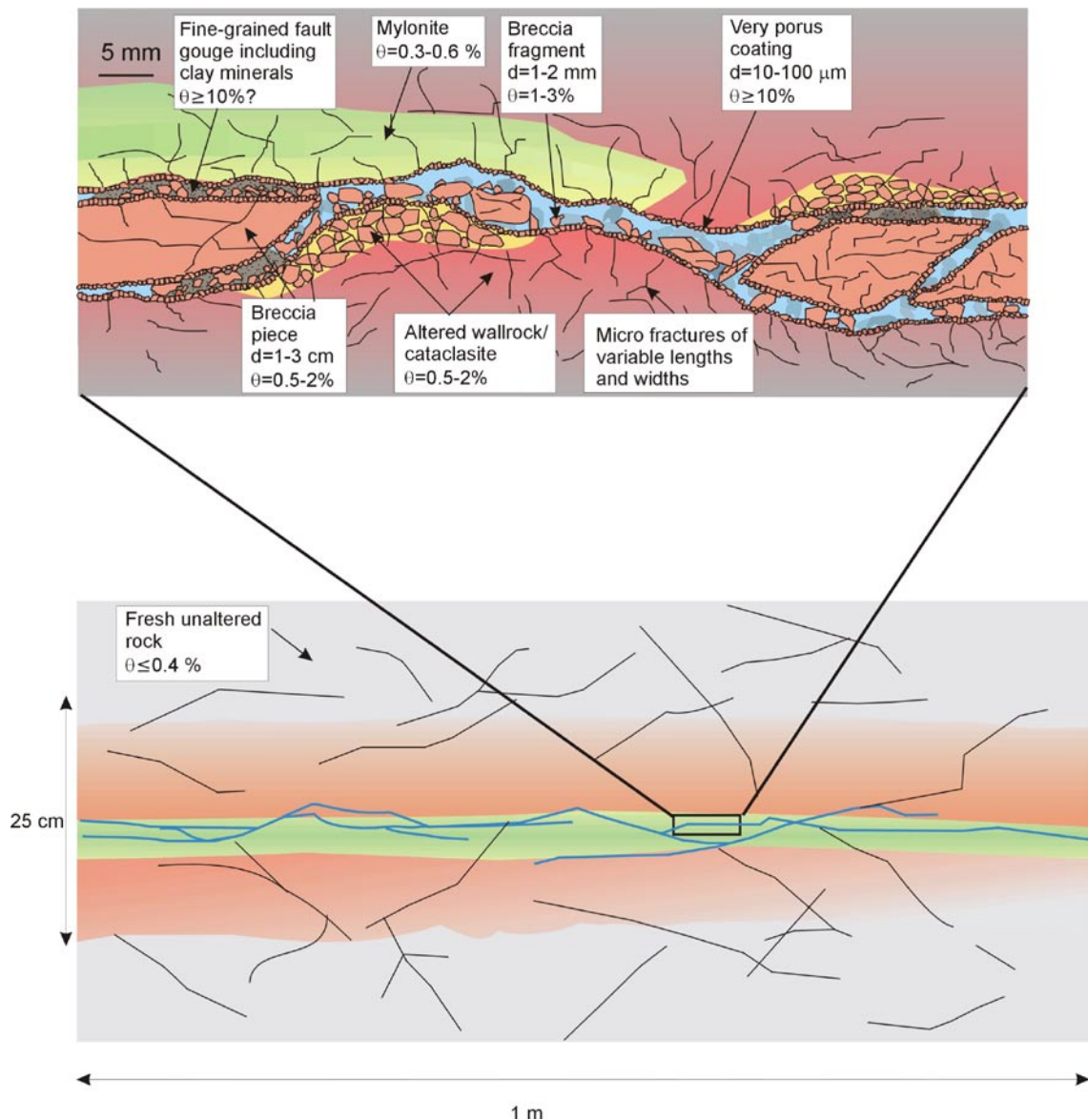
Figure 1-2. Example of a conceptualised description of transport processes in a natural fracture based on observations in the TRUE Block Scale Experiment at the Äspö Hard Rock Laboratory /Andersson et al. 2002/.

1.2.2 The process of development of the retardation model

The process of the development of a retardation model has been a work in which the selection of geological material for laboratory experiments for transport parameters has, for time reasons, been done parallel to the identification and successive refinement of the identification of the geological compartments (rock types, fracture types, deformation zone units) of the retardation model. As sorption and through-diffusion experiments are quite time-consuming (month-year only for the laboratory work, additional months for sample preparations), it was considered essential to identify and collect rock material of importance during the initial phase of the site investigations, i.e. based on the early geological models involving only a low number of boreholes. Therefore, the rock sampling for the laboratory programme started in March 2003. At this stage the aim was to collect rock samples from three or four drill sites located at the Simpevarp and the Laxemar subareas; KSH01–KSH03, KAV01–KAV04 and KLX02. One effect of this early stage sampling is that there are a relatively large number of rock core samples from the Simpevarp subarea.

Since that stage, on the basis of site descriptive model Simpevarp 1.2 and Laxemar 1.2, the Laxemar area has been focused on and the number of drill sites has increased. The improved knowledge of the site, as well as the focus on the area in the south-western part of the Laxemar area has

11

influenced on the rock sampling, which means that additional boreholes and geological features have been addressed in the sample collection. However, it has not been possible to include rock core samples from the last stages of the geological modelling work. For instance, the boreholes in the south-western part of the Laxemar area, which includes structures like e.g. ZSMNW042, are poorly represented. Nevertheless, the sample collection has been found representative for the site with respect to different rock types, fracture types and various types of altered rock within deformation zones.

The composition of the synthetic groundwater used for sorption and diffusion measurements was chosen during an early phase of the Site investigations, when the knowledge of the hydrogeochemistry was limited. Later on, the picture of the groundwater situation at Laxemar was modified and the previous water types chosen for the laboratory experiments were not considered to be completely representative for the site. Consequently, an additional water type was included in the batch sorption experiments (Water type V, cf. Section 2.2.3).

1.3   Outline of this report

The present report summarizes the bedrock transport properties of the Laxemar area in a retardation model and gives the background data that are used for the justification of this model. Thus, the report focuses primarily on the first and second bullet points in the strategy outlined in Section 1.1. The data and models used as input to the modelling are described in Chapter 2, including the inputs from other modelling disciplines. Furthermore in Chapter 2, based on a summary of the geological description of the site, an identification of the different geological structures (rock types, fracture types, deformation zone units) is done which will be used as the backbone of the retardation model. Chapter 3 presents the evaluation of transport data based on geological structures given in Chapter 2, whereas the resulting retardation model (a summary of the retardation properties for the identified geological structures) is described in Chapter 4.

2 Description of input data

2.1 Geology, hydrogeology and hydrogeochemistry

The following section is a brief summary of the geological, hydrogeological and hydrogeochemical models in the site description of the SDM-Site Laxemar. These models constitute the base for the evaluation of the results from the laboratory measurements of porosity, sorption and diffusion parameters, which are presented in Chapter 3 in this report. The synthesis of these parameters are summarised in a retardation model in Chapter 4 which besides the parameter values is intended to serve as a basis of the understanding of the transport properties of the rock.

For the establishment of a retardation model of the Laxemar site, the following features have been foreseen as essential:

- Rock types, variations in e.g. porosity, diffusivity and sorption properties between different rock types can easily be foreseen to have an impact on the transport and retardation properties.

- Rock domains, the possibility of correlating retardation properties to the domain sub-division of the bedrock of the site is necessary to address in a description of the retardation model.

- Deformation zones, a higher concentration of fractures are easily foreseen to constitute a larger part of the water flow through the bedrock. Due to the higher content of deformed and altered rock in deformation zones, special attention has to be drawn to the porosity, diffusivity and sorption properties of the geological elements that can be found in these zones.

- Rock alteration, since alteration is expected to have an impact on all retardation parameters, a general description of the alteration of the rock at the site has to be addressed in a retardation model.

- Fractures, water flow takes place in fractures and the impact of the different fracture types on sorption and diffusion, as well as the distribution of fracture types in the open and water conducting fractures, has to be addressed.

- Fracture domains, the possibility of addressing retardation properties to the sub-division of the bedrock based on a macroscopic fracture model of the site (the fracture domain concept) should be investigated.

- Hydrogeology and hydraulic rock domains, the possibility of assigning retardation properties to the sub-division of the bedrock based on the hydraulic description of the site (the hydraulic domain concept) should be investigated.

- Hydrogeochemistry, the impact of the groundwater composition on the chemical speciation and on the adsorption properties should be addressed.

Data of relevance for the bedrock transport properties description contained in the reports by /Wahlgren et al. 2008, Laaksoharju et al. 2009, La Pointe et al. 2008 and Rhén et al. 2008/ (including models and databases) are summarised in this chapter. Supporting descriptive data from the combined geological/hydrogeochemical interpretations of fracture mineralogy and wall rock alteration data are provided by /Drake and Tullborg 2009, Eklund and Mattson 2008/, as well as detailed studies of deformation zones are provided by /Viola and Venvik Ganerød 2007/.

2.1.1 Rock types

The bedrock in the Laxemar-Simpevarp area is dominated by 1.80 Ga intrusive rocks that formed during an intense period of igneous activity at the waning stages of the Svecokarelian orogeny. Magma mixing and mingling together with diffuse contact relationships are characteristic features of these rocks, which show compositions varying from true granites to quartz monzodiorite.

In the Laxemar 1.2 version of the bedrock geological map, the Laxemar subarea and its immediate surroundings were dominated by two rock types: a generally porphyritic Ävrö granite (501044) and quartz monzodiorite (501036). The Site descriptive model for Laxemar (model version 2.3) comprises a main modification compared to the latter version; a subarea of the originally defined Ävrö granite (501044) has been identified as Ävrö quartz monzodiorite (501046), i.e. a quartz-poor variety of the Ävrö granite (cf. Figure 2-1). This subarea is also characterized by a higher proportion of diorite/gabbro than the surrounding area.

The identification of the Ävrö quartz monzodiorite has given rise to a general subdivision of the Ävrö granite (501044) into the quartz-poor variety Ävrö quartz monzodiorite (501046) and the more quartz-rich variety Ävrö granodiorite (501056). However, since a geographical division of these two varieties is difficult to present, this remaining part of the 501044 area of the Laxemar local model volume is still marked as Ävrö granite (501044) on the bedrock geological map (Figure 2-1). The area defined on the map as Ävrö granite (501044) should therefore be considered to comprise a mix of Ävrö granodiorite (501056) and Ävrö quartz monzodiorite (501046). Nevertheless, for the rock samples used for laboratory determination of transport parameters dealt with in this report, the subdivision into 501046 and 501056 has been fully implemented and the results given for these two rock types separately. The 501044 rock type is therefore from now on not dealt with in this report.

Subordinate rock types in the Laxemar local model volume comprise fine-grained dioritoid (501030), diorite/gabbro (501033), granite (501058), fine-grained diorite-gabbro (505102) and fine-to medium-grained granite (511058). Dolerite (501027) is documented in a few boreholes in the westernmost part of Laxemar. A summary of the rock types and rock codes is presented in Table 2-1.
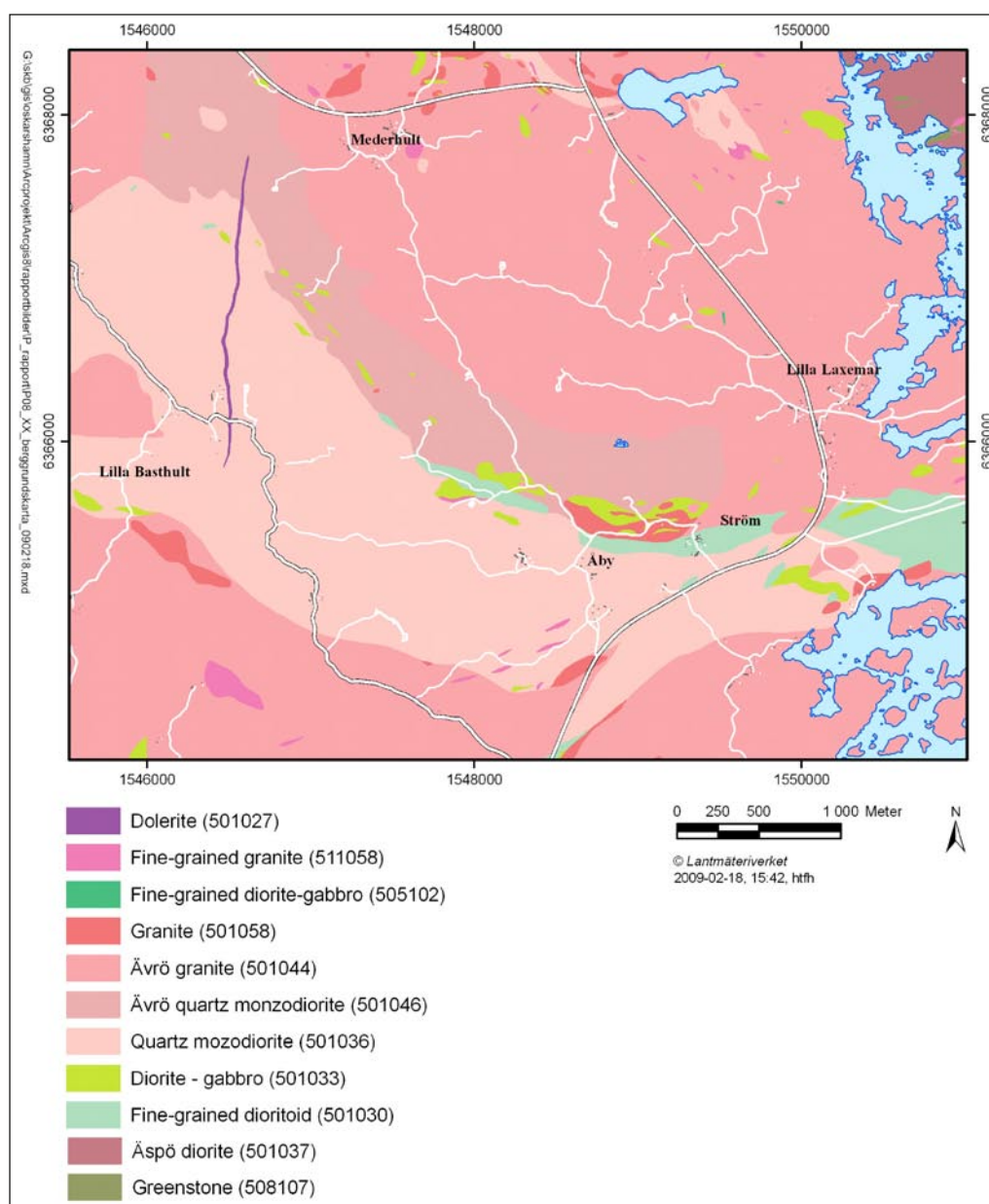

Figure 2-1. *Bedrock geological map of the Laxemar local model area, modified after /Wahlgren et al. 2008/. Note that Ävrö granite (501044) at the map comprises both Ävrö granodiorite (501056) and Ävrö quartz monzodiorite (501046).*

Table 2-1. Rock type nomenclature used by the Boremap mapping for the site investigation at Laxemar, after /Wahlgren et al. 2008/.

Rock type	Rock code
Dolerite	501027
Fine-grained dioritoid	501030
Diorite/gabbro	501033
Quartz monzodiorite	501036
(Ävrö granite)	(501044)
Ävrö quartz monzodiorite	501046
Ävrö granodiorite	501056
Granite	501058
Pegmatite	501061
Fine-grained diorite-gabbro	505102
Fine-grained granite	511058

2.1.2 Rock domains (RSM)

A rock domain refers to a rock volume in which rock units that show similar composition, grain size, degree of bedrock homogeneity, and degree and style of ductile deformation have been combined and distinguished from each other. The term rock domain is used in the 3D geometric modelling work. 13 rock domains are defined in the local model volume (Figure 2-2), of these domains RSMBA03 only occurs at depth in the southern part of the model volume. A short description of the rock domains that are of most importance in the local model volume is provided below, according to /Wahlgren et al. 2008/.

RSMA01: The commonly medium-grained and finely porphyritic Ävrö granite (501044) is the dominant rock type in the RSMA01 domain and constitutes about 82% of the volume. Subordinate rock types comprise fine-grained granite (511058), fine-grained diorite-gabbro (505102), granite (501058), fine-grained dioritoid (501030) and quartz monzodiorite (501036). The orientation of the faint to weak foliation and orientation of the subordinate rock types are fairly similar.

RSMD01: The RSMD01 domain is strongly dominated by equigranular, medium-grained quartz monzodiorite (Figure 2-3). Fine-grained granite (511058), fine-grained diorite-gabbro (505102) and pegmatite (501061) are the most important subordinate rock types and occur in relatively similar amounts in all boreholes.

RSMM01: The RSMM01 domain is characterized by a much higher proportion of diorite/gabbro (mean value about 16%) compared to the other rock domains (Figure 2-3). The Ävrö quartz monzo-diorite dominates and constitutes approximately 75% of the domain. The subordinate rock types are the same as in RSMD01 and constitute similar proportions (Figure 2-3). In contrast to the RSMD01 domain, the orientation of the subordinate rock types and the faint to weak foliation do not display the same similarities in the RSMM01 domain, especially there is no corresponding orientation of the subordinate rock types to the north-dipping foliation.

2.1.3 Deformation zones (DZ)

Definition of a deformation zone

Deformation zone is a general term referring to an essentially two-dimensional structure where there is a concentration of brittle, ductile or combined brittle and ductile deformation. These structures are referred to as regional, local major and local minor deformation zones (see Table 2-2).

Figure 2-4 illustrates a conceptual model of a brittle deformation zone including a transition zone and a core, surrounded by undeformed host rock. According to /Munier et al. 2003/ the host rock has a fracture frequency of less than 4 fractures per metres. The boundaries between the host rock, transition zone and core are commonly diffuse and difficult to define. The transition zone can range in thickness, from a few metres to several tens of metres. This part of the zone has an increased fracture frequency (between 4 and 9 fractures per metres) together with a more extensive alteration

Figure 2-2. *Horizontal cross section at the surface for a 3D-model of the rock domains in the Laxemar local model area SDM-Site Laxemar. The prefix RSM has been excluded in the denomination of the rock domains. The colours represent the dominant rock type in each domain, except for the P-domains which are characterized on structural basis, after /Wahlgren et al. 2008/. Note that the Ävrö granite comprises both granitic and granodioritic (501056), as well as quartz monzodioritic, compositions (501046).*

Figure 2-3. *Quantitative estimate in volume-% of the proportions of different rock types in rock domain RSMA01, RSMM01 and RSMD01 respectively, redrawn after /Wahlgren et al. 2008/. The translation of rock codes to rock types is provided in Table 2-1.*

Table 2-2. Terminology and general description of the brittle structures in the bedrock based on /Andersson et al. 2000/.

Terminology	Length	Width	Geometrical description
Regional deformation zone	> 10 km	> 100 m	Deterministic
Local major deformation zone	1 km–10 km	5 m–100 m	Deterministic (with scale-dependent description of uncertainty)
Local minor deformation zone	10 m–1 km	0.1 m–5 m	Statistical (if possible, deterministic)
Fracture	< 10 m	< 0.1 m	Statistical

BH 2   BH 1

— Target BH intercept, often BH ESHI intercept
— Modelled geometrical BH intercept -envelope thickness

▮ Fault core

▯ Transition zone

▢ Rock outside the brittle deformation zone
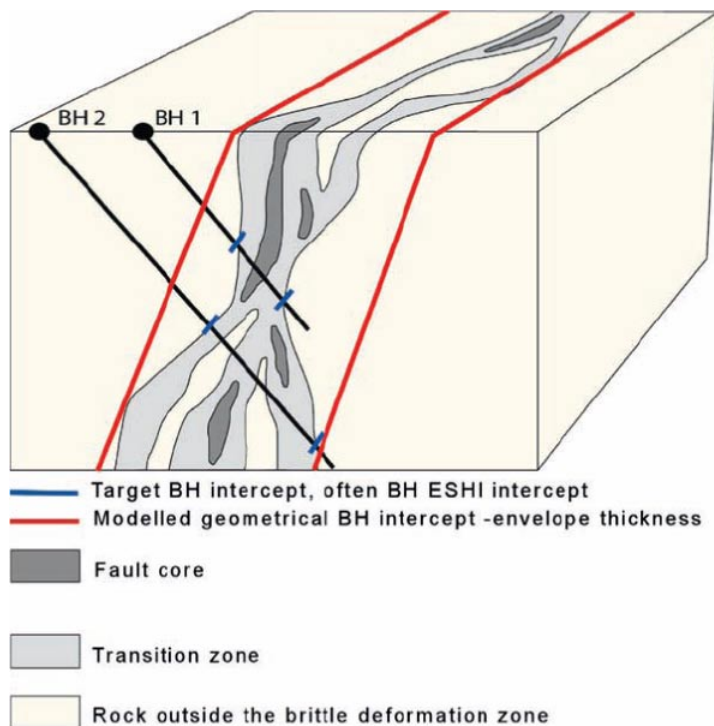
(redrawn after Caine et al. 1996)

Figure 2-4. *Three-dimensional illustration of a conceptual geometric model for a brittle deformation zone at Laxemar along which shear displacement has occurred (redrawn after /Caine et al. 1996/). Note the variable character of the deformation zone along the two borehole intersections /Wahlgren et al. 2008/.*

compared to the surrounding bedrock. However, the transition zone can contain segments that are unaffected with respect to both fracture frequency and alteration. Narrow zones or bands of fault rock may occur, especially closer to the transition to the fault core. The zone core is thinner than the transition zone and varies from a few centimetres to a few metres. The core has even higher fracture frequency (more than 9 fractures per metres) and is composed of sealed fractures (mainly in sealed fracture networks) as well as minor occurrences of fault rocks, mainly in the form of cemented breccia or cataclasite. Alteration, particularly hematite dissemination (oxidation), is abundant inside deformation zones, although the alteration is not always pervasive throughout the zone.

Laxemar deformation zones

Possible deformation zones have been identified through the extended single hole interpretation (ESHI) where a general description of each identified zone is given, based on geological and geophysical criteria. Deformation zones that are longer than 1,000 m are modelled deterministically and are included in the deformation zone block models in RVS (Rock Visualization System). All possible deformation zones that have been identified in a single borehole (i.e. through the estimated single hole interpretations, ESHI) and have an estimated thickness less than or equal to 10 metres are termed as minor deformation zones (MDZ). Deformation zones are distinguished in both the rock domain model as well as the fracture domain concept.

An overview of the location of the deformation zones, beside the rock domains interpreted and modelled deterministically in the local model area are presented in Figure 2-5. These zones are individually described in /Wahlgren et al. 2008, Appendix 14/. At the scale of local major and regional deformation zones there are no zones which are solely ductile. Many zones have a ductile origin but all show clear signs of brittle reactivation.

Figure 2-5. *An overview of the deformation zones and rock domains modelled deterministically in the Laxemar local model area /Wahlgren et al. 2008/.*

According to /Wahlgren et al. 2008/ the main zones are a series of five groups that are based on their overall orientation, origin and character:

- **Northeast-southwest striking, moderate to steeply dipping**. Three of the zones in this group are regional deformation zones and have a ductile origin and complex internal geometry. Other deformation zones in this group, located in the Laxemar local model area, have a ductile origin and have been subjected to brittle reactivation during multiple phases. Except for the regional zones, these structures are relatively narrow with thicknesses in the range of 10 to 35 metres and a zone core thickness of 1 to 5 metres.

- **North-south striking, moderate to steeply dipping**. Local major and regional zones in this group have a ductile origin and have been subject to multiple phases of brittle reactivation. A majority of these zones are narrow with thicknesses of 10 to 20 metres and multiple thin discontinuous highly fractured cores.

- **East-west to northwest-southeast striking, steep to moderate dip to the south**. All of the main zones show an original ductile fabric that has been heavily overprinted by brittle reactivation. Alteration, dominated by red staining, is also common to this group.

- **East-west to northwest-southeast striking moderate dip to the north**. This set is dominated by a specific 80 metres thick zone; ZSMEW007A-C. This zone has a completely brittle origin and character with well developed breccias and characteristic red-green fault gouge concentrated in 60 centimetres thick clay core. Thinner zones with similar character are found in the group.

- **Gently dipping**. Deformation zones in this group are interpreted to occur in Laxemar but their sizes are judged to be from around the lower range of what is termed Local major deformation zones to the minor deformation zones (MDZ) size range (Table 2-2). The character is varying from thicker discontinuous series of deformation zones and mafic intrusions to brittle with markedly open fractures.

The minor deformation zones (MDZ) mirrors the regional and local major deformation zones with respect to orientations and character, i.e. variations from ductile to brittle-ductile and brittle. The subhorizontal set represents about 70% of the total amount of MDZ. The spatial distribution of the identified MDZs was studied and implies that the upper 150 metres of the bedrock display a higher density of MDZs. A high proportion (65%) of minor deformation zones are associated with intrusions e.g. fine-grained granite, and have an increased frequency of open fractures /Wahlgren et al. 2008/.

2.1.4   Rock alteration

An estimate of the degree and different types of alteration has been carried out by use of the data set *rock alteration* in Sicada, as inferred from the Boremap mapping of the cored boreholes. The focus has been on the degree of alteration in the rock in between interpreted deformation zones and is presented in /Wahlgren et al. 2008, Appendix 7/. The degree (or intensity) is classified as faint, weak, medium or strong. For Laxemar in general, the degree of alteration in the bedrock in between the deformation zones is classified as faint to weak. It is found that up to approximately 20–25% of the bedrock is affected by alteration, although inhomogeneously distributed. Different types of mapped alterations are albitization, epidotization, oxidation (red staining), quartz dissolution, saussuritization, sericitization and in addition, silicification and carbonatization.

Red-stained, hydrothermally altered rock is a common feature adjacent to fractures in the Laxemar area. Almost 50% of the sealed fractures in the Laxemar local model area are bordered by red-stained wall rock. According to /Drake et al. 2008/, the main mineralogical features of the red-staining and hydrothermal alteration are pseudomorphic replacements of plagioclase by a paragenesis of albite, K-feldspar, sericite, Fe-oxide, prehnite and epidote, of biotite by chlorite and of magnetite by hematite. Increased intragranular porosity and higher amounts of micro fractures are also evident in the red-stained rock. The red-staining is associated with changes in concentrations of different elements such as Al, CaO, Sr, K_2O, Ba and Rb. The colour intensity of the red-staining is most prominent where minute Fe-oxide inclusions are present in porous secondary minerals, particularly in K-feldspar in the pseudomorphs after plagioclase. However, the hydrothermal alteration reaches further from the fracture than the red-staining, shown by biotite and plagioclase alteration in the reference samples.

The alteration in the rock domains described below is based on extended single hole interpretations of the rock between the identified deformation zones. The RSMA01 domain is dominated by oxidation (red staining), as can be seen in Figure 2-6. It is mostly of faint to weak character and affects about 25% of the domain. Alteration of subordinate character is saussuritization (approximately 3%) and very sparse epidotization (less than 1%).

The estimated alteration of the RSMD01 domain comprises equal proportions of faint to weak oxidation (red staining) and saussuritization, i.e. approximately 10% of each. Furthermore, epidotization is observed and constitutes about 2%.

The alteration in the RSMM01 domain is dominated by oxidation (red staining). It is mostly of faint to weak character and affects about 14% of the domain, with subordinate saussuritization (approximately 2%) and very sparse epidotization (less than 1%).

Alteration within deformation zones

Red staining caused by a fine-grained dissemination of hematite can be found associated with a majority of the zones. However, it seems to be particularly extensive and characteristic of the E-W trending zones, particularly the dominant zones ZSMEW002A, ZSMEW007A and ZSMNW042A. Most of the red stained bedrock is identified with an intensity of weak to medium. Hence, it must be taken into consideration that the degree of intensity of redstaining might be underestimated because of the original grey-red colour of some of the rock types.

An example of the proportion of altered bedrock inside deformation zones, beside various alteration types for rock domains RSMA01 and RSMD01 are displayed in Figure 2-7.
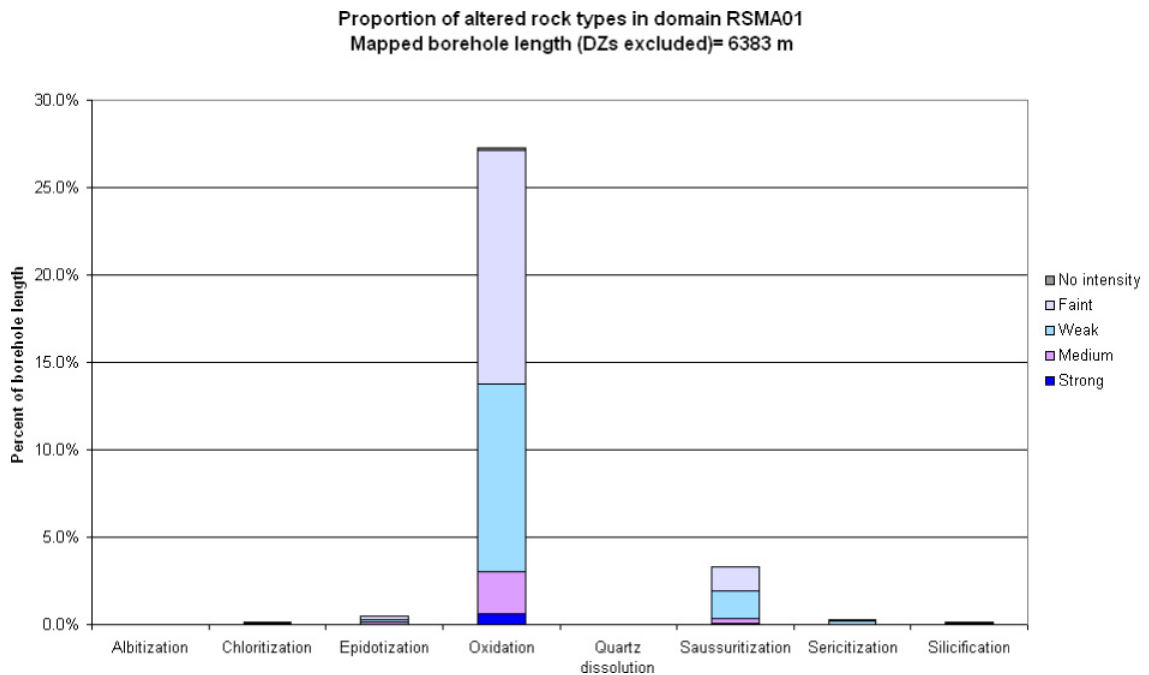
Figure 2-6. Different types of alteration within RSMA01 /Wahlgren et al. 2008/. The intensity of the alteration is marked with different colours.
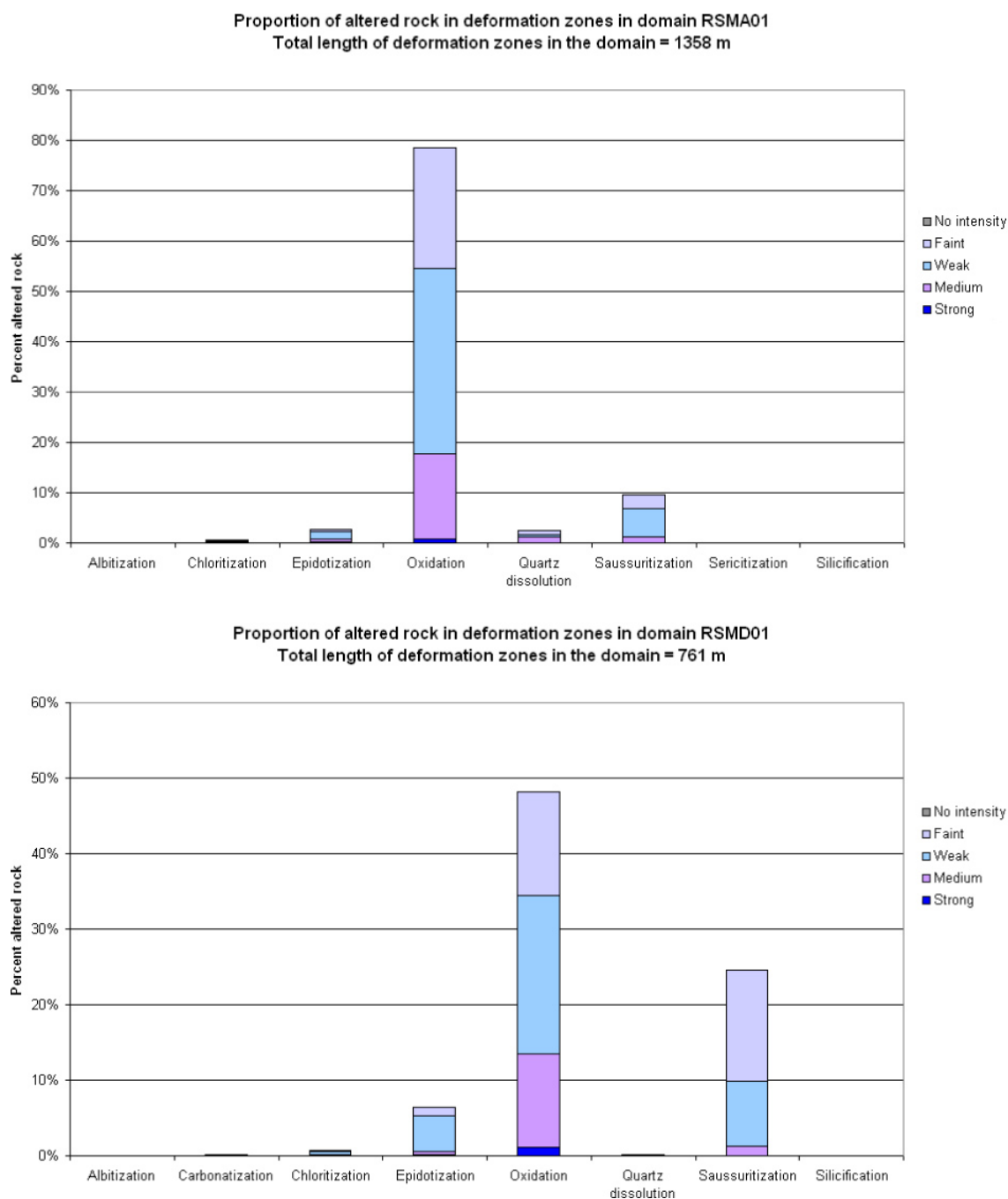
Figure 2-7. *Proportion of various types of alteration within deformation zones in rock domains RSMA01 and RSMD01. The intensity is marked with different colours.*

2.1.5 Fractures

Fracture generations

During detailed studies of the fracture mineralogy and wall rock alteration at the Laxemar-Simpevarp area /Drake and Tullborg 2009/, six sequences of events have been identified. These are presented in Table 2-3, and refer to both sealed and open fractures. The formation temperatures of the different generations range from moderate to low temperature conditions (greenschist to zeolite facies) grading into present conditions. This indicates that the fractures were initiated relatively early in the geological history and have been reactivated during several different periods. Re-activation is commonly observed, especially in deformation zones. It is assumed that especially the calcite and pyrite (and also Fe-oxyhydroxide near surface) formations are ongoing processes although the amounts of possible recent precipitates are low.

Table 2-3. Schematic fracture filling-sequence from the Laxemar subarea. After /Drake and Tullborg 2009/. Minerals within brackets are found in minor or trace amounts.

	Generation		Age
1.	Mylonite; quartz, epidote, (muscovite, chlorite, albite, calcite, K-feldspar)	(cf. zone unit 4 in Table 2-5)	>1.45 Ga, probably older than c 1.77 Ga.
2.	a) Cataclasite; epidote, quartz, chlorite, (K-feldspar, albite)	(cf. zone unit 4 in Table 2-5)	>1.45 Ga
	b) Cataclasite; K-feldspar, chlorite, quartz, hematite, albite, (illite)		
3.	a) Quartz, epidote, chlorite, calcite, pyrite, fluorite, muscovite, (K-feldspar, hornblende)	(cf. fracture type A, B, C D, E, F and I in Table 2-4)	
	b) Prehnite, calcite, (fluorite, K-feldspar)		1.42 Ga or older
	c) Calcite, laumontite, adularia, chlorite, quartz, illite, hematite, (albite, fluorite)		
4.	Calcite, adularia, laumontite, chlorite, quartz, illite, hematite, illite/chlorite-mixed layer clay, (albite, apatite)	(cf. fracture type B, D and I in Table 2-4)	1.42–0.7 Ga
	Sandstone		Cambrian
5.	Calcite, adularia, chlorite, hematite, fluorite, quartz, pyrite, barite, gypsum, mixed-layer clay (e.g. corrensite), apophyllite, harmotome, REE-carbonate, (galena, illite, chalcopyrite, laumontite, sphalerite, U-silicate, apatite, albite, analcime).	(cf. fracture type A, C, E, F, G and I in Table 2-4)	The earliest and major fillings ("warm brine" precipitates) were formed at c 448–400 Ma, but fillings formed at lower temperatures might be considerably younger.
6.	Calcite, pyrite, clay minerals, goethite (near surface)	(cf. fracture type A, F and I in Table 2-4)	Paleozoic to recent (possibly Quaternary)

As single fracture mineral, calcite is present in 78% of the mapped open fractures and in 48% of the mapped sealed fractures, while chlorite is present in 76% of the open fractures and in 33% of the sealed fractures (Figure 2-8) /Drake and Tullborg 2009/. A quantitative mapping of fracture minerals in transmissive fractures at Laxemar demonstrates that calcite generally covers 10–20% of the fracture surface and only rarely the whole fracture surface. Chlorite in turn usually covers the whole fracture surface, but it is generally coated by another fracture mineral, mainly by calcite /Eklund and Mattson 2008/.

Clay minerals, pyrite and hematite are most frequently found in open fractures, whereas epidote, adularia, quartz and prehnite are more frequent in sealed fractures /Drake and Tullborg 2009/. Generation 1 and 2 minerals, which occur in mylonites and cataclasites, are mainly mapped as minor rock occurrences with mylonitic/cataclastic as their structural description. Therefore, no specific mineral for mylonites and cataclasites is noted during the mapping of the drill core.

No clear correlation between mineralogy and fracture orientation is observed at the Laxemar-Simpevarp area. Many of the minerals, e.g. calcite and chlorite are found in several generations and because of the reactivation of fractures it may result in misleading interpretations of the fracture orientations. The different fracture orientations dominating in different fracture domains within the Laxemar local model area /Wahlgren et al. 2008/, is partly addressed to be associated to the orientations of older deformation zones which has influenced the formation of newly formed fractures nearby /Drake and Tullborg 2009/.

Water conducting fractures often exhibit non-cohesive and clayish coatings, usually of fault gouge type (i.e. mainly very fine-grained, loose fracture filling material). Many of the samples contain quartz, K-feldspar and albite in addition to calcite, chlorite and clay minerals. Altered wall rock fragments dominate the gouge material and it is therefore probable that most of the quartz and feldspars belong to these rock fragments or that the samples are contaminated with wall rock material. The total clay mineral content in the open fractures is very difficult to determine appropriately. Thin coatings attached to the fracture wall can consist of 90–100% chlorite and clay minerals. The amounts are relatively small as these coatings are usually thin (<100 μm) but their active surface can be very large. Swelling clays like corrensite and mixed-layer clays of illite/smectite type are common /Drake and Tullborg 2009/.
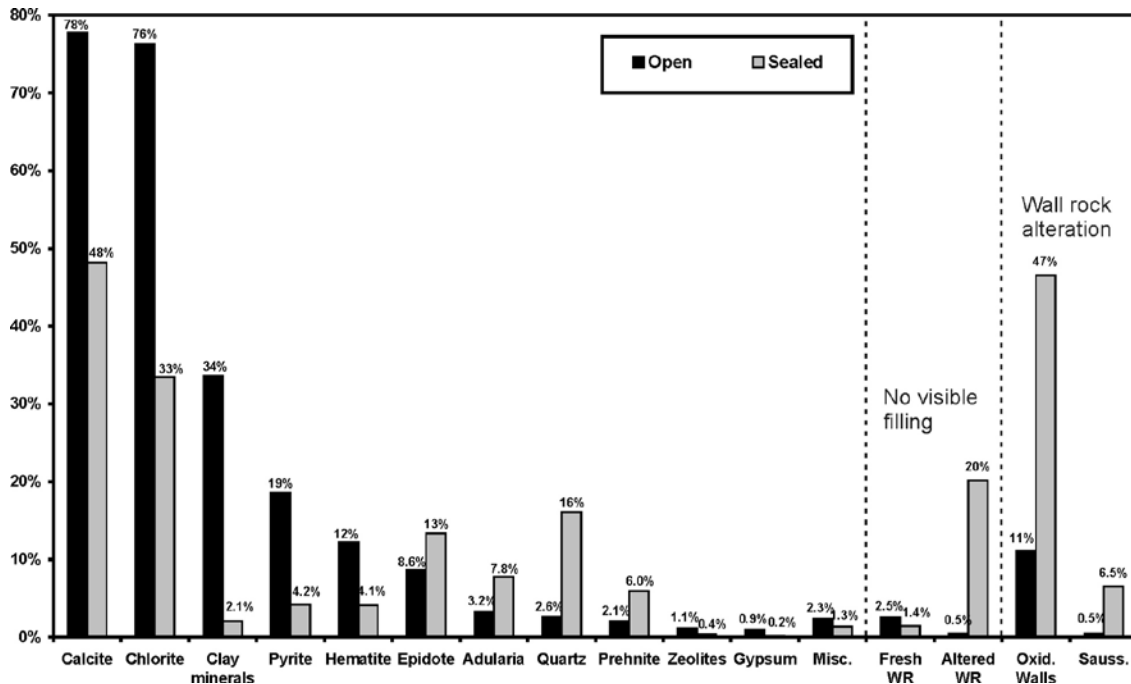
Figure 2-8. Frequency of fracture minerals (open as well as sealed) in KLX02–KLX29A. The number of sealed fractures is 69,229 and the number of open fractures is 33,499. Crush zones and sealed networks are excluded /Drake and Tullborg 2009/.

According to /Drake et al. 2006/ crush zones are mapped separately during the drill core mapping and often represent zones characterised by increased hydraulic conductivity. The term "crushed zone" correlates to an incohesive fault breccia according to the nomenclature of /Sibson 1977/. The fracture mineralogy in these crush zones is dominated by chlorite, calcite and clay minerals.

2.1.6 Fracture domains (FSM)

The term fracture domain refers to a rock volume outside deformation zones in which rock units show similar fracture intensity characteristics. Fracture domains at Laxemar are defined on the basis of the single-hole interpretation (SHI) and its modifications and extensions (ESHI).There are six identified fracture domains at Laxemar (FSM_C, FSM_EW007, FSM_N, FSM_NE005, FSM_S, and FSM_W), controlled by either influences of deformation zones or rock domains (Figure 2-9). Fracture domains are potentially hydraulically significant as the intensity and orientations of open fractures causes the permeability of the rock. Further descriptions of fracture domains are found in /La Pointe et al. 2008/.

2.1.7 Hydrogeology and hydraulic rock domains (HRD)

The following section is a very brief summary of parts of the hydrogeological model at Laxemar /Rhén et al. 2008/.

The hydrogeological SDM is based on data from cored boreholes which are characterised hydrauli-cally by usage of the PFL and the PSS method (further described in /Rhén et al. 2008/). Flowing fractures are detected with the so called PFL-f method (f stands for fracture or feature). These fractures are called "PFL-f features" or previously called PFL-anomalies. The PFL-f method can be used to detect individual flow anomalies down to a resolution of approximately 0.1 m and has a theoretical detection limit for transmissivity (T) of about $1 \cdot 10^{-9}$ m^2/s. About 9% of the detected flowing fractures are within crush zones and approximately 31% are within deformation zones. It is indicated that the hydraulic conductivity within a deterministically defined deformation zone is about 10 times larger compared to the rock between the deterministically defined deformation zones.
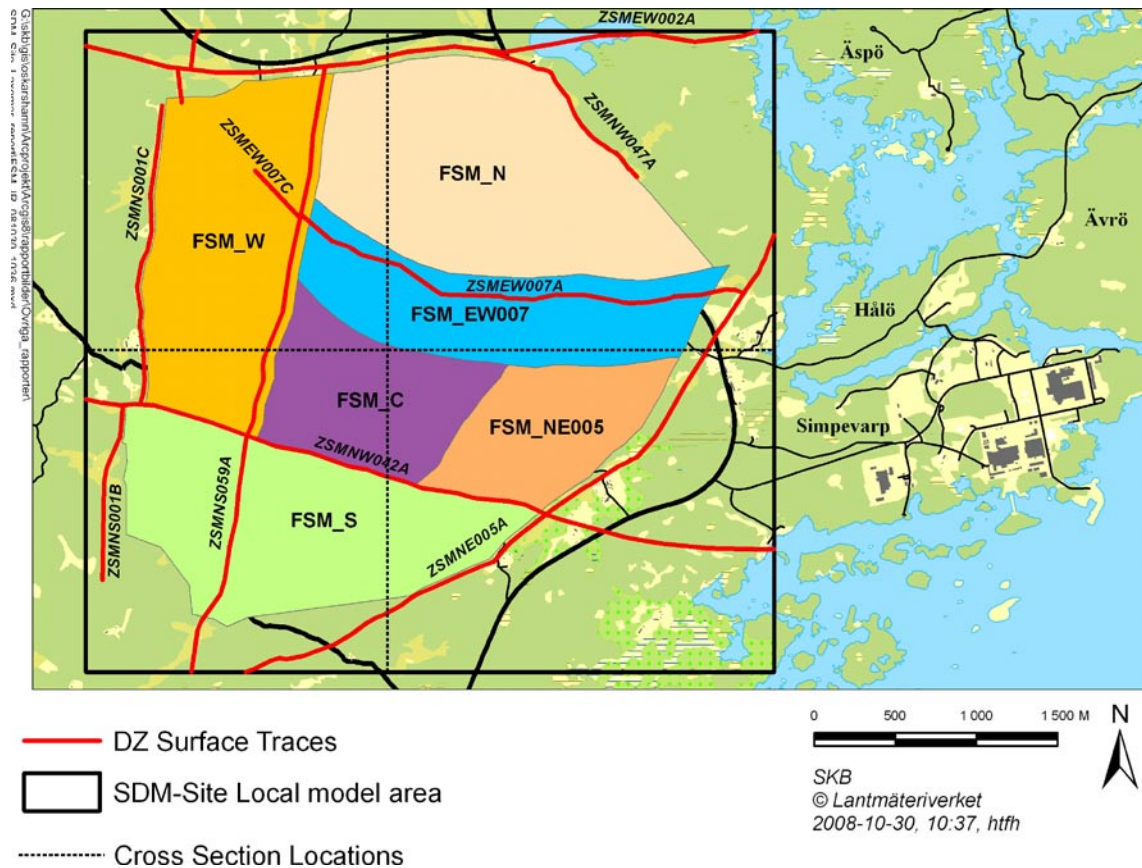
Figure 2-9. *Illustration of the SDM Site Laxemar Fracture Domain Model /La Pointe et al. 2008/.*

The groundwater system at Laxemar is divided into different hydraulic domains of which HCDs (hydraulic conductor domains) represents deformation zones as these may be of hydraulic importance both as planar conductive elements with higher permeability than the surroundings as well as hydraulic barriers by influence of geology, e.g. through association to dolerite dikes or fault gouge. HRDs (hydraulic rock domains) represent the fractured bedrock between the deformations zones. The hydraulic rock domains are defined based on the spatial distribution of hydraulic properties. After fracture analysis with the purpose to discover possible patterns in the occurrence and nature of open, interconnected, flowing fractures, it was shown that some of the fracture domains (cf. Section 2.1.6) can be used as hydraulic domains directly, whereas some fracture domains in combination act as hydraulic rock domains. Four hydraulic rock domains have been considered:

- HRD_EW007 corresponding to FSM_EW007,

- HRD_W corresponding to FSM_W,

- HRD_N corresponding to FSM_N, and

- HRD_C corresponding to the combination of FSM_C, FSM_NE005 and FSM_S.

The distribution of HRDs at the bedrock surface is shown in Figure 2-10.

2.1.8   Hydrogeochemistry

The following section is a very brief summary of the hydrogeochemical model at Laxemar /Laaksoharju et al. 2009/.

The groundwaters at Laxemar-Simpevarp area are characterised by compositions that range in salinity from fresh (less than 200 mg/L Cl) in the upper 100 metres, over to highly saline (about 45,000 mg/L) at approximately 1,500 m depth. Components of meteoric waters from cold and temperate climates as well as marine and deep saline groundwaters have been identified. The groundwaters have been subdivided into different groups based on their salinity, stable isotope
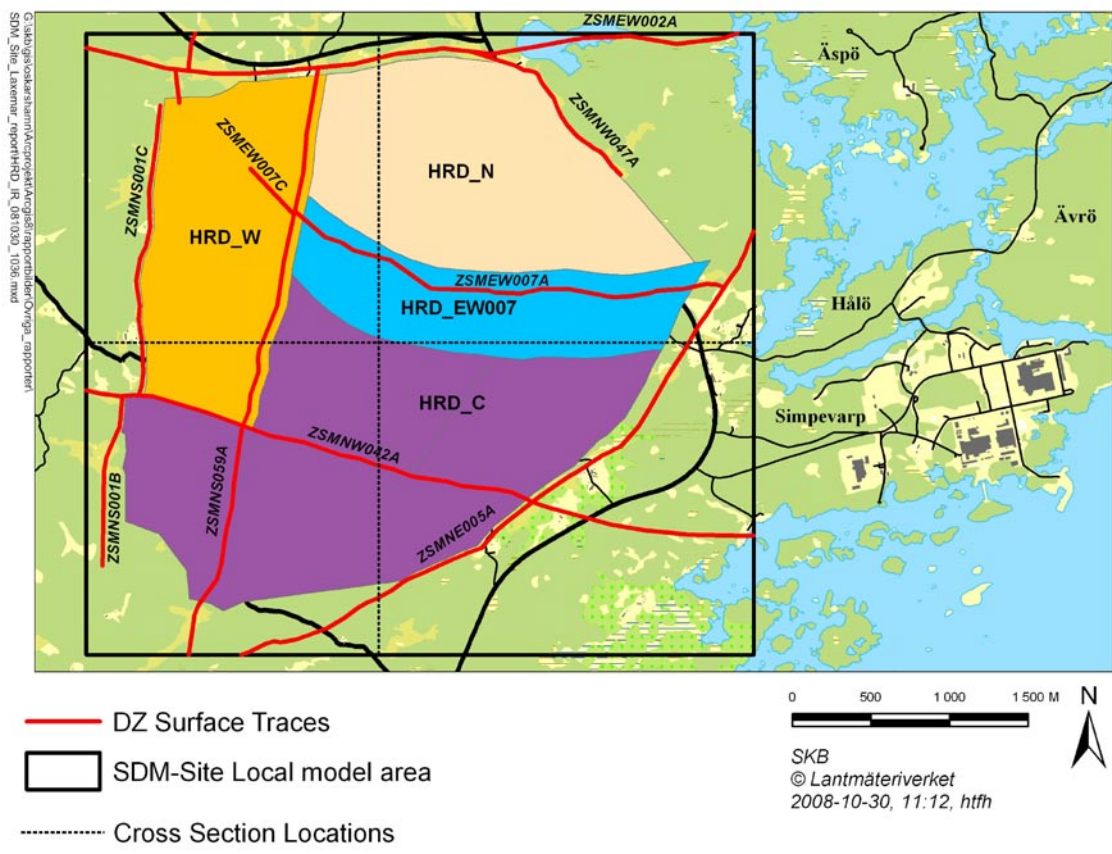
Figure 2-10. *Illustration of the SDM Site Laxemar Hydraulic Rock Domain Model /Rhén et al. 2008/.*

composition ($\delta^{18}O$; used to distinguish waters with a cold climate origin) and Mg contents (used as a marine indicator). The water types distinguished and used in the conceptual visualisation of the Laxemar-Simpevarp area (cf. Laaksoharju et al. 2009) are;

Fresh water; (<200 mg/L Cl; <1.0 g/L TDS (Total Dissolved Solids)) Meteoric in origin i.e. Na(Ca)-HCO$_3$-(SO$_4$) in type.

Brackish Glacial; (200–10,000 mg/L Cl; <1.0–18 g/L TDS); Last Deglaciation meltwater + Brackish Non-marine to Saline component; Ca-Na-Cl-(SO$_4$).

Brackish Marine (2,000–6,000 mg/L Cl; 3.5–10 g/L TDS; Mg>100 mg/L); variable Littorina Sea component (± modern Baltic Sea) + Last Deglaciation meltwater ± Brackish Non-marine to Saline component; Na-Ca-Mg-Cl-SO$_4$.

Brackish Non-marine (3,000–10,000 mg/L Cl; 5–18 g/L TDS; Mg <25 mg/L); Old Meteoric ± Old Glacial ± Last Deglaciation meltwater ± Saline component, i.e. Na-Ca-Cl-(SO$_4$) in type.

'Transition type' waters are sampled in the transition zone between Brackish Glacial and Brackish Non-marine groundwaters with a component of Brackish Marine. These waters range from 2,000–10,000 mg/L Cl.

Saline (10,000–20,000 mg/L Cl; 18–35 g/L TDS; Old Meteoric ± Old Glacial ± Last Deglaciation meltwater ± Highly saline component, i.e. Ca-Na-Cl-(SO$_4$) in type.

Highly saline (>20,000 mg/L Cl; >35 g/L TDS); Ca-Na-Cl-(SO$_4$) in type.

Note that Brackish Marine waters according to the definition above are not found at Laxemar, but are present as components in the 'Transition type' waters. This is a result of that only parts of the Laxemar area were covered by the Littorina Sea.

The conceptual model of the hydrogeochemistry (Figure 2-11) shows the distribution of these groundwater types along a WNW-ESE cross section.
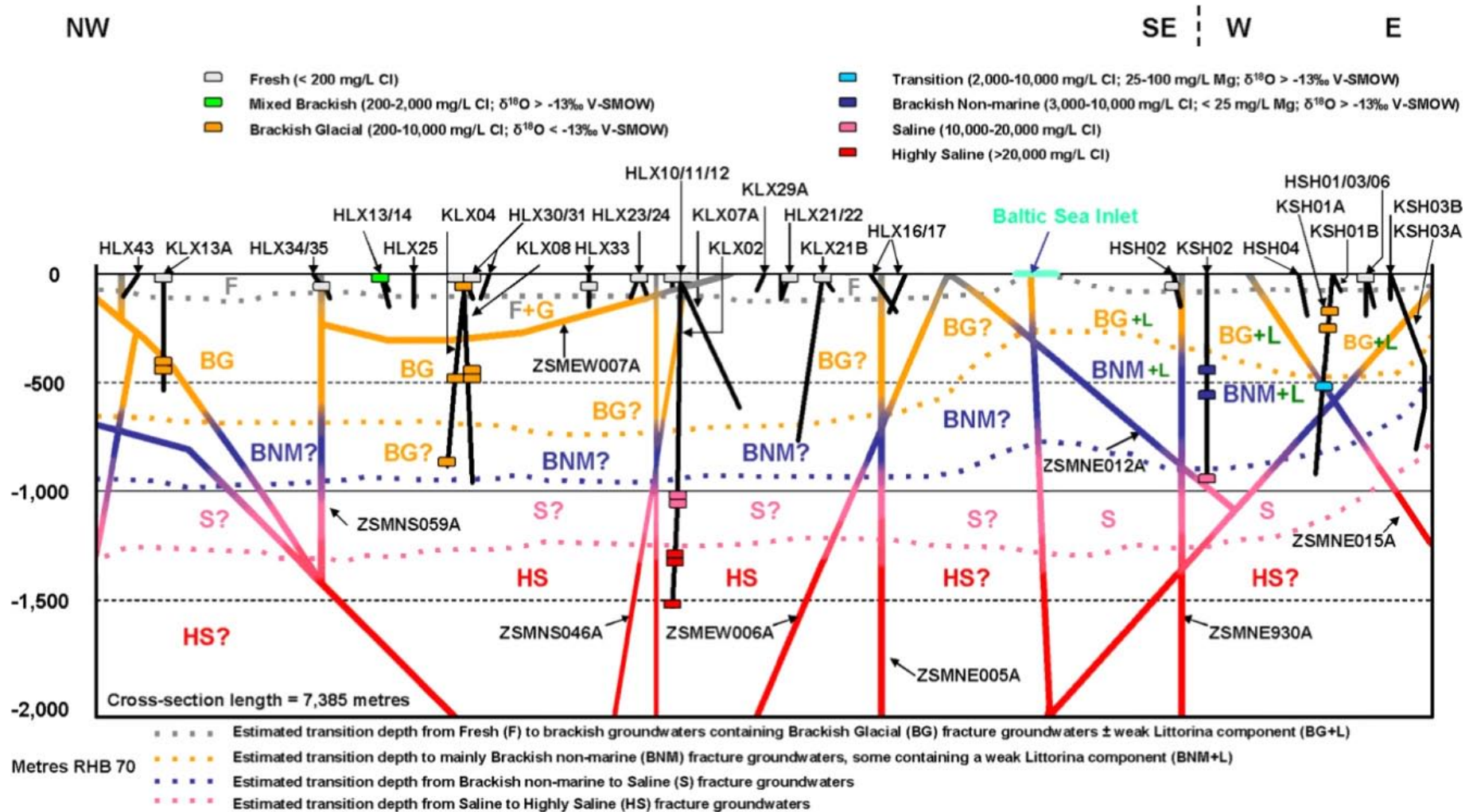
Figure 2-11. Conceptual model of the hydrogeochemistry at Laxemar along a WNW-ESE cross section showing the distribution of different groundwater types /Laaksoharju et al. 2009/.

The major features of the groundwater system at Laxemar are:

- The 0–20 metres depth interval is hydrogeologically active and dominated by recharge meteoric water or Fresh groundwater (<200 mg/L Cl) of Na-Ca-HCO$_3$-(SO$_4$) type showing large variations in pH and redox conditions.

- The 20–250 metres depth interval is dominated by Fresh–Mixed Brackish–Brackish Glacial groundwaters of Na-Ca-HCO$_3$-(SO$_4$) to Na-Ca-Cl-HCO$_3$ type, showing increasingly stable reducing conditions with increasing depth. The residence times of the groundwaters are in the order of decades to several thousands of years.

- The 250–600 metres depth interval is dominated by Brackish Glacial–Brackish Non marine–Transition groundwaters of Na-Ca-Cl-(HCO$_3$) type. Redox conditions are reducing and low Eh values (–245 to –303 mV) are typically controlled by the interplay between the iron and especially the sulphur systems. The significant portions of glacial waters at this depth interval, and the significant increase of non-marine groundwaters with depth, indicates that groundwaters older than 14,000 years are becoming increasingly important.

- The 600–1,200 metres depth interval is dominated by Brackish Non marine–Saline (±Brackish Glacial and Transition) groundwater of Na-Ca-Cl-(SO$_4$) to Ca-Na-Cl-(SO$_4$) type. This groundwater shows very low magnesium values and they are clearly reducing (–220 to –265 mV). Interpretation of chlorine-36 measurements on the saline groundwaters suggest long residence times of hundreds of thousands of years which is supported by low flow to stagnant hydraulic conditions.

- pH values are between 7.2 and 8.6 in the groundwaters and do not show any clear trend with depth. pH is mainly controlled by calcite dissolution-precipitation reactions and, probably, microbial activities. Influence of other common chemical processes, such as aluminosilicate dissolution-precipitation or cation exchange, are probably of secondary importance.

2.2 Data processing for the Retardation model

In this section, synthesis of the retardation relevant data from the geology, hydrogeology and hydrogeochemistry programmes (selection process described in Section 2.1) is made which gives the basis for the retardation model.

2.2.1 Fracture types

The mineralogical composition of the fracture coatings is important e.g. for the sorption interaction of released radionuclides, as well as the presence or absence of an altered zone in the wall rock adjacent to the conductive fractures, as these fractures constitute possible flow paths or, more probable, diffusion pathways. Due to the observed heterogeneity of the mineralogy of the fractures which was considered very likely to influence the retardation properties, a sub-division into a number of fracture types was essential in order to give a proper description of the retardation in fractures. For obvious reasons it is the open fractures that are of most interest for retardation model purposes and thereby the addressing of fracture statistics will be based on results for open fractures only.

As mentioned in Section 2.1.5 there is a sequence of fracture mineralization at Laxemar which includes both sealed and open fractures. The fractures have been developed during long time periods and many of them are reactivated several times which may give fracture minerals that not necessarily originate from the same period. Therefore, the described fracture mineralization in Table 2-3 might not reflect the current fracture assemblage in open fractures. However, using the fracture mineralogy (i.e. the fracture generations, cf. Section 2.1.5), together with feasible mapping units (i.e. fracture data from Sicada) and potential transport properties of different materials, nine different fracture types have been identified for the retardation model purposes (Table 2-4). These types are supposed to represent the present fracture assemblage in open fractures in the Laxemar local model volume. Oxidized walls, saussuritized walls as well as epidotized walls are noted in the mineral column in the software (i.e. Boremap mapping system) during the mineral identification work. Therefore these three types of alteration are included as minerals in the fracture types described in Table 2-4. Based on the work of /Drake and Tullborg 2009/ it has been concluded by the authors that the presently recorded fracture mineral distribution mainly will prevail over the life-time of a spent nuclear fuel repository.

Retardation properties for the various fracture types depends on their mineralogy and as a part of the work of developing the retardation model, statistics of the presence and relative distribution of the different fracture types have been compiled. The base for this statistics is the data from the boreholes from both Laxemar and Simpevarp, i.e. KLX02–KLX29, in addition to KSH01–KSH03. About 44,100 open fractures are included in this dataset. However, concerning the transmissive fractures the boreholes KLX02 and KLX27 is excluded from the dataset. In the analysis of the dataset, fractures with coatings according to the mineral specification in Table 2-4 were selected and extracted according to the procedure described in Appendix 2.

Beside the mineralization itself, the amount of fracture coating has an impact on the retardation capacity. This data was however not available at the time for the processing of fracture data. A work with quantitative mapping was later performed /Eklund and Mattson 2008/ but the results and the on-going analyzing work based on these data /Löfgren and Sidborn 2009/ has not been possible to include in the retardation model.

The following fracture type statistical representations have been compiled with the purpose to reflect possible differences with respect to elevation as well as the sub-divisions made and used by other disciplines (e.g. the geology and hydrogeology programme):

- Distribution and numbers of fracture types in the Laxemar-Simpevarp area, studied as a function of the elevation.
- Distribution of fracture types in the dominant rock domains within the Laxemar local model volume.
- Distribution of fracture types in the dominant fracture domains within the Laxemar local model volume.
- Distribution and numbers of fracture types in the deformation zones, studied as a function of the elevation.
- Distribution and numbers of fracture types within the group of transmissive fractures, studied as a function of the elevation.

Table 2-4. Identified types of fracture mineral assemblages identified for the retardation model, based on fracture mineralogy. The minerals included in each fracture type are defined in the fracture coating column. The following notations are used in the description; + = the mineral must be present; and/or = one or several of the minerals must be present; ± = the minerals may or may not be present.

Fracture type	Fracture coating	Thickness*	Wall rock alteration**	
A	***Chlorite + calcite + pyrite/ chalcopyrite*** ± any mineral	0.2–1 mm	≤ 10 mm	
B	***Epidote and/or prehnite and/or adularia*** ± chlorite ± calcite ± quartz	0.5–1 mm	≤ 20 mm	
C	***Hematite*** ± any mineral	0.5–5 mm	≤ 50 mm	

Fracture type	Fracture coating	Thickness*	Wall rock alteration**	
D	**Laumontite** ± *calcite* ± *chlorite*	0.2–2 mm	≤ 20 mm	
E	**Chlorite + calcite** ± oxidized walls ± saussuritized walls	0.2–0.5 mm	≤ 10 mm	
F	**Clay** ± *any mineral*	0.2–5 mm	≤ 50 mm	
G	**Chlorite** ± any mineral	c. 0.2 mm	≤ 50 mm	
H	**No mineral** ± oxidized walls ± saussuritized walls ± epidotized walls		≤ 10 mm	
I.	**Calcite** ± *any mineral*	c. 0.2 mm	≤ 10 mm	

* The thickness of the fillings for each fracture type is estimated as an average for the whole fracture surface. This is based on conclusions from general experiences of the drill core analysis made by geological expertise and was made before the work with quantitative mapping of fracture minerals Simpevarp-Laxemar (Eklund and Mattsson, 2008) was initiated.

** Referring to the wall rock close to the open fracture.

Frequency distribution of different fracture mineral types

Data are presented as number of open fractures versus elevation and the relative frequency of each fracture type is illustrated in Figure 2-12 and below. Note that right column in Figure 2-12 and 2-15, as well as Figure 2-16 reflect less borehole metres at great depth due to limited length and the angle of part of the cored boreholes.

As was pointed out in Section 2.1.5, chlorite and calcite are the most frequently occurring fracture filling minerals, and according to /Eklund and Mattson 2008/ they are also the most voluminous minerals. Consequently, chlorite and calcite may occur solely or together in all fracture types except for fracture type H (no mineral). Fracture type E (chlorite and calcite, with or without altered wall rock) and fracture type A (chlorite, calcite and pyrite/chalcopyrite) constitute about 23% and 7% respectively of the total amounts of open fractures (see Figure 2-13).

Clay occurs in approximately 34% of the mapped open fractures (Figure 2-8). The occurrence for fracture type F (clay ± any mineral) is lower, about 21% (Figure 2-13), but as clay is also present in fracture type C, the total amount of these two fracture types is approximately the same, i.e. 33%. However, according to /Drake and Tullborg 2009/ the clay mineral content is probably underestimated since most mapped chlorite bearing fractures also contain clay, while hematite is overrepresented due to its ability to discolour or stain other minerals like chlorite and feldspar.
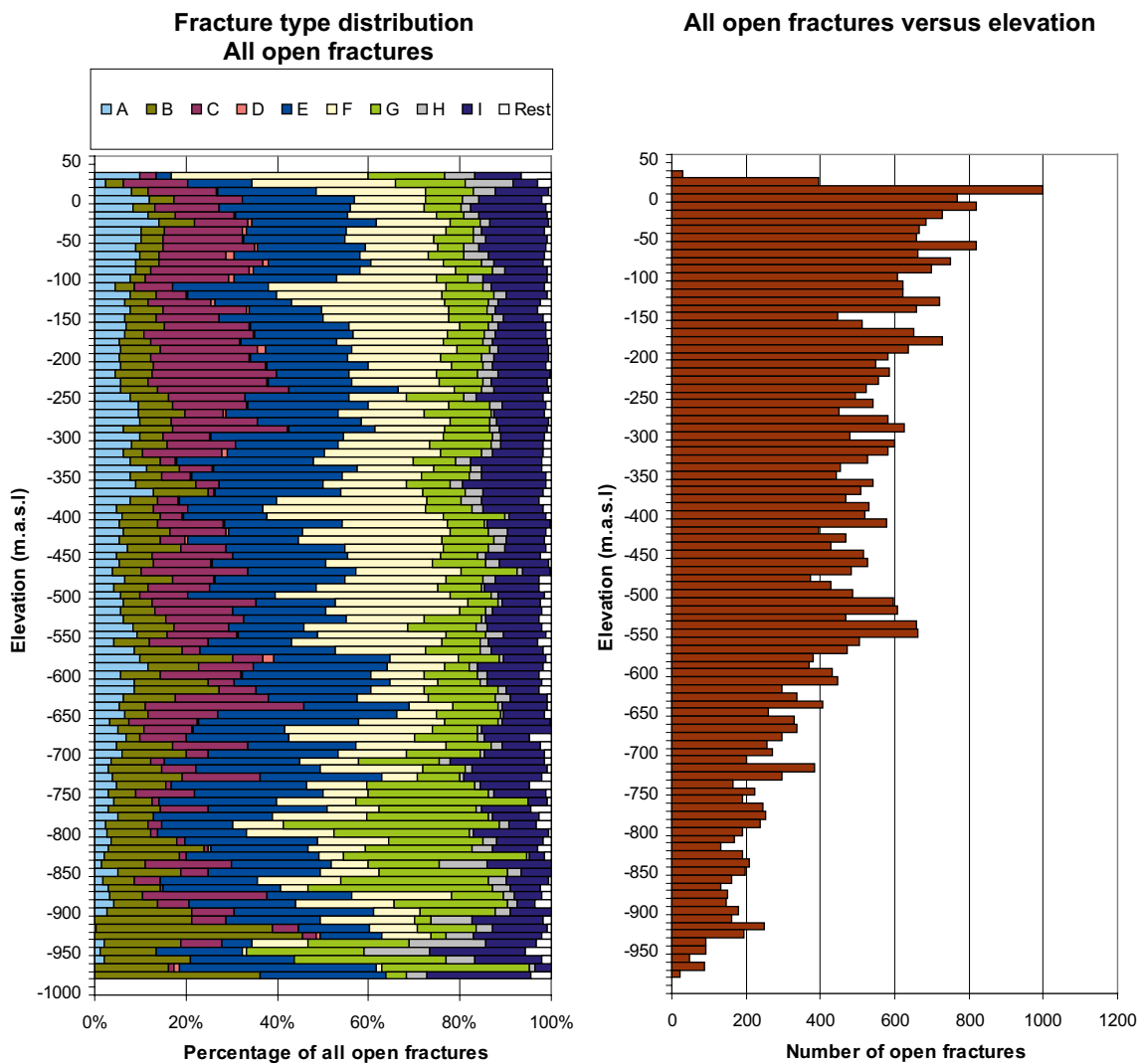
Figure 2-12. *Relative distribution of different fracture types in open fractures versus elevation at Laxemar-Simpevarp, based on borehole data from Sicada. The right figure shows the number of open fractures at differ-ent elevations. The decreasing amount of fractures towards depth is mainly explained by less borehole metres at larger depths and should therefore not be regarded as a generally decreasing fracture frequency with depth.*

31
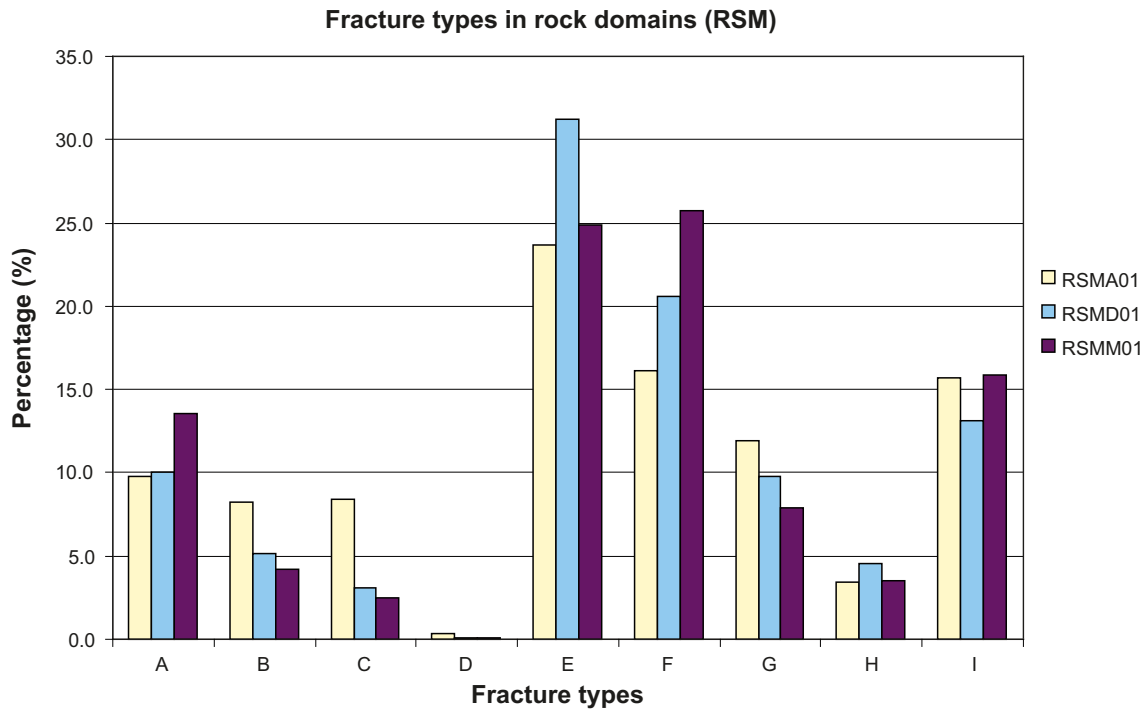
Figure 2-13. *Relative distribution of different fracture types in the dominant rock domains within the Laxemar local model volume, i.e. RSMA01, RSMD01 and RSMM01. Descriptions of the fracture types are presented in Table 2-4.*
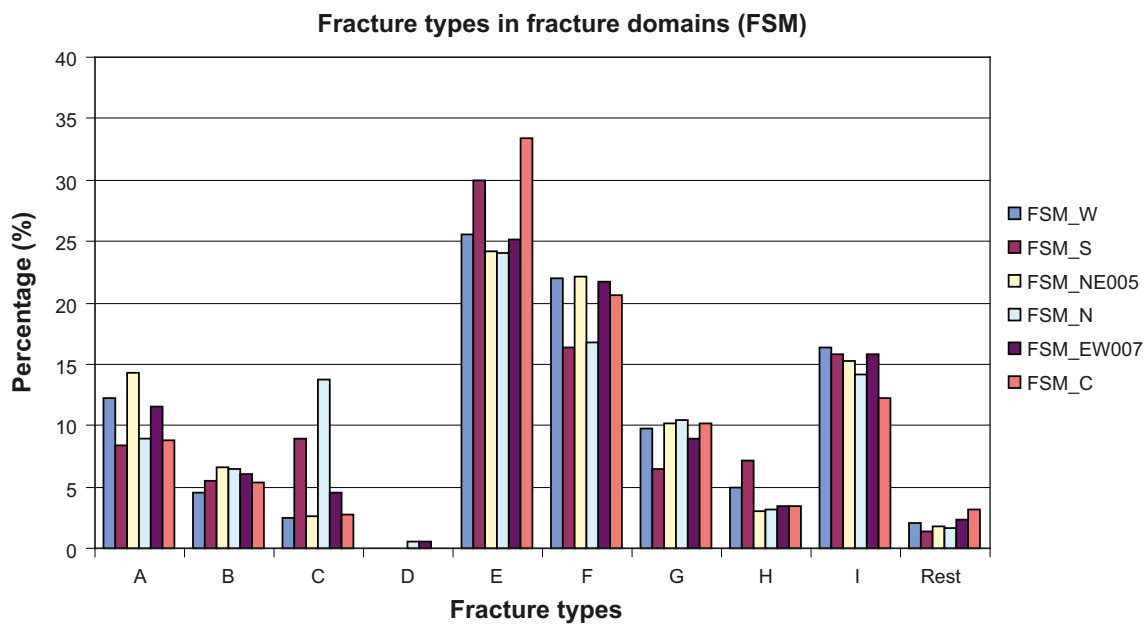
Figure 2-14. *The relative distribution of fracture types in the six fracture domains in the Laxemar local model volume. Descriptions of the fracture types are presented in Table 2-4.*
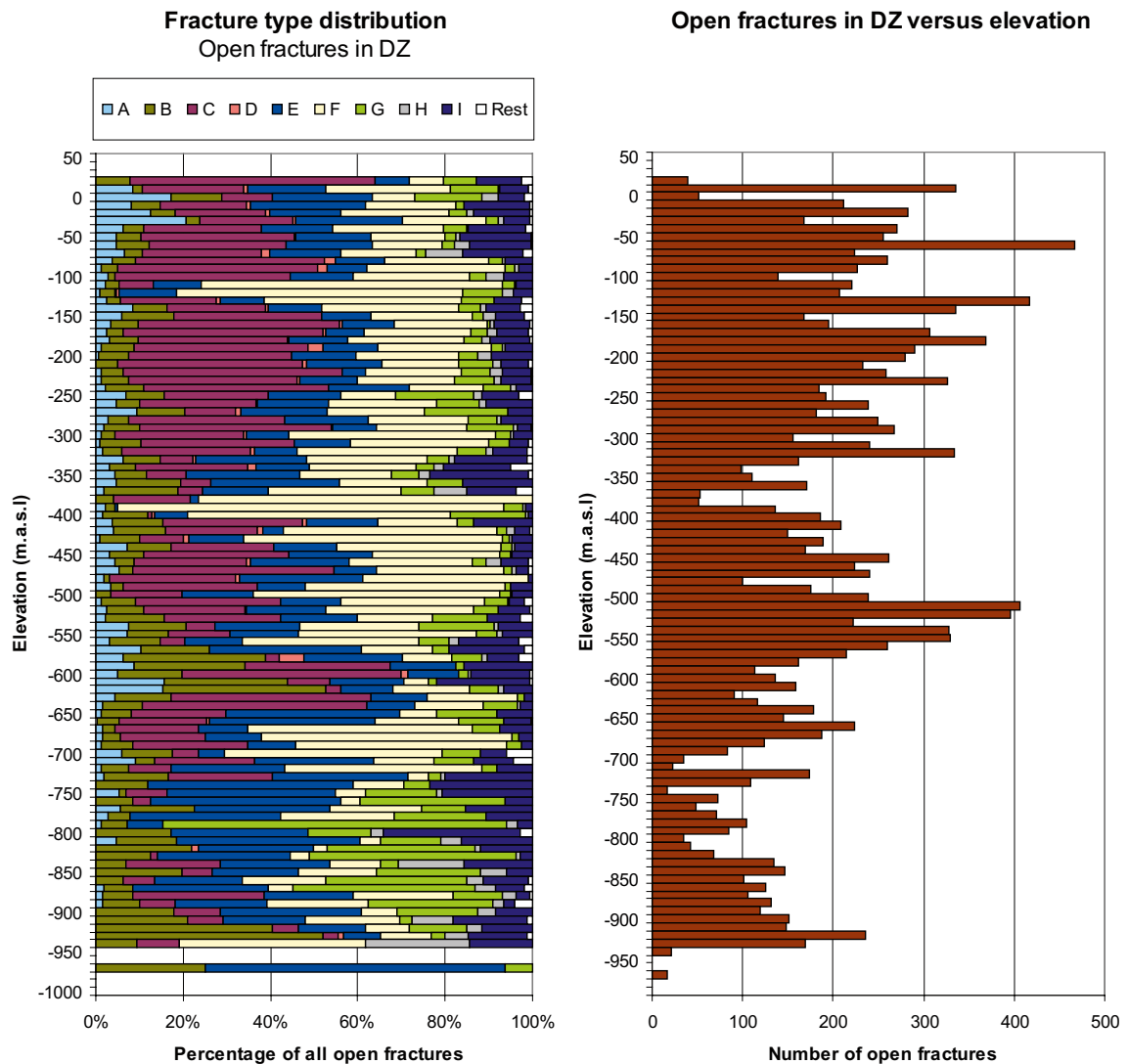
Figure 2-15. *Relative distribution of fracture types and fracture frequency (open fractures) within deformation zones. The right figure shows the number of open fractures within deformation zones at different elevations. The decreasing amount of fractures towards depth is mainly explained by less borehole metres at larger depths and should therefore not be regarded as a generally decreasing fracture frequency with depth.*

Hematite, i.e. fracture group C (hematite ± any mineral), is present in about 14% of the open fractures. According to single mineral statistics from /Drake and Tullborg 2009/ (Figure 2-8), the occurrence of hematite is slightly lower which probably is due to the fact that this data set does not includes fractures from Simpevarp.

The relative abundance of fracture type B (epidote/prehnite/adularia ± chlorite ±calcite ±quartz) is greater at depths below –800 m a s l. The reason for this is that younger fractures (≤ 450 Ma) are rare at greater depths. In addition, older epidote/prehnite/adularia filled fractures closer to the surface may have been reactivated and new fracture minerals may have precipitated.

Very few observations of open fractures containing laumontite filling (Fracture type D) and without visible fracture mineralization (Fracture type H) have been made. Furthermore, it has been suspected that the latter group actually has small amounts of fracture minerals; however, present in such low amounts that they can only be identified by using a microscope.

A comparison between the three rock domains covering most of the Laxemar local model volume show generally small differences (less than 5%) between the fracture types (Figure 2-13). However, some larger variations can be seen, especially for fracture type E (chlorite/calcite) and fracture type F (clay).
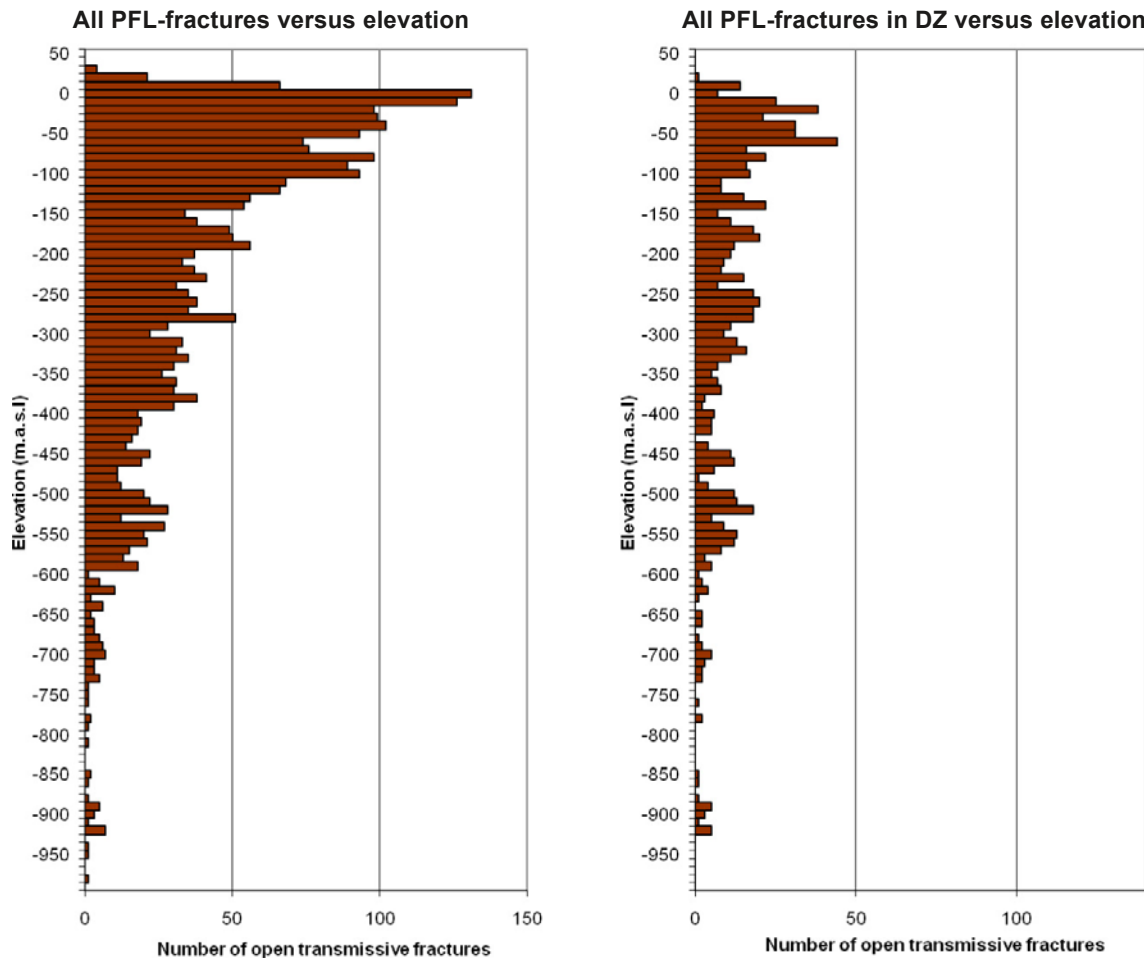
Figure 2-16. *The total number of open transmissive fractures versus elevation (to the left) compared to transmissive fractures solely inside deformation zones versus elevation (to the right). The decreasing amount of fractures towards depth is mainly explained by less borehole metres at larger depths and should therefore not be regarded as a generally decreasing fracture frequency with depth.*

An overview of the fracture mineralogy within the fracture domains (Figure 2-14) displays a similar pattern with relatively small variations in the fracture type distribution between the different fracture domains. The largest variations (although less than about 10%) are observed for fracture types C (hematite) and E (chlorite/calcite).

Fractures within deformation zones

The proportion of the fracture mineral types within deformation zones (Figure 2-15) is somewhat different compared to the overall fracture statistics described above. Most significant is the increased amount of hematite filled fractures (fracture type C) and the clay filled fractures (fracture type F) besides the decrease of chlorite and calcite filled fractures (fracture type E).

Transmissive fractures

For the retardation model, the hydraulically conductive parts of the rock are of greatest interest. Transmissive fractures are identified in parts of deformation zones, but deformation zones are not always found to be hydraulically conductive. In addition, single transmissive fractures appear in the rock matrix, between the deformation zones. Figure 2-16 compares the total number of transmissive fractures with the number of transmissive fractures within deformation zones and shows a relatively large number of transmissive fractures outside deformation zones.

The distribution of fracture types (Figure 2-17) in the transmissive fractures displays a small increase of fracture types A, F and I compared to the overall fracture type distribution (Figure 2-12), and a decrease of primarily fracture types B, C and G.
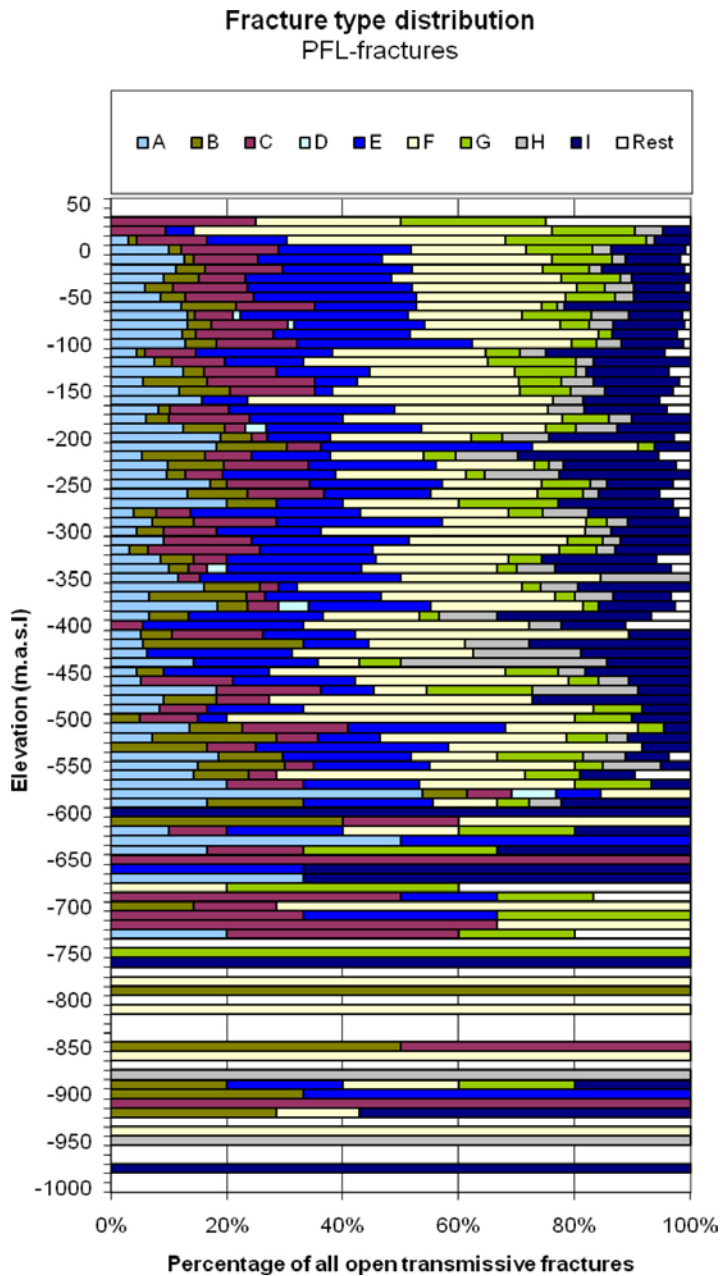
Figure 2-17. *Relative distribution of fracture types in open fractures with a detected flow anomaly. Note that the statistical basis below –600 m is poor.*

2.2.2 Deformation zone units

For the retardation model, five different segments of altered bedrock have been distinguished as recurrent units within (or close to) deformation zones (Table 2-5), besides the single fractures. These units represent both features which are commonly abundant in deformation zones as well as features that are not so common but nevertheless considered to may give significant contribution to the total retardation capacity of the deformation zones. The identification of these units was based on macroscopic observations of altered parts of the drilled rock cores during the initial phase of the rock sampling for the laboratory programme (cf. discussion in Section 1.2.2). Furthermore, the units can occur individually or together within a deformation zone.

Table 2-5. Identified segments of altered bedrock within deformation zones, further called zone units. Comparisons for retardation properties are done relative to typical intact rock.

1. **Fault rock/gouge (strongly tectonized and partly incohesive material).**

   Generally, altered rock fragment, mineralogy partially depending on host rock together with chlorite, saussurite and clay.

   Potential impact on retardation: Partly very fine-grained material which may have significantly increased surface areas available for adsorption. Increased porosity due to poor consolidation.

2. **Chlorite (green gouge, primarily close to mafic rock types).**
   Chlorite ± corrensite

   Potential impact on retardation: Partly very fine-grained material which may have significantly increased surface areas available for adsorption. Increased porosity due to poor consolidation.

3. **Porous episyenitic wall rock.**

   Secondary mineral formation of prehnite, adularia, calcite, laumontite, epidote and hematite ± quartz,

   Quartz dissolution as well as quartz redistribution occur.

   Potential impact on retardation: Presumably an increased sorption capacity where hematite precipitation occurs. Increased porosity in case of a net quartz dissolution

4. **Cataclasite (with mylonitic banding).** Altered rock fragments sealed with epidote, adularia, quartz, hematite ± laumontite in various portions.

   Potential impact on retardation: Increased porosity for cataclasite, increased amount of sealed fractures. Mylonitic banding may give decreased porosity with a directional dependency that may act as a barrier for diffusion.

5. **Oxidized (medium to strong alteration) wall rock.**

   Hydrothermally altered host rock, with a mineralogy related to initial rock type. Red staining due to small hematite grains, K-feldspar, saussurite, plagioclase, quartz, chlorite is common in granitic variants

   Potential impact on retardation: Contains micro grains of hematite which may have an impact on adsorption of radionuclides influenced by surface complexation. Enhanced porosity in altered plagioclase grains. Increased amount of micro fractures.

Summarizing the retardation properties of a deformation zone is a complicated process because of the heterogeneity. Most of the deformation zones have been reactivated during different geological events and display a wide spectrum of alteration types, brittle and ductile. As described earlier, a deformation zone is divided into transition zones and cores. A deformation zone might be intersected by several boreholes and yet, it appears in different ways in those intersections (Figure 2-4). The core and transition zone in the deformation zone may contain one or several of the five segments of altered bedrock presented in Table 2-5. In addition to this, the fracture frequency and fracture mineralogy varies as well. Concerning transport properties (sorption, porosity and diffusion), it might be a considerable diversity between these different segments, between the single fractures and finally the combination of all those in the deformation zone. A task during the retardation model work has been to specify how detailed the description and parameterization of deformation zones is required to be and how detailed it possibly can be done. In Figure 2-18 three different ways to deal with these questions are illustrated. In its simplest approach (a) retardation properties could be given to the zone in its entirety as an average of all the geological features involved in the deformation zone. A slightly more sophisticated model (b) could be to divide the deformation zone into high transmissive and low transmissive units and list retardation properties to the different units. The most complicated model (c) would be to besides that also include the different segments/parts of a zone (i.e. core and transition zones).
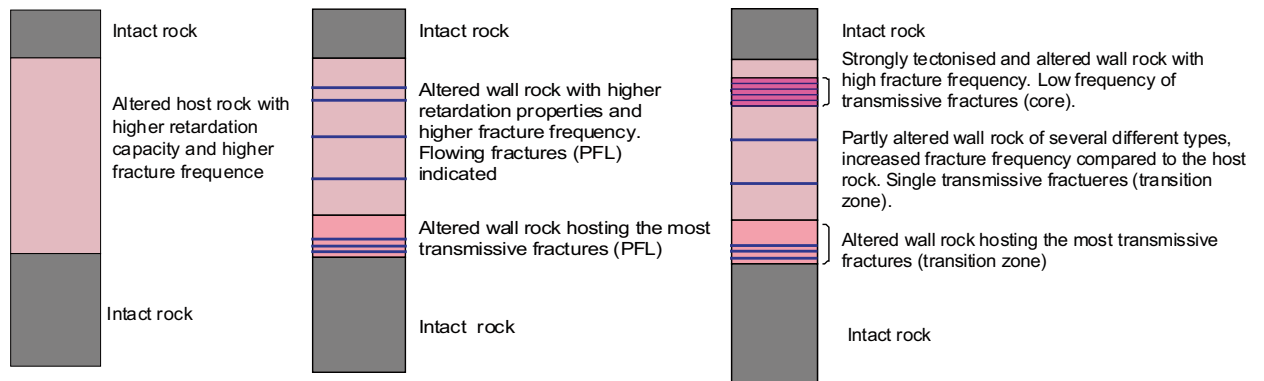
Figure 2-18. *Schematic illustration of alternative ways to describe a deformation zone with respect to retardation capacity a) the deformation zone considered as one unit with higher retardation capacity than the surrounding bedrock; b) the deformation zone divided into high and low transmissive units; c) variation including core and transition zone, the latter divided into a high and a low transmissive unit.*

The present report does not specify or give any recommendation of which of the three given alternatives that should be used for transport modelling but does only outline different ways to include retardation data to the deformation zones in the site description and/or performance assessment. Nevertheless, an example is given below where a parameterisation of the ZSMEW002A zone is done according to the (c) concept.

Of the mapped deformation zones at the Laxemar local model volume, special attention has been given to the deterministically identified ZSMEW002A, also called the Mederhult deformation zone. An attempt to describe the retardation properties for this zone has been performed. A possible methodology for this work is presented below.

1. Summarizing the information about the deformation zone;
   a) Obtain specific information from single hole interpretations (SHI) and extended single hole interpretations (ESHI).
   b) Recognition of open fracture frequency within the specific deformation zone using Boremap data and estimation of the mineralogical distribution of these fractures with the help of Single hole interpretations (SHI) and Boremap.
   c) Identification of transmissive fractures and/or parts of the deformation zone through PFL-f data (cf. Section 2.1.7).

2. Application of available transport laboratory data (porosity, diffusion and batch sorption) for the core and transition zone within the deformation zones; i.e. data from different fracture types and various types of altered bedrock.

According to /Viola and Venvik Ganerød 2007/ the general properties of the ZSMEW002A deformation zone can be summarized as consisting of narrow, highly fractured segments (cores) that enclose less fractured rock (transition) in a complex network. The fracture mineralogy is heterogeneous in the zone that intersects in different boreholes.

A simplified example from the parameterisation of ZSMEW002A as it appear in the intersection in borehole KLX06 (DZ2 in the ESHI) is presented in Figure 2-19. The heterogeneity of the zone is illustrated in this figure, including examples of the deformation zone units described in Table 2-5. The division into cores and transition zones in the figure has been performed in previous work by /Viola and Venvik Ganerød 2007/ but the zone has been considered wider in the single hole interpretation. The section contains a narrow zone of crushed rock and a distinct fault core containing brittle fault rocks that overprint a rather pervasive foliation. The fault core consists of pro-tomylonites, cataclasites and red gouge. The protomylonites are affected by later brittle deformation as suggested by the presence of mylonitic fragments in the crosscutting cataclasites. The transition zone consists of foliated granites with localized brittle-ductile deformation bands. The main fracture minerals in the zone are: chlorite, calcite, clay, hematite, pyrite, adularia, quartz, laumontite, epidote and fluorite. The distribution of the transmissive fractures is marked as well.
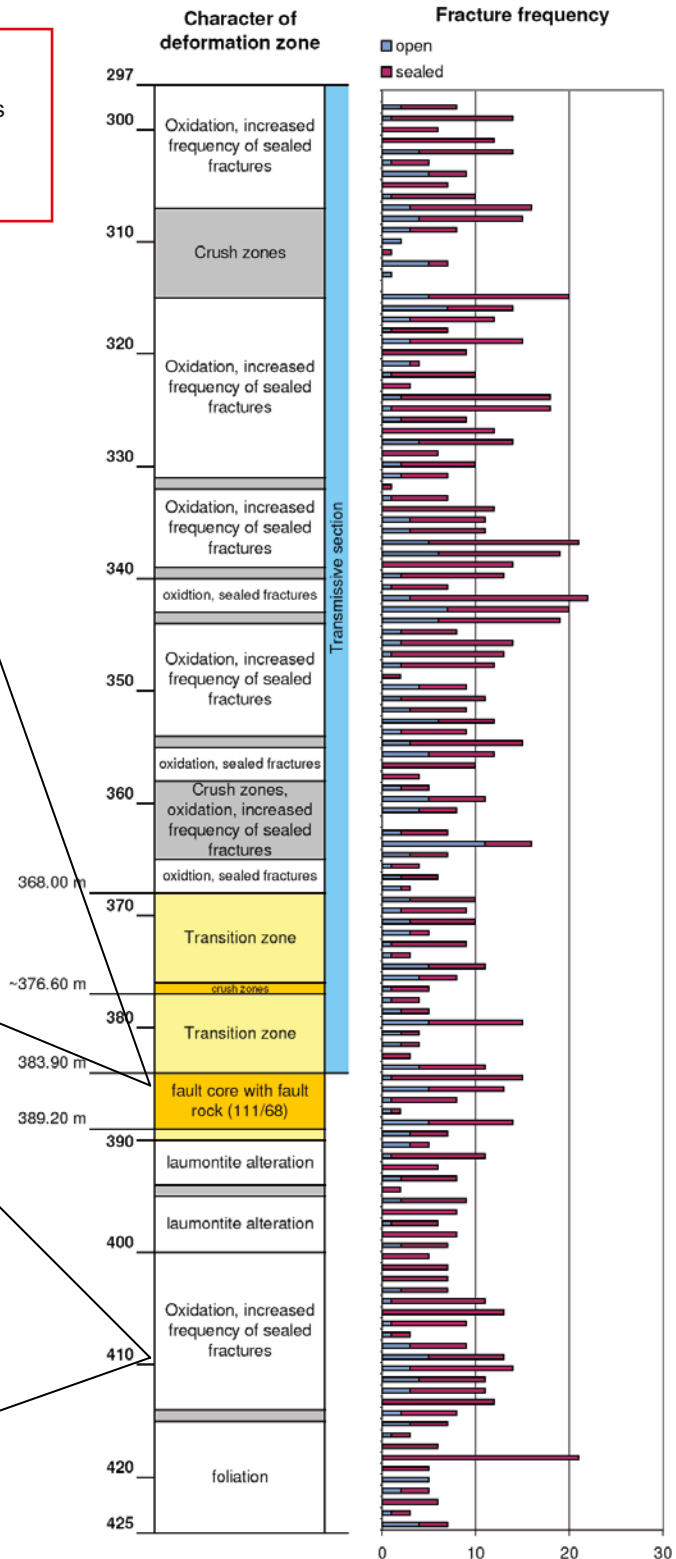
Figure 2-19. Schematic illustration of ZSMEW002A from the intersection in KLX06 (DZ2). Both sampled zone units and fracture frequencies (number of fractures per metres) of open and sealed fractures are shown. The zone core and transition zones are defined by /Viola and Venvik Ganerød 2007/(marked in yellow/orange), and the outer rim encountered in the zone definition in the SHI (marked in white/grey).

38

2.2.3 Hydrogeochemistry

Selected water types for laboratory measurements

For the laboratory measurements of transport properties it has been important to choose experiment waters that reflects the present water composition at repository depth but also to represent wider ranges of compositions that cover potential variations in groundwater compositions during the future phases of the potential repository. For the batch sorption measurements especially, the water chemistry plays an important role and five different groundwater compositions have therefore been selected for use in the laboratory experiments:

I. **Fresh diluted Ca-HCO₃ water;** Fresh groundwater now present in the upper –100 metres of the bedrock, but also a water type that can be found at larger depths during late phases of glacial periods. In Laxemar the fresh water is dominantly of Na-HCO₃ type. This water type corresponds to the Fresh water described in Section 2.1.8.

II. **Brackish groundwater with marine character, Na-(Ca)-Mg-Cl (5,000 mg/L Cl);** This water type has been found at depth around 100 to 400 metres in a few boreholes mainly at Äspö and beneath the Baltic Sea. It is comparable with the Brackish Marine water type in Section 2.1.8.

III. **Brackish groundwater of dominantly non-marine origin Na-Ca-Cl type (5,400 mg/L Cl);** this is a water with higher Ca and lower Mg compared to the Type II water. This water type is presently found at Laxemar at depth below 450 to 650 metres depending on location. Compared to the water types described in Section 2.1.8, this is a mix of Brackish Non-marine and Marine water and referred to as "Transition type" waters.

IV. **Brine type water of very high salinity, Ca-Na-Cl type water with Cl content of 45,000 mg/L;** during a glacial period, brine type waters can be forced to more shallow levels than at present (1,500 m depth). The water type corresponds to the Highly saline water in Section 2.1.8.

After the first part of the Site investigations at Simpevarp/Laxemar, which means also after the execution of the first part of the Transport programme it was evident that the picture of the groundwater situation at Laxemar with dilute water prevailing down to 1,000 m depth followed by an abrupt change to very saline water was an over-simplification not valid for the area. Therefore a fifth water type was included in the laboratory experiments (batch sorption):

V. **Brackish water of non-marine Na-Ca-Cl type (2,000 mg/L Cl).** This water has lower salinity than groundwaters of type II and III. This water type is common in the Laxemar subarea at repository depth. Corresponding water type in Section 2.1.8 is Brackish Glacial.

In all experiments done, synthetically prepared groundwaters were used; naturally sampled groundwater were avoided due to the risk of oxidation and colloid formation because of difficulties to maintain natural reducing conditions during the sampling procedure.

Especially for the batch sorption measurements, the chemical composition of the groundwater is expected to play an important role and attempts were therefore made to mimic the exact chemical composition of these groundwaters. However, for the diffusivity measurements in the laboratory programme, tritiated water (H³HO) was the only tracer used and the demand of addressing the groundwater composition in these experiments was not considered necessary. Consequently, a water composition of Type II was chosen for the through-diffusion experiment and only the major components, Ca^{2+}, Na^+, Cl^- and SO_4^{2-}, were included in the synthetic groundwater used in the diffusion experiments. The compositions of the groundwater types I–V are specified in Table 2-6 below, referring to specific sampling intervals (expressed in meter borehole length) in the boreholes.

Table 2-6. Chemical composition of the groundwater types used in the diffusivity and sorption measurements for the Simpevarp and Laxemar subareas. Data is based on water samples at specific boreholes and borehole lengths (in brackets). Concentrations are given in mg/L.

	Type I (HSH02 0–200 mbl)	Type II (KFM02A 509–516 mbl)	Type III (KSH01A 558–565 mbl	Type IV (KLX02 1383–1392 mbl)	Type V (KLX04 510–515 mbl)
	Fresh water	Brackish groundwater with marine character	Present ground-water at repository level	Brine type water of very high salinity	Brackish groundwater of non-marine character
Li^+	1.60E-2	5.10E-2	5.80E-1	4.85E+0	1.52E-2
Na^+	1.27E+2	2.12E+3	3.23E+3	7.45E+3	6.91E+2
K^+	2.16E+0	3.33E+1	1.24E+1	3.26E+1	3.19E+0
Rb^+	(2.52E-2)[A]	6.28E-2	4.24E-2	1.78E-1	4.24E-2
Cs^+	(1.17E-3)[A]	1.79E-3	1.37E-3	1.86E-2	1.37E-3
NH^{4+}	(9.47E-2)[A]	4.00E-2	4.00E-2	5.60E-1	3.19E-2
Mg^{2+}	1.43E+0	2.32E+2	4.47E+1	1.20E+0	6.9E+0
Ca^{2+}	5.21E+0	9.34E+2	2.19E+3	1.48E+4	2.34E+2
Sr^{2+}	6.95E-2	7.95E+0	3.23E+1	2.53E+2	4.67E+0
Ba^{2+}	(1.29E+0)[A]	1.88E-1	1.88E-1	2.40E-2	1.88E-1
Fe^{2+}	(3.64E-1)[C]	1.20E+0	6.86E-1	3.45E+0	9.00E-2
Mn^{2+}	2.00E-2	2.12E+0	4.60E-1	1.11E+0	1.09E-1
F^-	3.03E+0	9.00E-1	9.67E-1	(1.60E+0)[D]	2.7E+0
Cl^-	2.15E+1	5.15E+3	8.80E+3	3.68E+4	1.48E+3
Br^-	(2.00E-1)[B]	2.20E+1	7.10E+1	5.09E+2	1.34E+1
SO_4^{2-}	8.56E+0	5.10E+2	2.21E+2	1.21E+3	1.04E+2
$Si(tot)$	6.56E+0	5.20E+0	4.70E+0	2.60E+0	6.63E+0
HCO_3^-	2.52E+2	1.24E+2	1.20E+1	4.20E+1	5.14E+1
S^{2-}	(1.00E-2)[B]	5.00E-2	5.00E-2	5.00E-2	6.00E-3
pH	8.58	7.1	7.45	6.8	7.83

A) No measurements available, data imported from comparable water sample; KSH01 156–167 mbl.

B) Based on detection limit.

C) Based on the Fe-tot measurement.

D) No measurements available, data imported from comparable water sample; KLX02 1,420–1,705 mbl.

2.3 Data from the laboratory programme

Laboratory investigations within the Transport programme are proposed to give site-specific porosity, sorption and diffusion properties for different rock materials. Rock core samples for these measurements were selected, in accordance with /Widestrand et al. 2003/, from a large number of the cored boreholes at Laxemar-Simpevarp. However, since the laboratory measurements of diffusion and sorption are very time consuming, a large part of the rock samples were collected from early cored boreholes, i.e. KSH01, KSH02, KLX02 and KLX04. The improved knowledge of the Laxemar local model volume later influenced the rock sampling by including additional boreholes in the sample collection. Eventually the total sample collection consists of about 400 rock samples from fourteen boreholes (Figure 2-20). The sample collection has been found to be representative for the target volume although it has not been possible to include all different fracture types in the laboratory measurements (discussed below).

In order to describe the heterogeneity of the retardation parameters and the possible effects of stress release, rock samples were selected from various depths in the boreholes. For instance, in KSH01A, KSH02 and KLX02 samples were taken every 20 metres. Features as major rock types as well as the minor rock types, various fracture types and altered rocks of different style and degree in deformation zones are represented in the sample collection. The selection of rock types has been controlled by available geological descriptions at the current time performed by the Geology programme.

The selection of samples from open fractures was controlled by the indications of water flow, as recorded in flow logs, when available and with support from hydrogeological and hydrogeochemical expertise. Another parameter that influenced on the fracture type sampling was the accessibility
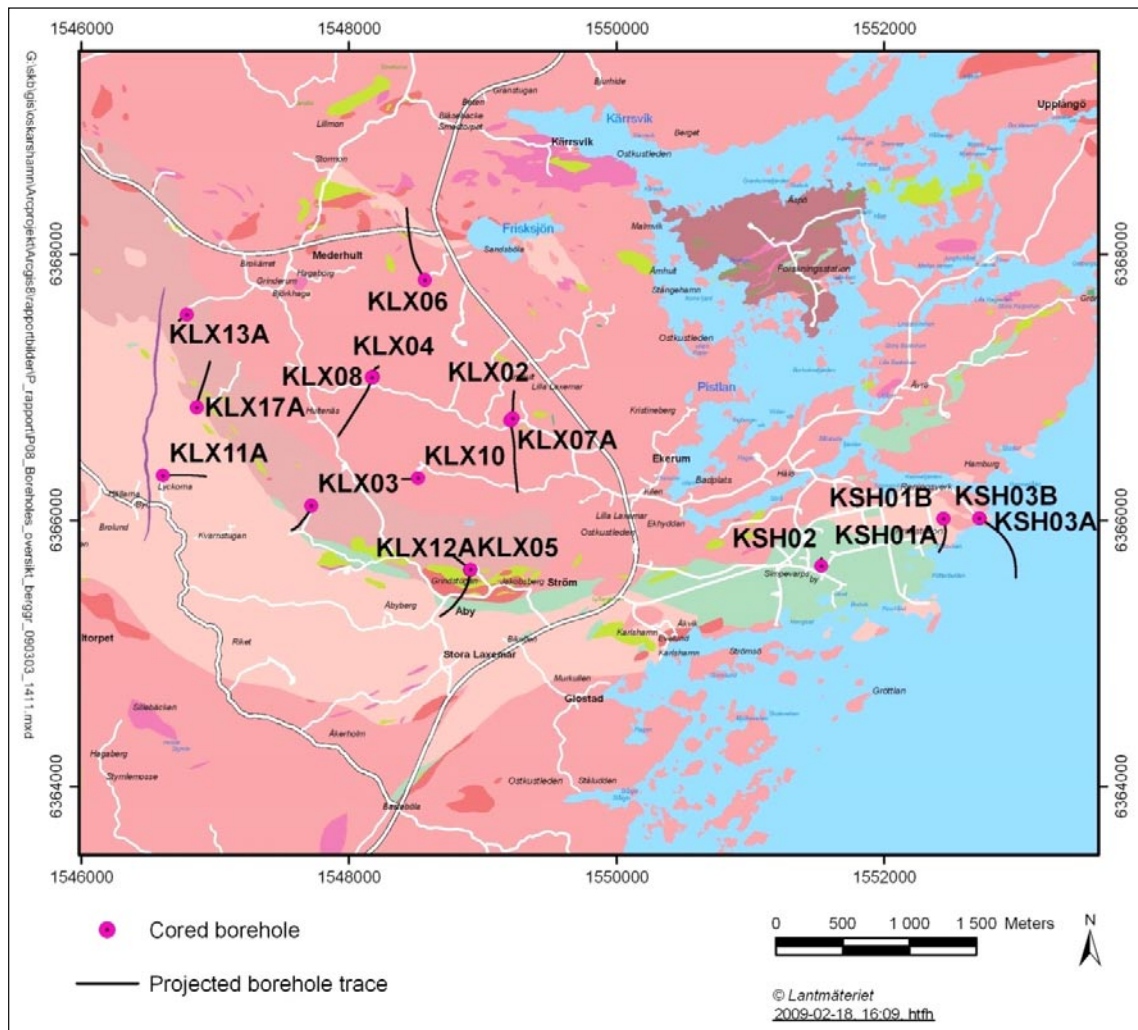
Figure 2-20. *The cored boreholes at the Laxemar-Simpevarp area included in the sample collection for the laboratory measurements of porosity, sorption and diffusion.*

of sufficient amount of loose fracture filling material for the laboratory experiments, e.g. sorption measurements require a minimum of about 0.5 g of fracture filling material for a single batch experiment only (i.e. one tracer and one water type without duplicate or triplicate). For some fracture types e.g. Fracture type I (Calcite ± other), it was therefore not possible to collect material at all.

For deformation zone units, rock alteration, in addition to the water flow were the controlling parameters for the sampling. The purpose of the deformation zone unit sampling was to identify segments of altered rock within deformation zones that might reflect divergent characteristics than the intact rock with respect to porosity, diffusion and sorption. A summary of the available transport laboratory data are found in Table 2-7, the detailed description of the measurements together with the results are presented in /Selnert et al. 2009/. Note that the numbers given in Table 2-7 reflect the data obtained in the different measurements and not the originally collected number of rock samples. One original rock sample with e.g. sample-ID KLX04_482.00–482.10, may have been further subdivided in several of the methods presented below. Thus, the number of data exceeds the number of rock samples.

Table 2-7. Rock sample data included in the retardation model; i.e. the number of measurements for the respective method used in the laboratory investigations.

Method	Total number of measurements	Number of rock type measurements	Number of fracture type measurements	Number of measure-ments from deforma-tion zone units
Porosity	333	324	0	9
PMMA	3	0	1	2
Electric resistivity	42	42	0	0
Through diffusion	90	84	0	6
BET (crushed rock)	197	154	26	17
CEC	15	9	5	1
Batch sorption (crushed rock)	436	263	85	88

3 Analyses and evaluation of Transport data

This chapter deals with the task of identifying retardation data (i.e. porosities, diffusivities and sorption coefficients) for the different geological features (i.e. rock types, fracture types and deformation zone units) identified in Chapter 2. The primary source for the data is the report of the Transport laboratory programme /Selnert et al. 2009/ and for all data used in this chapter, it is referred to that report unless stated otherwise.

3.1 General model

In this chapter, the data used (site-specific and/or imported from other works) for establishing the retardation models are described. According to the basic conceptual model for radionuclide retardation, Section 1.2.1, the considered retardation processes can be described as:

A. Adsorption on surfaces of materials present in or at the fracture walls, which are considered to be directly accessible (no significant diffusion needed) during the transport. These fracture surface reactions are considered to be independent of the flow rate and the residence time in the fracture, and can thus be simply described by an equilibrium surface sorption coefficient, K_a (m). The retardation obtained by this process can be described by a retardation factor, R_f, defined as:

$$R_f = 1 + \frac{2K_a}{b} \qquad \text{(Eq 3-1)}$$

where b is the aperture of the fracture.

B. Diffusion into the rock matrix and a potential adsorption on the inner surfaces of the rock material. This process is dependent on the following parameters:

a. The amount of inner volume (pores) in the rock matrix that is available for diffusion, i.e. the porosity, θ_m (-).
b. The rate at which the radionuclide diffuses in the rock matrix, i.e. the effective diffusivity, D_e (m^2/s).
c. The partitioning coefficient describing the distribution of the radionuclide between the inner surfaces of the pores and the water volume of the pores, K_d (m^3/kg).

In the time perspective relevant for storage of nuclear waste, the A process can often be neglected compared to the B process. However, the pure surface retardation process can have an effect on the early arrival of tracers in fast flow paths and should therefore also be considered.

3.2 Uncertainty of data and statistical representation

Concerning the data for the retardation parameters given to be used in the retardation model, an important issue is the uncertainty and how it should be addressed in this work. One can roughly divide the uncertainty into two parts:

1. Uncertainty of the qualitative sub-division of the geological units used in the retardation model, i.e. the judgement made and described in Chapter 2 in this report. These types of uncertainties cannot be based on quantitative estimations and are therefore difficult to present in numbers. This must therefore be acknowledged as an underlying conceptual uncertainty.

2. Uncertainty in the numerical values of the experimentally measured retardation parameters.

In this chapter where the transport data are analysed, the latter uncertainty is addressed. One can easily foresee that with the large number of identified geological units the variation and/or uncertainty of the numerical parameters presented will be important.

An important underlying issue concerning the sampling and investigation of the rock material has been to identify possible extremes, i.e. material with strong deviations from the average values of the different transport properties, e.g. porosity, diffusivity and sorption capacity. This material has almost exclusively been sampled from deformation zones. The rationale behind this sampling

strategy is obvious; it is necessary to obtain an identification of specific flow paths in any geologic medium that significantly could contribute to a fast spreading of any dispersed radionuclide. However, from this perspective, one may argue that a general uncertainty has been introduced since a general overrepresentation of different deformation zone material compared to its actual occurrence in the rock volume is introduced.

Contrary to the earlier version of the retardation model /Byegård et al. 2006/ the uncertainty of the different retardation parameters will be given using an approach consisting of:

- In the cases where 3 or more measurements have been made of a single parameter, the measurement is presented giving the average, the standard deviation (1σ confidence level), median together with the minimum and maximum values of the measurements.

- In the cases where only 2 measurements are available, these are reported as the minimum and maximum values available.

- In the cases where only a single measurement is available, uncertainty is (where appropriate) presented using the estimation of the uncertainty in a single measurement. For example, the uncertainty of the sorption coefficients are based on the counting statistics uncertainty in the radioactivity measurements and for the cation exchange capacity (CEC) measurements, the uncertainty is based on the general uncertainty in the ICP-AES measurement of Mg^{2+}.

The comparatively large variation for some of the parameters causes that the standard deviation in some cases will be larger than the average, which strictly conceptually would involve acceptance of negative values. This is, of course, not the case and the minimum value presented should in these cases be considered as the realistic lower limit of the interval of this parameter value.

One has to acknowledge, however, that a considerable part of the uncertainty involved with a retardation model of this kind is due to the different geological and hydrogeological classifications on which the retardation model relies. Examples of such classifications are:

- Fracture type classification
- Groundwater type classifications

The strict identification of such groups used in this model is certainly a simplification; a large range of intermediates between the different groups do most probably exist. The uncertainty caused by such most probably rather subjective decisions are difficult to address in quantitative terms but, nevertheless, has to be acknowledged as an underlying qualitative uncertainty.

Furthermore, the question of to which extent the observations made from a relatively few number of boreholes give a good representation of the whole rock mass is certainly another source of qualitative uncertainty which is difficult to address in quantitative numbers.

3.3 Porosity

3.3.1 Methods

Porosity, in this context, refers to the volume of the rock that is filled with water and available for diffusion. With the concept used in this work, the porosity in the micro scale is considered to be homogeneously distributed in the rock matrix.

The porosity data used in the site descriptive transport modelling has mainly been obtained from measurements done on rock samples intended for diffusion and sorption studies. The method used for determination /SS-EN 1936/ involves drying of the rock sample, followed by water saturation in vacuum. The drying of the samples is done at a temperature of 70° C, which differs from the temperature (105° C) used in the method for porosity measurements in the geology programme of the site investigation. The reason for this is that the samples in the transport programme are designated for other laboratory investigations afterwards. For the interpretation of these laboratory investigations (diffusion and sorption measurements), it is important to avoid the extra chemical and mechanical degradation of the samples that could result from the higher drying temperature. The measurement uncertainty of a single porosity value determined by the water saturation method is 0.05 vol-%, given with 1σ confidence.

Estimations of the porosity for the deformation zone units have, due to its general heterogeneity combined with problems with consolidation, been shown to be complicated. For this reason, the

mainly used technique for porosity measurement (water saturation) has been complemented using PMMA-impregnation measurements /Penttinen et al. 2006/ from which spatial location as well as porosity distribution information was available.

3.3.2 Results and analysis

Major rock types

The results of the porosity measurements are summarized in Table 3-1. In the material used, measurements on drill core samples with lengths of 0.5–5 cm are included, however the majority of the samples are of 3 cm length (288 of the 324 samples used for the summary of the porosity results, given in Table 3-1).

The porosity range is in the interval of 0.1% to 0.5% for the majority of the samples as can be seen in Figure 3-1. Generally, the more fine- to medium-grained rock types (e.g. 501030, 505102, 501036 and 511058) have lower porosities than the medium- to coarse-grained or porphyritic rock types (e.g. 501046 and 501056).

The porosity for different sample thicknesses is presented in Figure 3-2. A slight increase in porosity was indicated for the 0.5 and 1 cm sizes relative to the porosity of the 3 cm size. The effect of including shorter sample sizes in the total results for a rock type is therefore small, especially when considering that the shorter samples are less than 15% of the total amount of samples. Increased porosity in shorter samples can be caused by e.g. a larger contribution of sawing induced porosity and/or a too small sample size relative to the mineral grain size.

Figure 3-3 shows porosity as a function of the sampled borehole length for the major rock types. No clear dependency of porosity with borehole length can be observed which indicates that no dependency with depth (e.g. increased stress release during the sampling process) is observed either. One should be aware of that the sampled borehole length does (due to the borehole inclination) not exactly correspond to the elevation of the sample.

A division of the samples has also been made with respect to their respective location, i.e. whether they originate from deformation zones or not. The results (cf. Table 3-1) indicate that this gives practically no difference in the average values of the respective porosity. This may seem surprising, but it can be explained by the presence of large parts of undeformed rock within the defined volumes of the deformation zones (cf. discussion in Section 2.1.3). It is thus important to note that the rock within a deformation zone not necessarily is deformed and that the division based on sample location therefore may give a poor indication of the impact of sample deformation. The quartz monzodiorite (501036) is the only rock type that shows a clearly increased porosity in samples from deformation zones which is due to the observed alteration of 8 of these 10 samples (cf. Table 3-2).

The detailed geological characterisation performed using a binocular microscope has shown several samples having small micro fractures that are 3–15 mm in length and with a width of up to 0.5 mm, in both fresh and altered rock samples /Selnert et al. 2009/. These fractures are thus larger than intragranular micro fractures, and cut right through mineral grains. Comparison of the porosities determined for samples with and without having observable micro fractures (cf. Table 3-1, 501030 and 501056 for the rock types with largest number of micro fracture containing samples), indicates that the presence of micro fractures increase the porosity.

A further division has been performed in which the visible alteration of the samples has been used as a parameter for the porosity interpretation. The results (Table 3-2, e.g. 501030, 501036, 501046 and 501056 samples outside deformation zones) indicate that the porosities of the altered samples, both inside and outside of deformation zones, are higher than the samples without strong or medium alteration. An exception is the Ävrö granodiorite (501056) samples inside deformation zones, where the opposite is observed. However, the visual judgement of alteration is more subjective and difficult for the naturally red-coloured rock types compared to the more greyish rock types. A closer look at the samples in the group "without observation of medium to strong alteration" show that it contains three high porosity samples that were classified as "weak to medium alteration" (these three samples contain sealed fractures and micro fractures in one case). Hence, the uncertainty in the visual judgements of alteration should be acknowledged which affects the basis for the conclusions of the impact of alteration on porosity.

The combined effect of alteration and micro fracturing is exemplified in Figure 3-4, where the fine-grained dioritoid was sorted in groups of less altered/unfractured (no micro fractures and no or faint

45

Table 3-1. Porosities (vol-%) of different rock types from the Laxemar-Simpevarp areas, the median min and max values from the numbers (N) of samples involved in the study. The division of samples in inside or outside deformation zones is based on the extended single hole interpretation. This division only defines if the sample is located within a deformation zone or not, it does not mean that a specific sample necessarily is altered or not. Average is the arithmetic mean value, σ is the standard deviation of the samples and N is the number of samples.

Rock type (SKB code)	Inside or outside def. zone	All rock samples						Rock samples without visible open micro fractures						Rock samples with visible open micro fractures					
		Median	Min	Max	Average	σ	N	Median	Min	Max	Average	σ	N	Median	Min	Max	Average	σ	N
Fine-grained dioritoid (501030)	Outside	0.15	0.00	1.49	0.23	0.26	76	0.12	0.00	1.49	0.19	0.22	59	0.21	0.08	1.33	0.36	0.33	17
	Inside	0.12	0.04	0.75	0.19	0.19	18	0.09	0.04	0.41	0.13	0.11	13	0.31	0.07	0.75	0.35	0.26	5
Diorite to gabbro (501033)	Outside	-	0.05	0.06	0.06	-	2	-	0.05	0.06	0.06	-	2	-	-	-	-	-	0
	Inside	-	-	-	-	-	0	-	-	-	-	-	0	-	-	-	-	-	0
Quartz monzodior- ite (501036)	Outside	0.13	0.00	1.32	0.19	0.19	61	0.13	0.00	1.32	0.19	0.19	59		0.12	0.47	0.30	-	2
	Inside	0.77	0.17	1.59	0.75	0.40	10	0.78	0.17	1.59	0.78	0.41	9	0.45	-	-	-	-	1
Ävrö quartz mon- zodiorite (501046)	Outside	0.40	0.05	0.60	0.35	0.14	28	0.40	0.05	0.60	0.35	0.14	26	-	0.15	0.58	0.37	-	2
	Inside	0.36	0.25	1.45	0.63	0.52	6	0.28	0.25	0.42	0.31	0.08	4	-	1.12	1.45	1.29	-	2
Ävrö granodiorite (501056)	Outside	0.28	0.13	0.99	0.31	0.15	60	0.26	0.13	0.80	0.30	0.12	54	0.38	0.30	0.99	0.47	0.26	6
	Inside	0.36	0.15	0.89	0.40	0.20	19	0.35	0.15	0.89	0.39	0.20	18	0.63	-	-	-	-	1
Granite (501058)	Outside	-	0.38	0.84	0.61	-	2	-	0.38	0.84	0.61	-	2	-	-	-	-	-	0
	Inside	0.76	-	-	-	-	1	0.76	-	-	-	-	1	-	-	-	-	-	0
Pegmatite (501061)	Outside	0.02	-	-	-	-	1	-	-	-	-	-	0	-	-	-	0.02	-	1
	Inside	-	-	-	-	-	0	-	-	-	-	-	0	-	-	-	-	-	0
Fine-grained diorite-gabbro (505102)	Outside	0.18	0.03	0.21	0.15	0.07	6	0.18	0.03	0.21	0.15	0.07	6	-	-	-	-	-	0
	Inside	0.33	0.05	1.15	0.46	0.50	4	0.33	0.05	1.15	0.46	0.50	4	-	-	-	-	-	0
Fine-grained granite (511058)	Outside	0.24	0.07	1.15	0.27	0.19	26	0.24	0.07	0.40	0.23	0.07	23	0.20	0.20	1.15	0.52	0.55	3
	Inside	0.14	0.05	0.25	0.15	0.08	4	0.16	0.13	0.25	0.18	0.07	3	0.05	-	-	-	-	1
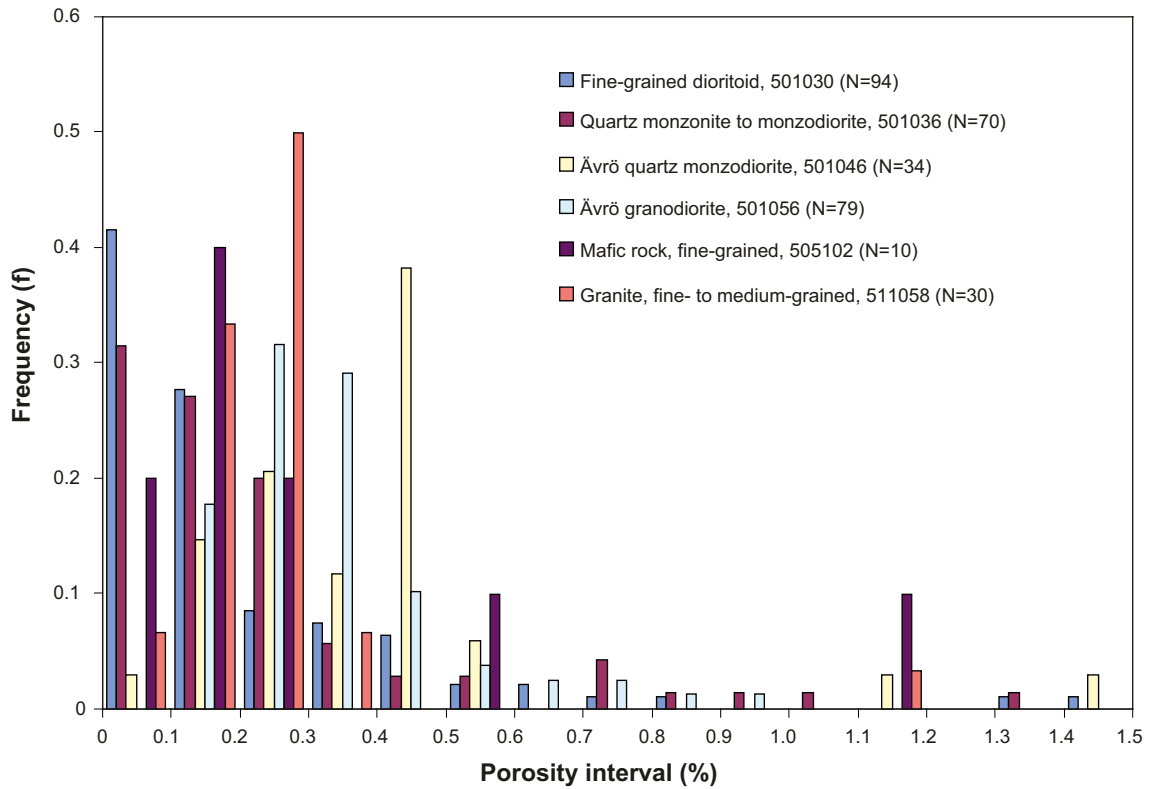
Figure 3-1. *Porosity frequency of rock types for all rock type samples from Laxemar and Simpevarp subareas. The frequency is normalised by the total number of samples (N) for each rock type and represents the fraction of observations in each 0.1% interval (e.g. the frequency for 511058 is about 0.5 in the 0.2 to 0.3% interval).*
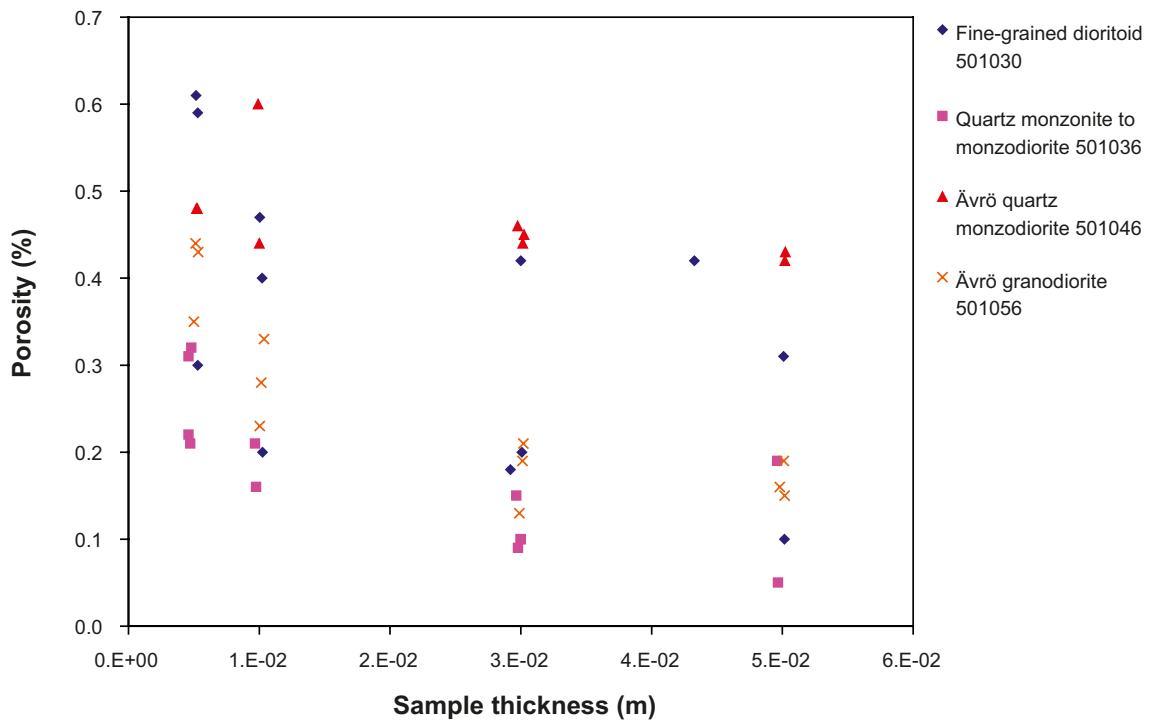
Figure 3-2. *Porosity versus sample thickness for major rock types. One relatively homogeneous sample of about 30 cm core length for each rock type was cut into sub-samples of 0.5, 1, 3 and 5 cm sizes.*
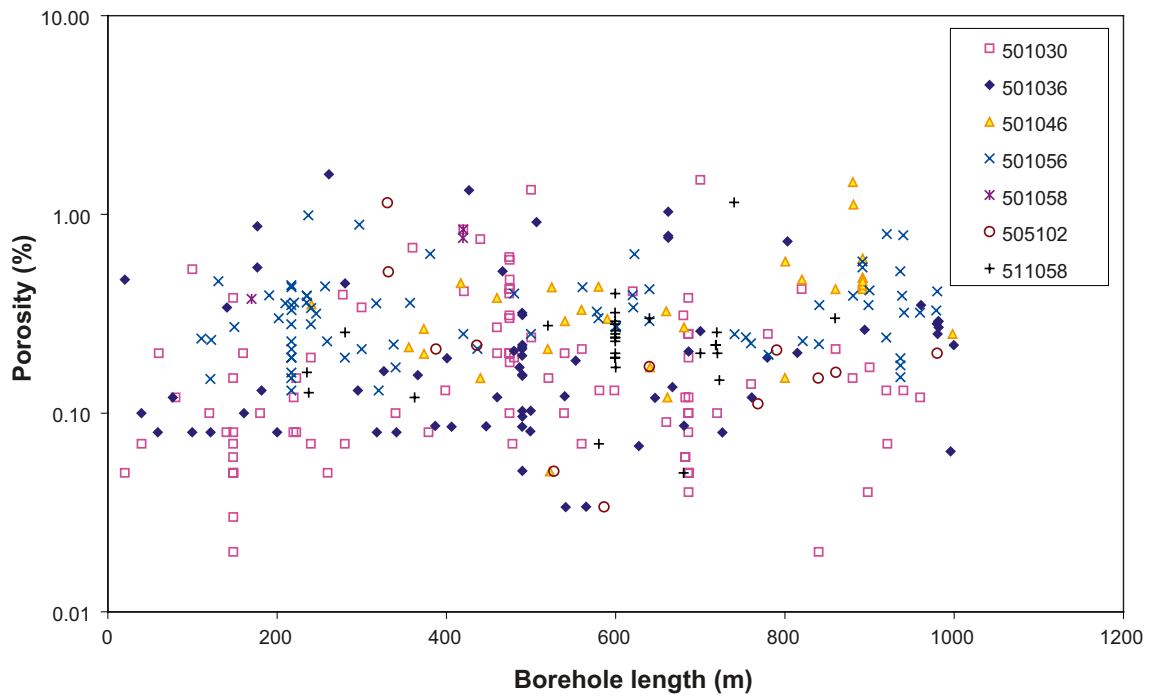
Figure 3-3. *Porosity as a function of borehole length for all rock type samples from Laxemar and Simpevarp subareas.*
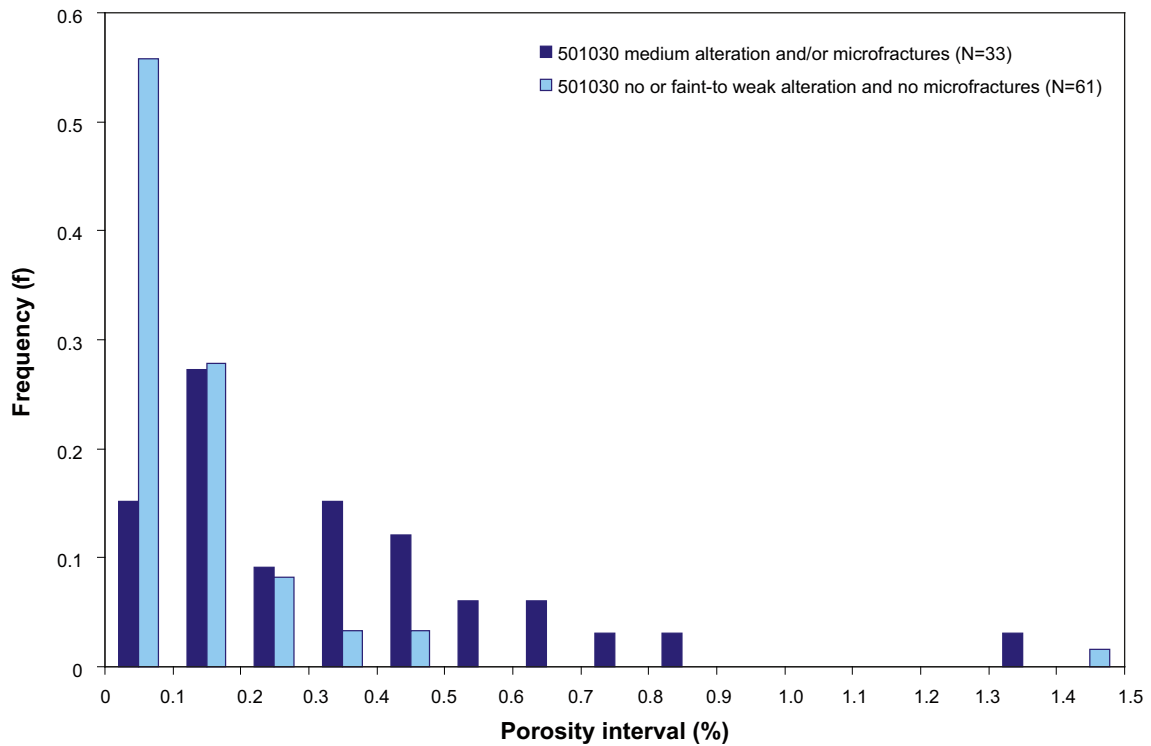
Figure 3-4. *Porosity frequency of 501030 samples sorted in a group with medium alteration and/or micro fractures (dark blue) and a group with no or faint to weak alteration and no micro fractures (light blue). The frequency is normalised by the total number of samples (N) for each rock type and represents the fraction of observations in each 0.1% interval.*

48

Table 3-2. Porosities (vol-%) of some different rock types from the Laxemar and Simevarp areas based on the alteration of the samples. The alteration analyses based on the binocular inspection of the individual drill core samples. The division of samples in inside or outside deformation zones is based on the extended single hole interpretation. This division outside/inside deformation zone only defines if the sample is located within a deformation zone or not. Average is the arithmetic mean value, σ is the standard deviation of the samples and N is the number of samples.

Rock type (SKB code)	Outside/Inside deformation zone		Median	min	max	Ave-rage	σ	N
Fine-grained dioritoid (501030)	Outside	All samples	0.15	0.00	1.49	0.23	0.26	76
		Samples with observation of medium or strong alteration	0.84	0.21	1.33	0.79	0.56	3
		Samples without observation of medium or strong alteration	0.13	0.00	1.49	0.20	0.22	73
	Inside	All samples	0.12	0.04	0.75	0.19	0.19	18
		Samples with observation of medium or strong alteration	-	0.19	0.75	0.47	-	2
		Samples without observation of medium or strong alteration	0.11	0.04	0.41	0.16	0.13	16
Quartz monzodiorite (501036)	Outside	All samples	0.13	0.00	1.32	0.19	0.19	61
		Samples with observation of medium or strong alteration	-	-	-	-	-	0
		Samples without observation of medium or strong alteration	0.13	0.00	1.32	0.19	0.19	61
	Inside	All samples	0.77	0.17	1.59	0.75	0.40	10
		Samples with observation of medium or strong alteration	0.83	0.45	1.59	0.87	0.35	8
		Samples without observation of medium or strong alteration	-	0.17	0.34	0.25	-	2
Ävrö quartz monzodiorite (501046)	Outside	All samples	0.40	0.05	0.60	0.35	0.14	28
		Samples with observation of medium or strong alteration	0.15	-	-	-	-	1
		Samples without observation of medium or strong alteration	0.42	0.05	0.60	0.36	0.14	27
	Inside	All samples	0.36	0.25	1.45	0.63	0.52	6
		Samples with observation of medium or strong alteration	1.12	0.25	1.45	0.94	0.62	3
		Samples without observation of medium or strong alteration	0.29	0.13	0.42	0.33	0.08	3
Ävrö granodiorite (501056)	Outside	All samples	0.28	0.13	0.99	0.31	0.15	60
		Samples with observation of medium or strong alteration	0.39	0.23	0.99	0.55	0.33	5
		Samples without observation of medium or strong alteration	0.27	0.13	0.58	0.29	0.10	55
	Inside	All samples	0.36	0.15	0.89	0.40	0.20	19
		Samples with observation of medium or strong alteration	0.25	0.15	0.79	0.36	0.25	6
		Samples without observation of medium or strong alteration	0.36	0.22	0.89	0.43	0.18	13

Rock type (SKB code)	Outside/Inside deformation zone		Median	min	max	Ave-rage	σ	N
Fine-grained diorite-gabbro (505102)	Outside	All samples	0.18	0.03	0.21	0.15	0.07	6
		Samples with observation of medium or strong alteration	-	-	-	-	-	0
		Samples without observation of medium or strong alteration	0.18	0.03	0.21	0.15	0.07	6
	Inside	All samples	0.33	0.05	1.15	0.46	0.50	4
		Samples with observation of medium or strong alteration	-	-	-	-	-	0
		Samples without observation of medium or strong alteration	0.33	0.05	1.15	0.46	0.50	4
Granite (511058)	Outside	All samples	0.24	0.07	1.15	0.27	0.19	26
		Samples with observation of medium or strong alteration	-	0.12	1.15	0.64	-	2
		Samples without observation of medium or strong alteration	0.24	0.07	0.40	0.24	0.07	24
	Inside	All samples	0.14	0.05	0.25	0.15	0.08	4
		Samples with observation of medium or strong alteration	-	-	-	-	-	0
		Samples without observation of medium or strong alteration	0.14	0.05	0.25	0.15	0.08	4

to weak alteration) and more altered/fractured (containing micro fractures and/or medium to strong alteration) samples. For the lower porosity range, unaltered samples are in majority while for the porosities above 0.4% the majority of the samples are in the altered or micro fractured group.

According to /Wahlgren et al. 2006/, there is a difference in tectonic influence and in the degree of deformation with relatively more deformation on Simpevarp than on Laxemar. Higher fracture frequencies and more developed alteration of the bedrock is found on the Simpevarp side of the NE trending set of regional deformation zones that intersects the area. Since approximately half of the porosity data in the transport programme are sampled in the Simpevarp subarea, a comparison was done in order to evaluate if differences for the intact (undeformed) rock would occur between the two subareas. The comparison was done for rock samples with no or faint to weak alteration and without micro fractures. The results are presented in Table 3-3 and it shows only small differences in the rock type porosities between the two sites. Consequently, the impact of the site location on porosity of the intact rock is small and thus it seems motivated to import Simpevarp data to the Laxemar retardation model without restrictions to its geographical origin.

Deformation zone units

For the five different deformation zone units that have been identified (cf. Section 2.2.2), porosity measurements using the PMMA method /Penttinen et al. 2006/ have been applied. The major reason for this is that these materials are complex and heterogeneous in their structure; hence porosity distribution information was considered essential. Three of these were also measured using the water saturation technique. The results are presented in Table 3-4 and can be summarized as:

- For the Deformation zone unit 1 (Fault rock/gouge, strongly tectonised and partly incohesive material), cf. Figure 3-5, an average porosity of approximately 3% has been estimated using the PMMA technique. The porosity is strongly heterogeneously distributed. Low porosity rock fragments are surrounded by highly porous material (clay, hematite, chlorite),

- Deformation zone unit 2 (Chlorite, green gouge, primarily close to mafic rock types), cf. Figure 3-6, have a PMMA-measured porosity of 12%. The pore structure is congruent with altered chlorite phases, which form a connective network of highly porous veins.

- The water saturation measurements show median porosities of approximately 6% for Deformation zone unit 3 (Porous episyenitic wall rock). The PMMA measurement shows that the porosity pattern is strongly heterogeneous. A highly porous clayish fracture coating had a porosity >10%.

- For Deformation zone unit 4 (Cataclasite, with mylonitic banding), an average porosity of approximately 3% is obtained by the water saturation measurements. A heterogeneous porosity pattern is observed by PMMA, ranging from very low porosity in dense mylonite parts (less than 0.1%), typical matrix porosity levels in between fractures (0.5%) to very high porous areas in more altered parts.

- Deformation zone unit 5, Oxidized (medium to strong alteration) wall rock, has a water saturation porosity of approximately 0.7%. Micro fractures cutting through the sample were clearly visualised with the PMMA technique.

Fracture type samples

Alteration near an open fracture was studied by the PMMA-method in a Fracture type G sample from a deformation zone, cf. Figure 3-7 and Table 3-4. The fracture coating had a porosity of about 0.9% /Penttinen et al. 2006/. Due to their limited sample thickness and to the fact that the samples sometimes were not consolidated, porosity determinations were not possible to perform with satisfying results for more than one Fracture type sample.

Table 3-3. Comparison of porosities for samples with no or faint to weak alteration and without micro fractures from Simpevarp and Laxemar areas for dominating rock types. The median, min, max, average arithmetic and sample standard deviation (σ) values from the numbers (N) of samples involved in the study are presented.

Rock type (SKB code)	Site (Simpevarp or Laxemar)	Samples with no or faint to weak alteration and no micro fractures						Comments
		Median	Min	Max	Average	σ	N	
Fine-grained dioritoid (501030)	Simpevarp	0.10	0.00	0.42	0.12	0.09	54	
	Laxemar	0.07	0.04	1.49	0.32	0.53	7	One sample of 1.49% porosity causes the increase in average value
Quartz monzodiorite (501036)	Simpevarp	0.13	0.08	0.35	0.17	0.10	19	
	Laxemar	0.15	0.00	1.32	0.20	0.22	42	
Ävrö quartz monzodiorite (501046)	Simpevarp	0.45	0.12	0.60	0.44	0.12	11	9 of these 11 Simpevarp samples are from a series of deep samples in KSH01A 891.69–891.94 m which are coarse grained and of higher porosity which increases the porosity of the group
	Laxemar	0.29	0.05	0.43	0.29	0.11	16	
Ävrö granodiorite (501056)	Simpevarp	0.37	0.24	0.58	0.40	0.13	6	The Simpevarp samples are from KSH01 in the range of 880–940 m depth
	Laxemar	0.28	0.13	0.89	0.31	0.13	54	

a   b   c
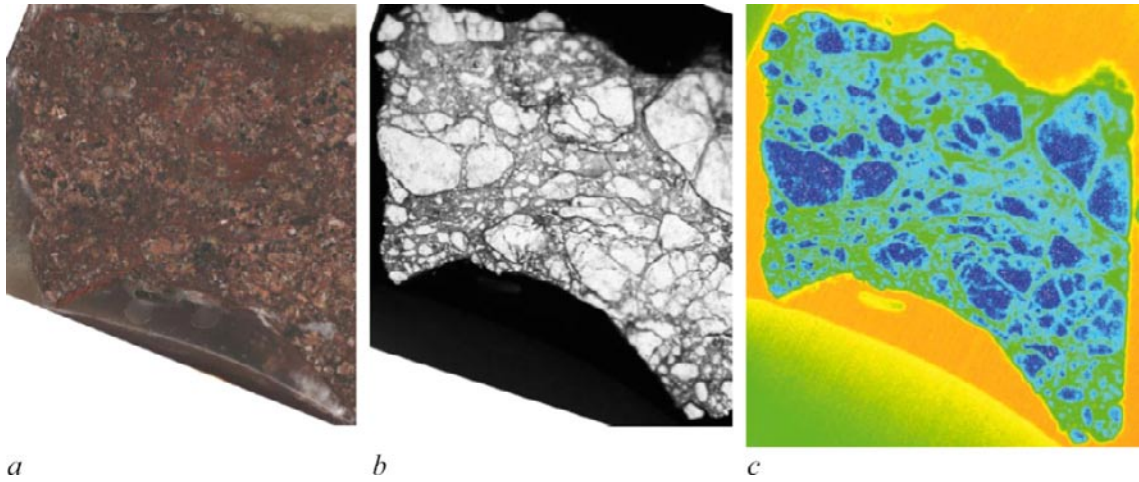
Figure 3-5. a) Photograph of the analysed rock surface of a Deformation zone unit 1, b) its corresponding film autoradiograph where white areas represent low porosity and dark areas high porosity, c) its corresponding digital autoradiograph where the dark blue colour is illustrating the lower porosity areas while green colour represent higher porosity .

a   b   c
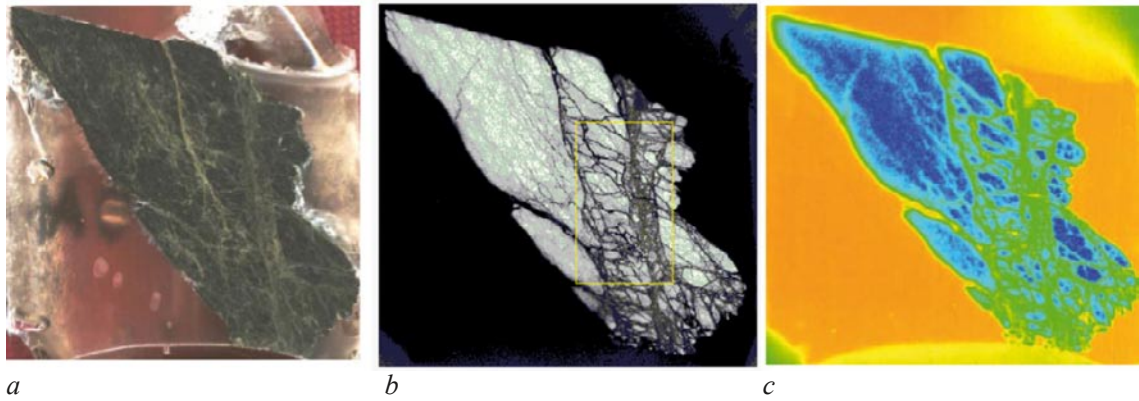
Figure 3-6. a) Photograph of the analysed rock surface of a Deformation zone unit 2, b) its corresponding film autoradiograph with evaluated porosity area marked in yellow, white areas represent low porosity and dark areas high porosity, c) its corresponding digital autoradiograph where the dark blue colour is illustrating the lower porosity areas while green colour represent higher porosity.
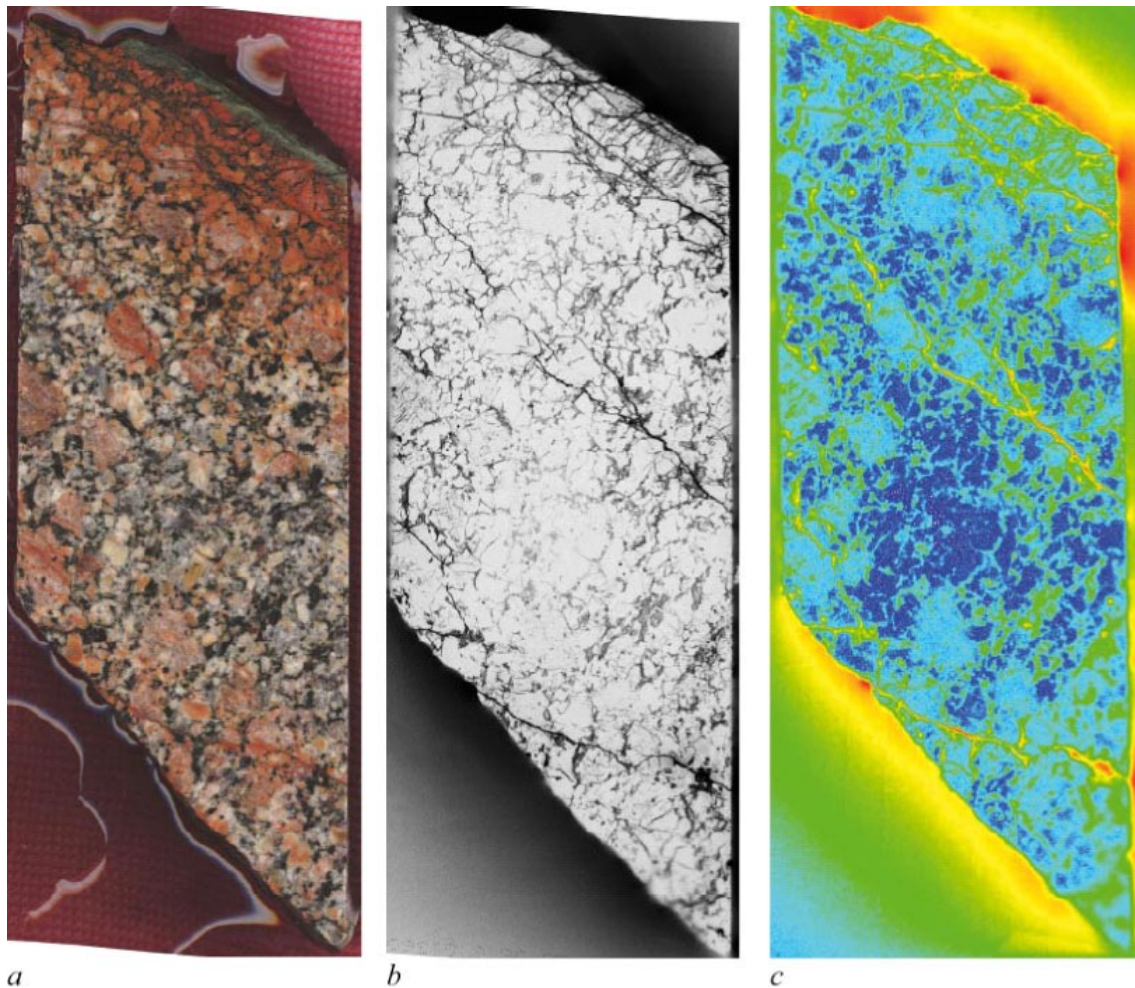
Figure 3-7. a) Photograph of the analysed rock surface of a Fracture type G sample, b) its corresponding film autoradiograph, white areas represent low porosity and dark areas high porosity, and c) its corresponding digital autoradiograph where the dark blue represent the lower porosity and yellow to red is illustrating the higher porosity. The fracture surface is on the top side and the fade green-coloured chlorite coating is seen in the photograph (a).

Table 3-4. Porosities (vol-%) of different deformation zone unit samples and one fracture coating from the Laxemar-Simpevarp area. The median, min, max, average (arithmetic mean), samples standard deviation values and numbers (N) of samples involved in the study are presented. The results originate from water saturation measurements of 30 mm rock core samples or alternatively from PMMA measurements of rock core samples evaluated for average porosity.

| Deformation zone unit / Fracture type | | Water saturation porosity (vol-%) | | | | | |
ID	Geological description	Median	Min	Max	Average	σ	N
Fracture type G	Chlorite ± other	-	-	-	0.9[A,C]	-	1[A]
Def. zone unit1	Fault rock/gouge (strongly tectonised and partly incohesive material).	-	-	-	3[A]	-	1[A]
Def. zone unit 2	Chlorite (green gouge, primarily close to mafic rock types)	-			12[A]	-	1[A]
Def. zone unit 3	Porous episyenitic wall rock	-	4.2	8.3	6.2	-	2
Def. zone unit 4	Cataclisite (with mylonitic banding)	3.4	0.7	5.8	2.8	1.8	7
Def. zone unit 5[B]	Oxidized (medium to strong alteration) wall rock	0.8	0.2	1.6	0.7	0.4	19

[A] Based on PMMA measurement.

[B] Selected from medium and strongly altered samples of all rock types located within deformation zones.

[C] Data valid for the fracture coating only.

3.3.3 Statistical representation

Since the porosity measurements represent the laboratory measurement method with the highest number of samples, an attempt to study the statistical representation of the material has been performed with respect to these results. In the study, all the 501030, 501036, 501046 and 501056 rock type samples have been organized using a linear distribution model (Figure 3-8) and a logarithmic distribution model (Figure 3-9). Deformation zone unit samples (i.e. the strongly altered samples as described in Section 3.3.2) were not included in the study. Besides, no filtering is done and the samples included may thus be located both inside and outside of the deformation zones. From the results, a slight indication is obtained that the logarithmic distribution gives a better Gaussian shape compared to the linear distribution which may be regarded as a verification of a log-normal distribution as the best statistical representation of the porosity (and probably therefore also to the closely related parameter, diffusivity). However, it is the opinion of the authors that it is not motivated from these findings alone to consequently in this report use a log-normal distribution of the retardation parameters. This becomes even more obvious when including the sorption studies where a very low number of measurements have been done.

3.3.4 Alternative representations of the porosity data

As has been described in Chapter 2, different methods for rock sub-divisions have been developed during the Laxemar site investigation programme. Besides the method mainly used in this report, i.e. sorting according to the:

• Rock type,

the following alternative sorting methods are available:

• Rock domains

• Fracture domains

• Hydraulic rock domains
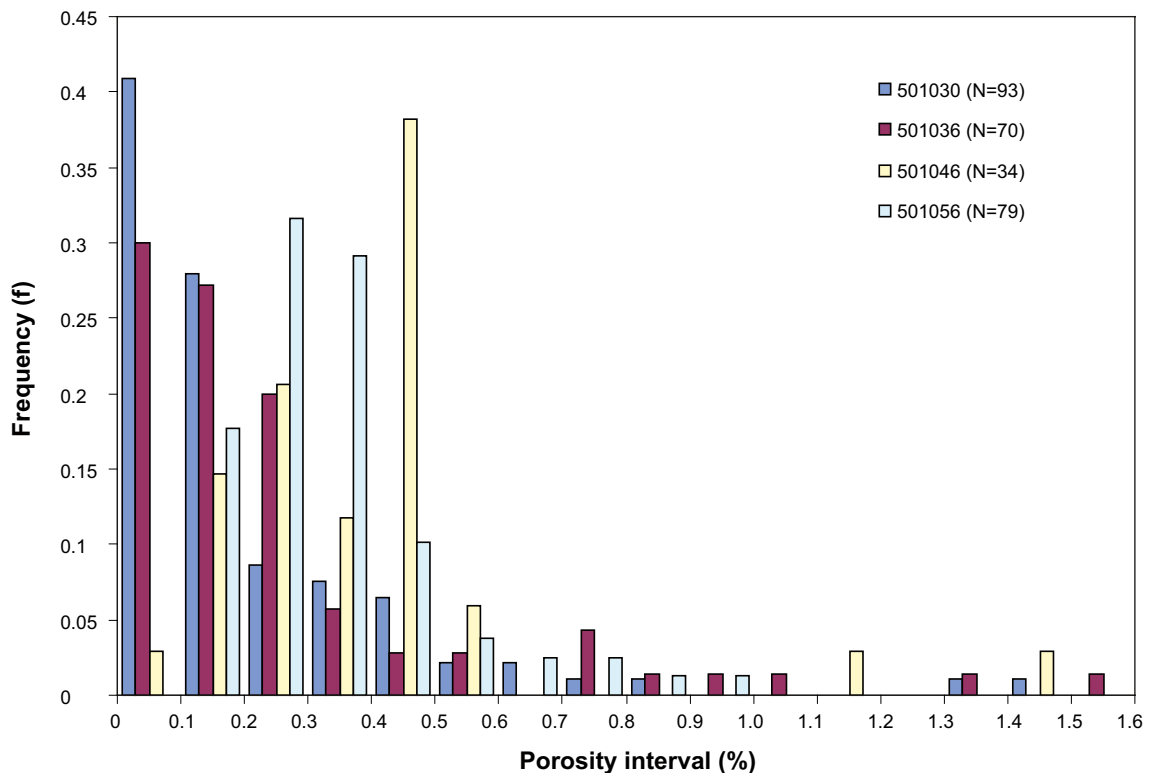
Figure 3-8. *Histogram representing the linear distribution of porosity for rock types 501030, 501036, 501046 and 501056. The frequency is normalised by the total number of samples (N) for each rock type and represents the fraction of observations in each 0.1% interval.*
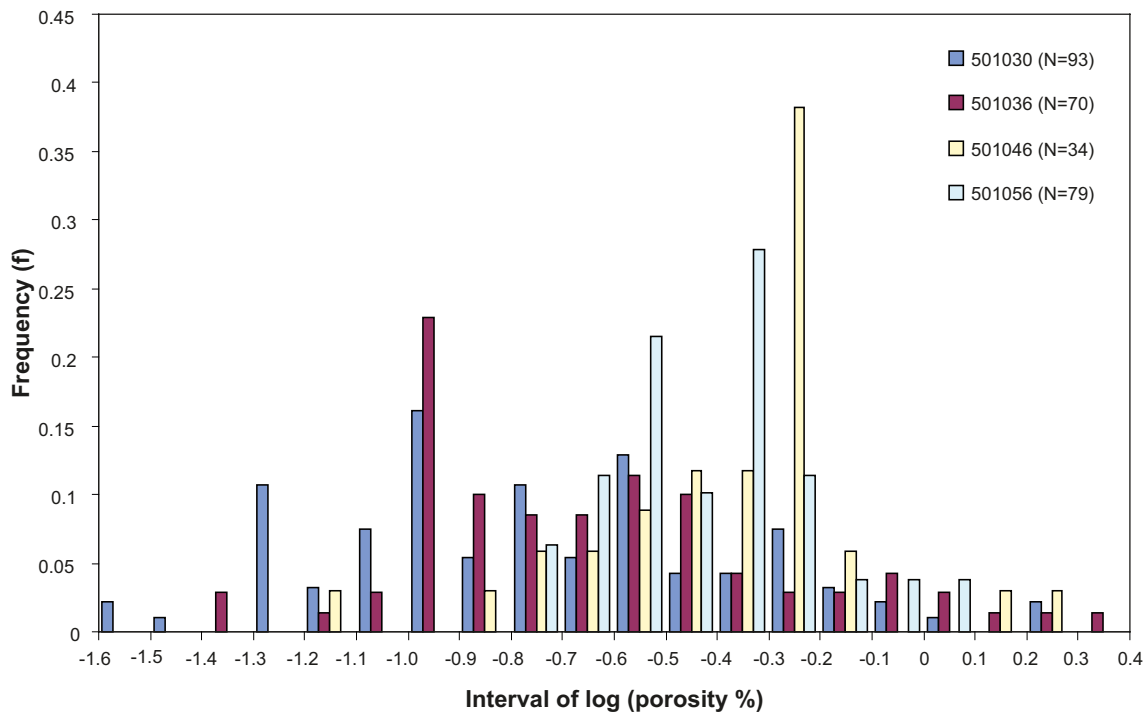
Figure 3-9. *Histogram representing the logarithmic distribution of porosity for rock types 501030, 501036, 501046 and 501056. The frequency is normalised by the total number of samples (N) for each rock type and represents the fraction of observations in each 0.1% interval.*

Since data concerning the porosity is the transport parameter which has the largest quantitative representation, attempts have been performed to make sub-divisions of the porosity data also to the three latter methods. This is done in order to investigate the possibility that alternative sub-division methods give less variation in the results within the sub-divided groups which would be an indication that describing retardation properties based on alternative domains would be a better alternative than using the rock type method.

The results of this exercise are represented in Figure 3-10 where the standard deviations (1 σ) of the different methods are displayed. Besides that, the uncertainties of the average value ($\sigma/N^{1/2}$) are also illustrated in the figure. At a first glance, it seems as the fracture domain concept as well as the hydraulic rock domain concept produces less variation compared to the rock type concept. However, one has to consider that the hydraulic rock domains and the fracture domains refer to concepts in which the deformation zones are excluded; for comparisons to the rock type concept and rock domain concept one should therefore exclude the deformation zone samples. Doing so, one can conclude that no improvement of any of the alternative sub-divisions is obtained compared to the rock type concept.

An extended summary of the different methods of sorting the porosity data is given in Appendix 1, where the numerical data as well as the elevation dependence of the porosity are presented.
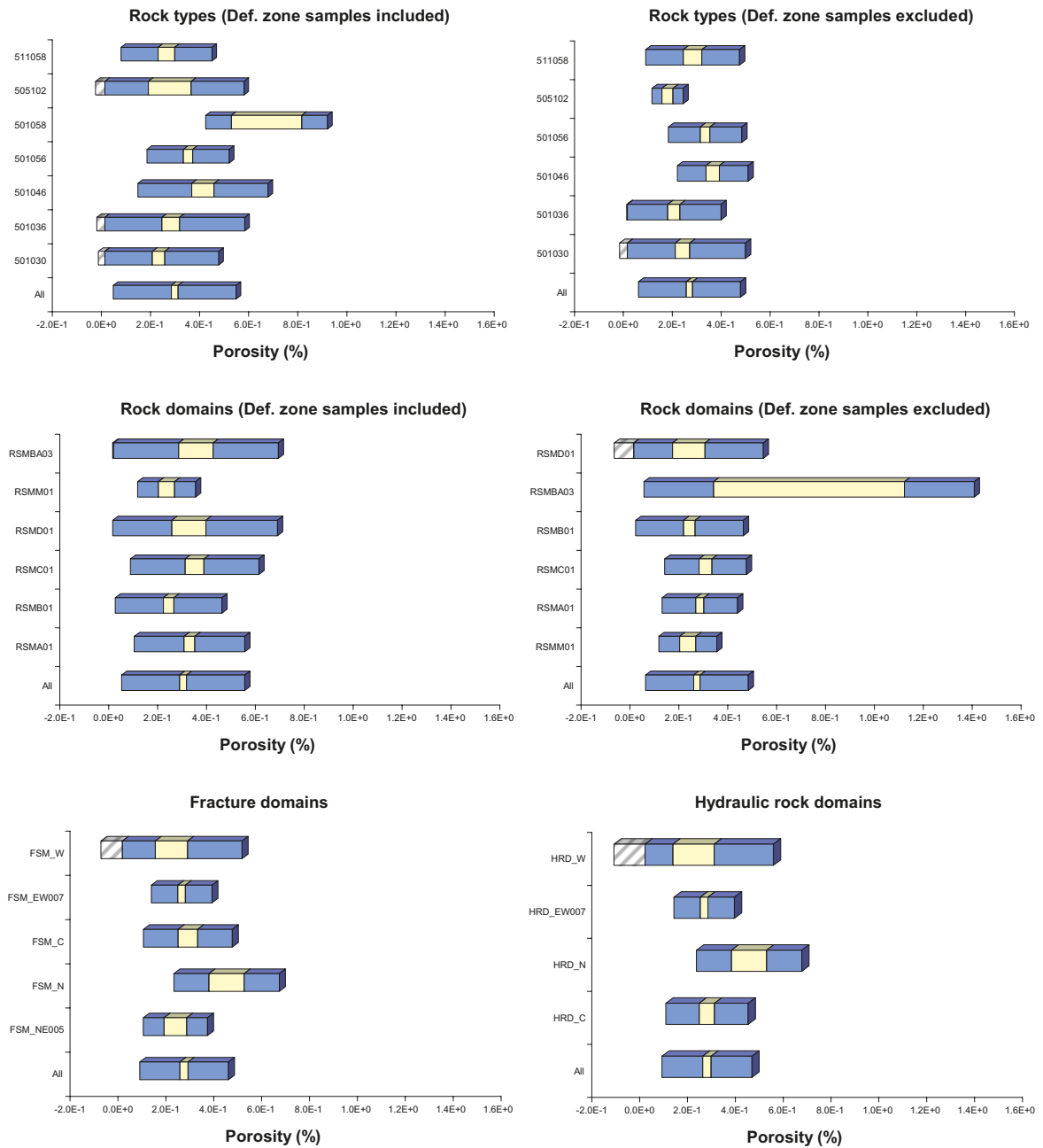
Figure 3-10. *Illustration of the intervals of the porosity measurements, divided as rock types (top), rock domains (middle), fracture domains (bottom, left) and hydraulic rock domains (bottom, right). The average value for each population is located in the middle of each box while the length of the blue boxes refers to the average values given with sample standard deviation (1σ). The intervals going in to the negative areas have been illustrated with a striped box; for obvious reasons, no sample results are found within this interval. The length of the yellow boxes refers to the average values given with standard deviation of the average values (1σ/N^{½}) where N is the number of measured samples.*

3.4 Diffusion

3.4.1 Methods and parameters

In this work, the term diffusion refers to the process in which a tracer can diffuse from the fracture water volume into the micro fractures of the rock matrix. Thereby, an interaction can occur in which the inner surfaces of the rock matrix can be available for sorption, and the tracers can be significantly retarded in their transport. This work addresses diffusion processes in the aqueous phase only; potential diffusive mobility in the adsorbed state (so-called surface diffusion /Ohlsson and Neretnieks 1997/) has not been considered.

In this work, primarily two methods are used for the determination of the diffusivity of the rock materials /Widestrand et al. 2003/:

- Through-diffusion measurements; a method where the effective diffusivity, D_e (m²/s), is determined by studying the diffusion rate of tritiated water (HTO) through a rock sample (HTO is used in the site investigations; the method can be applied also with other tracer solutions).

- Resistivity measurements; a method where the information on the diffusivity is obtained from the resistivity of electrolyte-saturated rock samples. The concept implies that electrical conduction in this rock can only exist in the electrolyte-saturated pores (no conduction within the nonporous grains of the crystalline rock) and that the ability of the rock to perform electrical conductance is a similar process to the ability of the tracer to diffuse in the pores.

The diffusion process is quantified in terms of the formation factor, F_f (-). This parameter quantifies the reduced diffusion rate obtained in the rock material relative to the diffusion rate in pure electrolyte. It is thus calculated from the results of the through-diffusion studies, as:

$$F_f = \frac{D_e}{D_w}$$ (Eq 3-2)

where D_w (m²/s) is the diffusivity of tritiated water in pure water. In this work, a water diffusivity of $2.1 \cdot 10^{-9}$ m²/s has been used, which is based on the /Mills and Lobo 1989/ using a temperature compensation for the somewhat elevated temperatures obtained in the glove box in which the through-diffusion experiments has been performed. It should be noted that solely based on the temperature variation and uncertainty involved therein, one must at least acknowledge an up to 10% additional uncertainty in the values. Nevertheless, this uncertainty is considered to be low compared to the other uncertainties in the concept.

Through-diffusion measurements are performed according to SKB MD 540.001 (SKB internal document). The determination of diffusivity is performed by studying the diffusion of tritiated water (HTO) through a slice of rock. A slice of water-saturated rock is mounted in a diffusion cell, where the start cell is filled with water spiked with HTO tracer and the other side is filled with non-spiked water. The diffusion is determined from the rate of the in-growth of the HTO tracer in the originally non-spiked water volume. The effective diffusivity, D_e (m²/s) and the rock capacity factor, α (-) is calculated by fitting the model equation:

$$C_r = \frac{C_2 V_2}{C_1 Al} = \frac{D_e t}{l^2} - \frac{\alpha}{6} - \frac{2\alpha}{\pi^2} \sum_{n=1}^{\infty} \frac{(-1)^n}{n^2} \exp\left\{ -\frac{D_e n^2 \pi^2 t}{l^2 \alpha} \right\}$$ (Eq 3-3)

where C_2 (Bq/m³) is the accumulated tracer concentration in the target cell at the time t (s), V_2 (m³) is the volume of the target cell, C_1 (Bq/m³) is the tracer concentration in the start cell (the low diffusivities gives a concentration decrease that is negligible), A (m²) is the geometric surface area of the rock sample, and l (m) is the length of the rock sample.

The relative measurement uncertainty of a single diffusivity value determined by the through-diffusion method is estimated to 12%, given with 1 σ confidence level, for samples from the Forsmark site investigation. The uncertainty was estimated by an analysis of the impact of modelling assumptions, either using a fitted porosity or fixing the porosity based on the water saturation measurements. A similar analysis is presented in /Selnert et al. 2009/ based on Laxemar and Simpevarp data.

For the resistivity measurements, F_f (-) is the parameter produced by the method, i.e. the ratio of the resistivity of a given electrolyte to the resistivity of the rock sample with the pores saturated with the same electrolyte.

The resistivity can be measured both in laboratory experiments (where the rock samples are saturated with 1 M NaCl) and in borehole in situ experiments. For obvious reasons, no saturation of the rock matrix with a known electrolyte can be done in in situ experiments. In this case, the composition of the pore liquid must be estimated based on hydrochemical sampling and analysis, commonly assuming the same composition in the matrix as in the groundwater in neighbouring fractures. A further complication is that at a lower salinity than 1 M NaCl, which likely could be present in the pores in in situ rock according to /Ohlsson and Neretnieks 1997/, a significant part of the conductivity could be a result of the surface ion mobility, which would overestimate the in situ measured formation factors.

3.4.2 Through-diffusion studies

Site-specific data

Site specific rock materials from the Simpevarp and Laxemar subareas have been sampled and measured using the through-diffusion method as described above. The results of the through-diffusion experiments are presented in Table 3-5 and Figure 3-11. From the results it can be concluded that formation factors in the range of $3.1 \cdot 10^{-5}$ to $4.6 \cdot 10^{-4}$ is observed for rock type samples outside deformation zones. Generally, the formation factor ranges seem to reflect the porosity range in the rock types, i.e. lower formation factor is found e.g. for the lower porous 501030 type while higher formation factor is obtained for the more porous 501046.

An attempt has been made to study the influence of the porosity on the formation factor. The different formation factors determined by through-diffusion experiments are presented in Figure 3-12 as a function of their porosity measured by water saturation technique. As expected, a relationship is indicated and two functions are presented for the interpretation; the Archie law $F_f=0.71 \cdot \varepsilon^{1.58}$ /Parkhomenko 1967/ and a fit of a similar equation to the actual data in this investigation. The large variation observed in experimental data is an indication that one has to deal with a sample heterogeneity which probably cannot be covered by a simple porosity-diffusivity relation as proposed by e.g. Archies law or the relationship established by the fit of the experimental values involved in this work.

Only small differences in formation factors are observed for rock type samples located inside deformation zones compared to those located outside deformation zones, which is in accordance with the porosity results. A drawback is, however, that the numbers of measurements from samples inside deformation zones are very low and the statistical basis for these observations can be questioned.

The formation factors for altered samples originally selected as typical deformation zone unit samples (Zone 3, 4 and 5 in Table 3-5) range from approximately $1 \cdot 10^{-4}$ to $1 \cdot 10^{-3}$ which is in accordance with the higher porosity of those samples.

In the material used for through-diffusion experiments, measurements on drill core samples with lengths of 0.5–5 cm are included, however the majority of the samples (approximately 60%) are of 3 cm length and 13% each are of 0.5, 1 and 5 cm lengths. The diffusivity as a function of sample length is presented in Figure 3-13 for large and relatively homogeneous rock samples (approximately 30 cm) that was subdivided into the 0.5 to 5 cm sizes. It is indicated that 0.5 and 1 cm sizes have a slightly increased diffusivity compared to the 3 and 5 cm sizes, which is in accordance with the porosity increase indicated for the same samples (Figure 3-2). However, the normal variation within a given size is typically larger than the size effect. The effect of including shorter sample sizes in the total results for a rock type is therefore small. Increased porosity (and thus increased effective diffusivity) in shorter samples can be caused by e.g. a larger contribution of sawing induced porosity and/or a too small sample size relative to the grain size of the minerals which may increase available porosity.

Table 3-5. Formation factors (F_f) of different rock types and deformation zone unit types from the Laxemar and Simpevarp areas, determined from the through-diffusion experiment. The median, min and max values from the numbers (N) of samples involved in the study are presented. The division of samples in inside or outside deformation zones is based on the extended single hole interpretation.

Rock type (SKB code)	Inside or outside of deformation zones	Median	Min	Max	Average	σ	N	Comments
Fine-grained dioritoid (501030)	Outside	3.1E-5	1.1E-6	4.0E-4	6.6E-5	1.1E-4	19	
	Inside	8.4E-6	1.4E-6	1.5E-5	8.6E-6	4.9E-6	5	
Quartz monzodiorite (501036)	Outside	6.1E-5	2.0E-6	4.7E-4	1.1E-4	1.2E-4	15	
	Inside	1.4E-4	1.1E-5	3.7E-4	1.8E-4	1.4E-4	7	
Ävrö quartz monzodiorite (501046)	Outside	4.6E-4	7.5E-6	5.2E-4	4.1E-4	1.6E-4	9	8 of these 9 samples are from a series of deep samples in Simpevarp KSH01A 891.69-891.94 m which are coarse grained and of higher porosity which increases the formation factor of the group
	Inside	-	-	-	-	-	0	
Ävrö granodiorite (501056)	Outside	7.0E-5	1.3E-5	6.1E-4	1.5E-4	1.7E-4	20	
	Inside	6.0E-5	3.8E-5	8.1E-5	5.9E-5	2.1E-5	3	
Mafic rock, fine-grained (505102)	Outside	-	-	-	9.8E-5	-	1	
	Inside	-	-	-	-	-	0	
Granite, fine- to medium-grained (511058)	Outside	4.4E-5	2.3E-5	6.0E-5	4.5E-5	1.5E-5	5	
	Inside	-	-	-	-	-	0	
Deformation zone unit, type 3	Outside	-	-	-	1.1E-3	-	1	Outside deformation zone but defined as crushed zone in boremap.
Deformation zone unit, type 4	Inside	-	-	-	7.6E-3	-	1	
	Outside	9.4E-4	7.6E-4	2.1E-3	1.3E-3	7.4E-4	3	Outside deformation zone but defined as crushed zone in boremap.
Deformation zone unit, type 5	Inside	1.4E-4	3.8E-5	3.7E-4	1.5E-4	1.3E-4	9	Selected from medium and strongly altered samples of all rock types located within deformation zones
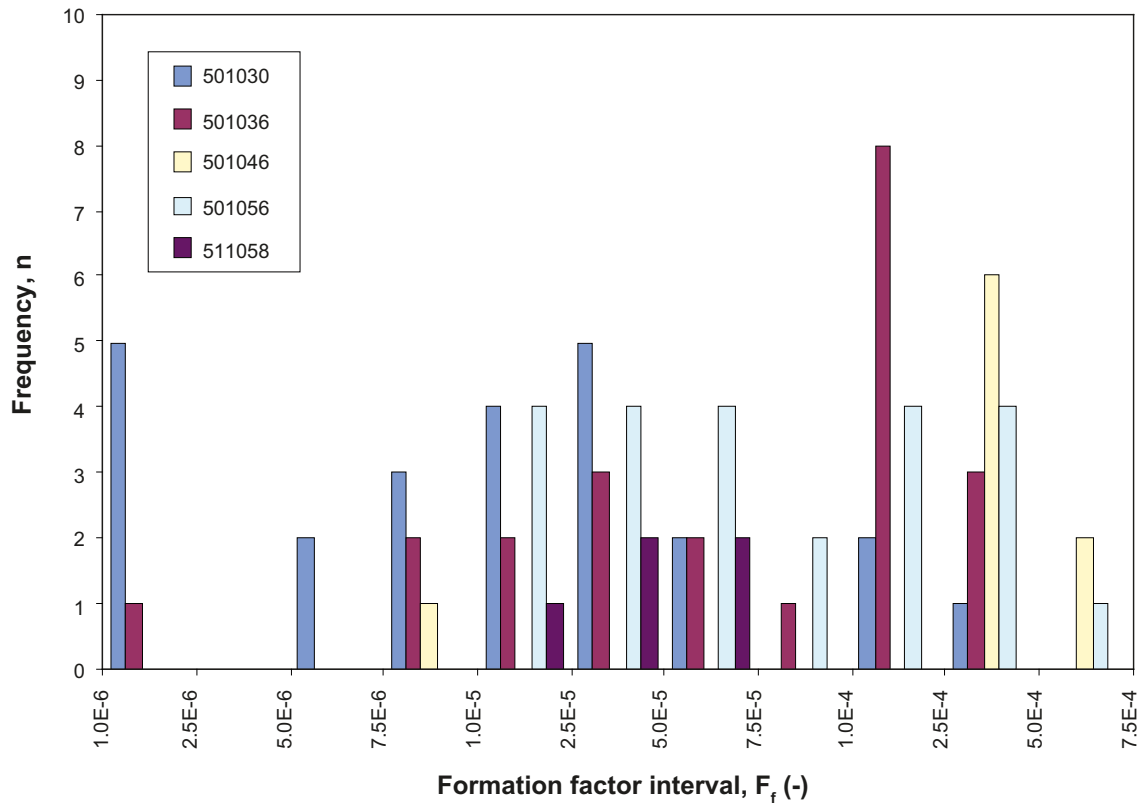
Figure 3-11. *Histogram representing the distribution of the formation factor for major rock types analysed in the laboratory programme.*
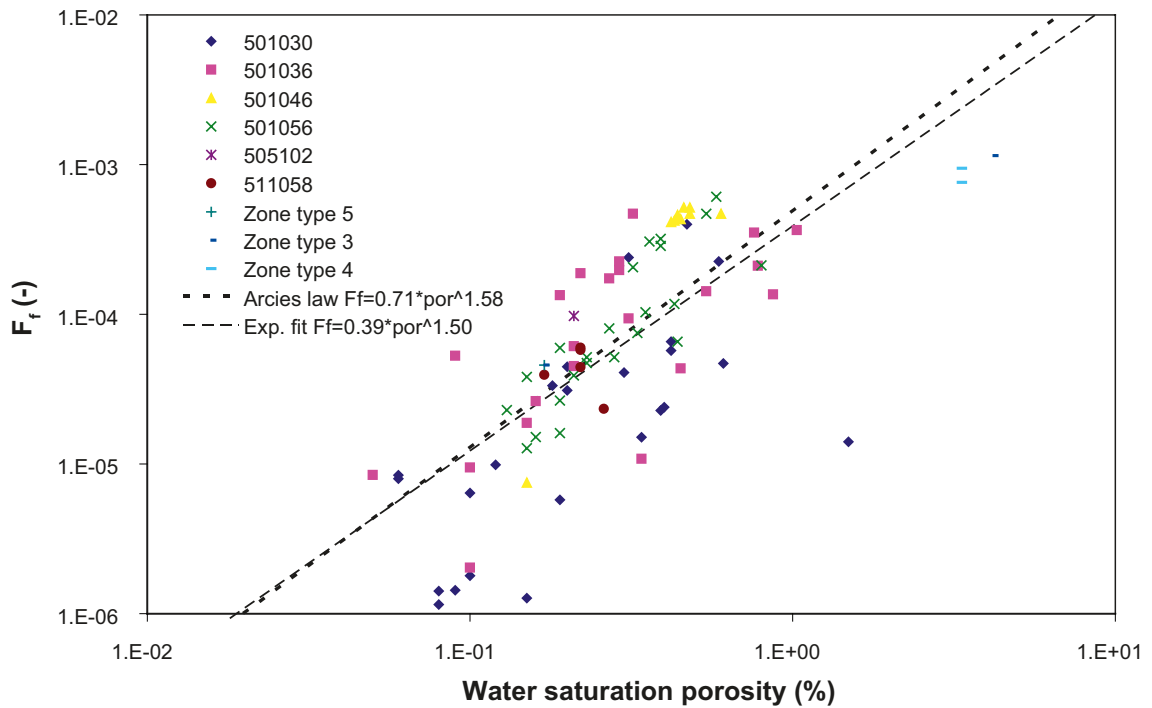
Figure 3-12. *Formation factor versus the porosity, with formation factor determined from through-diffusion experiments. Comparisons are made to a representation of Archie's law (Parkhomenko 1967) and to a fit of a similar equation to the actual results in this investigation. The porosities have been measured using the water saturation method (SS-EN 1936).*
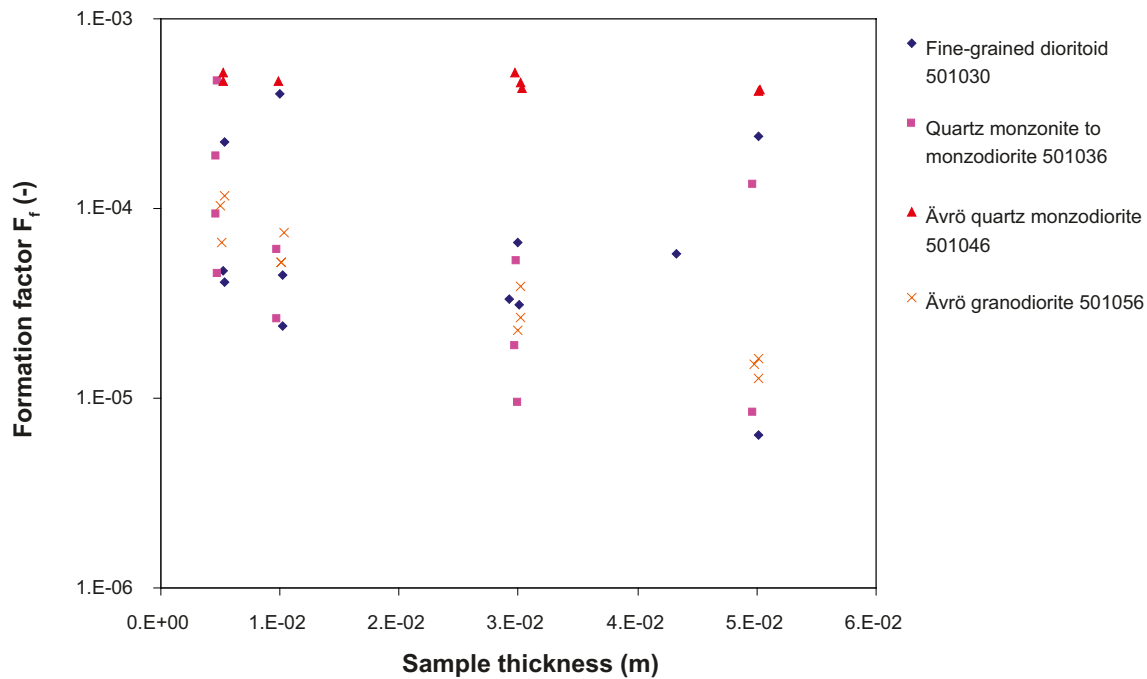
Figure 3-13. Formation factor versus the sample thickness determined from through-diffusion experiments. One relatively homogeneous sample of about 30 cm core length for each rock type was cut into sub-samples of 0.5, 1, 3 and 5 cm sizes.

3.4.3 Electrical resistivity

A thorough investigation has been made where 42 samples earlier exposed for through-diffusion experiments, were measured for their formation factor by the resistivity measurement method /Thunehed 2005a, 2005b, 2007a, 2007b/. The results (Figure 3-14) indicate a positive correlation between the two methods and that the resistivity measurements give a somewhat higher formation factor compared to the through-diffusion results. There are, however, a large variation in the results; the ratio between the resistivity measurement and the through-diffusion measurement has been found to be 2.1 on average but the range varies from 0.7 to 9.9 (median value 1.5). Although surface conduction bias is thought to play a certain role in this, the magnitude of the deviation is larger than expected and the source of the discrepancy is therefore not fully understood at present.

Comparisons have also been made between the samples used for through-diffusion experiments and the results of the in situ resistivity measurements /Löfgren and Neretnieks 2005a, 2005b, Löfgren and Petterson 2006, Löfgren 2007/ for the exact location of the sample used in the laboratory investigation. The results from the in situ resistivity measurements have been divided into two groups of measurements namely "fracture"; measurement points in proximity (≤ 0.5 m) to known open fractures and "matrix"; measurement points distant (> 0.5 m) from known open fractures. The results (Figure 3-14) indicates that, contrary to the laboratory resistivity measurements, the in situ resistivity measurements for the matrix group give significantly lower formation factors compared to through-diffusion. In this group 19 of 23 in situ samples are lower than the through-diffusion measurement and the factor $F_{f, HTO}/F_{f, in\ situ}$ is 19±17. Furthermore, the in situ data seem to be relatively uncorrelated to the through-diffusion measurements. However, it should be noted that the matrix group is based on a restricted number of rock sample positions; a 30 cm drill core sample from KLX04 489.48–489.78 m subsequently divided into 11 samples, a similar drill core sample from KSH01A 891.66–891.94 m which were cut into 12 samples and one sample from KLX04 719.37 and KSH01A 940.80 m respectively. The KLX04 489 m samples have a factor $F_{f, HTO}/F_{f, in\ situ}$ of 5±7 while the factor for the KSH01A 891 m samples is 38±5. It is consequently very difficult to estimate a general factor between in situ resistivity and through-diffusion data since the comparison practically is based on four sampled rock positions.
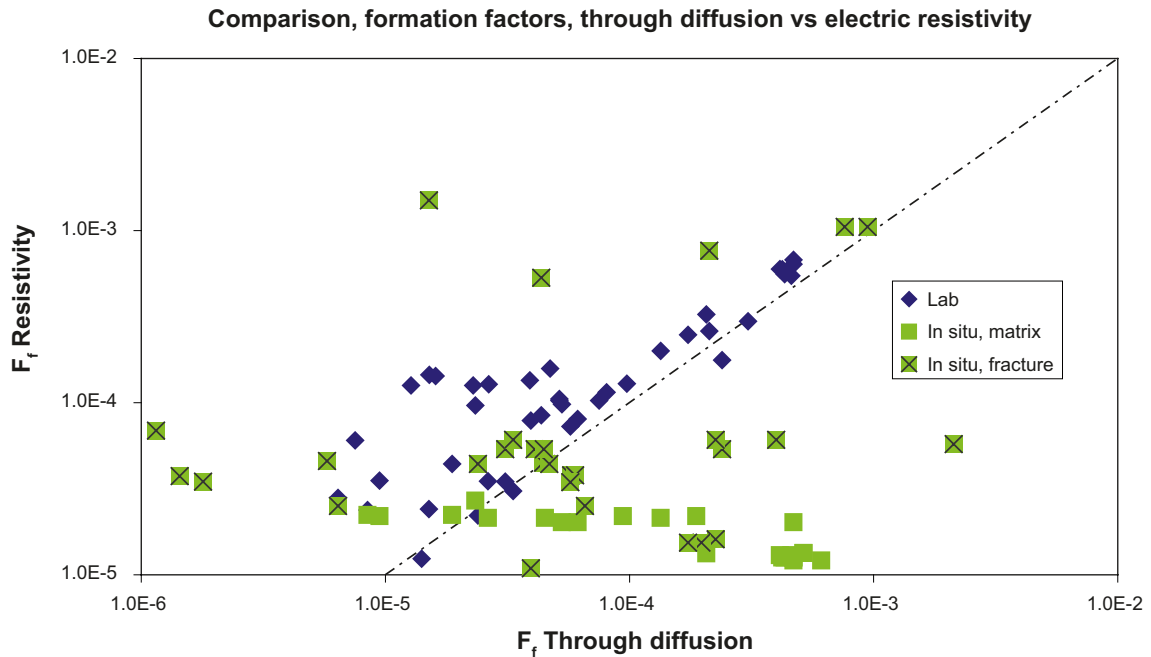
Figure 3-14. *Comparison of the results of the formation factor measurements determined by the electrical resistivity (Y-axis) and by through-diffusion (X-axis).The blue dots refers to comparisons of of the results of samples where laboratory resistivity measurement and laboratory through diffusion measurement has been made on the same drill core sample. The green dots refers to the results obtained for a particular through diffusion measurement given in relation to the results obtained for the* in situ *electrical resistivity electrical at the exact borehole location of the origin for the rock sample used in the through diffusion experiment. The results concerning the* in situ *resistivity measurements have been divided into two groups of measurements namely "fracture" (measurement points in proximity, ≤ 0.5 m, to known open fractures) and "matrix" (measurement points distant,> 0.5 m, from known open fractures).*

The in situ resistivity formation factors of the fracture group vary considerably, both relative to the matrix group and the through-diffusion data. The fracture group results are nearly equally distributed relative to the 1:1 line (16 samples are larger than the through-diffusion values and 13 samples lower than the through-diffusion results). These results are in accordance with the fact that that this sample group is close to fractures and is expected to have a larger variation in electrical conductivity/resistivity properties than the less fracture-influenced matrix rock.

Several different explanations for the differences between the results of the different methods are possible, e.g.:

- The drill core samples have been exposed to stress release and/or mechanical disturbances during the drilling/sampling. There are earlier works (e.g. /Skagius and Neretnieks 1986, Birgersson and Neretnieks 1990/) which have indicated that stress strongly influences the porosity and diffusivity of rock samples. This explanation seems plausible for the difference of the in situ resistivity (matrix group) to the laboratory methods (and possibly also an explanation to the variation in laboratory determined formation factors).

- Uncertainty concerning the actual pore water composition in the in situ electrical resistivity method.

- Possible influence of surface conduction in the electrical resistivity methods.

- Uncertainty concerning the temperature and its influence on the water diffusivity rate, this in combination with the general uncertainty for the tabulated water diffusivity.

Since the through-diffusion technique is the method that best mimics the actual physical process aimed to be studied, the formation factors which will be presented in the retardation model tables (Chapter 4) in this work are the ones obtained by through-diffusion measurement. Nevertheless, the possible overestimation of these values due to stress release and/or mechanical damage is

acknowledged so an optional decrease of the formation factors in future modelling, e.g. for conservative purposes, is acknowledged. It should in this context be mentioned that the retardation tables in Chapter 4 more should be regarded as comparisons of retardation properties between the different geological elements and not necessarily as the strictly recommended numerical values of the retardation parameters.

For a further discussion concerning the method and results of the resistivity measurements, it is referred to Appendix C in /Crawford and Sidborn 2008/.

3.5 Sorption

The process "sorption" is in this work defined as the adsorptive interaction of radionuclides with the surfaces of the rock material which therefore causes retardation of the transport of the tracer compared to any non-sorbing solute. In the somewhat simplified approach taken in this work, sorption is considered to be:

- Linear (i.e. no concentration effect on the sorption).

- Fast and reversible compared to the considered time perspective (no chemical kinetic effects are addressed for the sorption processes).

The concept used for the sorption processes is the same as was outlined in the "laboratory strategy report" /Widestrand et al. 2003/. This means that the source of sorption data will be batch laboratory experiment mainly performed using crushed and sieved rock material. It is outlined that the results from the measured distribution of tracer between the rock and water phase will be interpreted in the terms of:

- Adsorption of the tracers on the outer surfaces of the rock material, determined by the surface sorption parameter, K_a (m).

- Adsorption of the tracers on the inner surfaces of the rock material, determined by the volumetric sorption parameter, K_d (m^3/kg).

During the coarse of this work, it was identified that fracture filling material would play an important role in the retardation process; mainly due to high BET surface area and/or high sorption coefficients. This material was obtained by simple sampling from the fractures in the drill cores (in some cases a careful scraping was used to extract the material) and therefore never underwent any crushing process. It was therefore obvious that a different approach, compared to the strategy outlined for the crushed material, had to be addressed for the implementation of the sorption results of the fracture material; a material which was used in the sorption experiments in their natural form as it was found in the fractures. Further discussion concerning the strategy for the transfer of laboratory sorption data to the retardation models will be presented in Section 3.5.1.

The sorption properties of the rock material can be regarded as closely related to the active surface and its general ability to interact with solute species. Therefore, the specific surface area measurements by gas adsorption, i.e. the BET measurement according to Brunauer, Emmet and Teller /Brunauer et al. 1938/ and Cation Exchange Capacity (CEC) will give general information of the sorption properties and will therefore also be discussed in the context of sorption.

3.5.1 BET surface area measurements

Since the adsorption of radionuclides is taking place on the surfaces of the rock material, the quantification of available surface areas is a useful proxy for the estimation of the sorption capacity of the rock material. For example, different ferric oxides have significant surface areas and have been shown to be a highly adsorbing mineral for cations that adsorb with surface complexation, see, e.g. /Jakobsson 1999/, this of course in combination with the fact that ferric oxides surface groups are strong ligands for surface complexation. Furthermore, presence of clay minerals (as a group identified as a significant potential sink for Cs$^+$) will also cause increased surface areas in the measurements on rock samples.

An establishment of a direct quantitative relationship between the BET-surface and the sorption strength would require detailed knowledge of the exact proportionality of sorptive surface area distributed amongst different minerals. Since literature values of the sorption site densities of a number of surface ligands in various oxides, carbonates and aluminosilicates are available, a detailed knowledge of the mineralogy of the rock sample would together with the results of the BET surface area measurement provide data for determining the total ligand density of the material. However, such an exercise has been considered to be outside the scope of this work and the BET measurement should therefore only be considered as a proxy for sorption capacity of the rock material.

BET measurements have been performed on site-specific materials according to the ISO 9277 standard method. Three types of measurements have been performed for the Laxemar site specific material:

1. For samples taken from drill core, crushing and sieving has been performed. The size fractions 63–125 μm and 2–4 mm were measured in duplicate samples for each fraction. The results of these measurements are given in Table 3-6. Attempts have also been made to use these results to establish a division of the measured BET surface area, A_d (m²/g), as a sum an inner surface area, A_i (m²/g), of the rock (i.e. the part of the measured surface area which was present in intact rock before it was crushed) and an outer surface, A_{out} (m²/g), of the rock (i.e. the part of the measured surface area that is associated surfaces obtained during crushing process), i.e.:

$$A_d = A_i + A_{out} \qquad \text{(Eq 3-4)}$$

The concept involves the following assumptions:

a. Spherical particles of the diameter d_p (m) are obtained during the crushing process, thus having an outer geometrical surface, A_{geo} (m²/g), of:

$$A_{geo} = \frac{4\pi r^2}{m} = \frac{4\pi r^2}{\rho V} = \frac{3}{\rho r} = \frac{6}{d_p \rho} \qquad \text{(Eq 3-5)}$$

where r (m) = $d_p/2$ is the average radius of the particle, m (g) = ρV is the mass of the particle, V (m³) = $4\pi r^3/3$ is the volume of the particle and ρ (g/m³) is the density of the rock.

b. The amount of inner surfaces remains the same after the crushing process and is independent of the size fractions.

c. The amount of outer surface areas created during the crushing process is proportional to the geometrical outer surface of the presumed spherical particles, i.e.:

• $$A_{out} = kA_{geo} = \frac{6k}{d_p \rho} \qquad \text{(Eq 3-6)}$$

Inserting (Equation 3-6) into (Equation 3-4) gives:

• $$A_d = A_i + \frac{6k}{d_p \rho} \qquad \text{(Eq 3-7)}$$

where k (-) is a proportionality constant between the geometric surface area and the BET surface area (cf. Equation 3-6). A graph of the measured BET surface area as a function of $1/d_p$ will thus give a line with an intercept corresponding to inner BET surface area (A_i) and a slope corresponding to $6k/\rho$. Examples of such representations are given in Figure 3-15 and a summary of the evaluated A_i for 101057 rock type are given in Figure 3-16.

2. For natural fracture samples, scraping of the fracture surfaces was performed and the <125 μm fraction was isolated through sieving of the scraped material and measured in duplicate samples. The results of these measurements are given in Table 3-7.

3. Attempts have been made for a small number of samples to measure the BET surface area for non-crushed pieces of drill core, i.e. more or less intact rock. This has been made according to the methods and strategy outlined in /André et al. 2008 ab/.

Comparison of the results for different rock types

The results of the BET surface area measurement are presented in Tables 3-6 and 3-7. The major finding is the large difference between the non-altered samples compared to the rock material from fractures. The latter group has in this work a larger representation of samples in the small size fraction which, due to geometrical reasons, is presumed to give higher BET surface areas. Nevertheless, comparisons of the results within the smaller size fractions group (Figure 3-15) shows that fracture material in several cases gives up to 100 times higher than the lowest value obtained for the intact rock in the smallest size fraction. From these results alone, it can be assumed that the rock material in or adjacent to the fractures could constitute a considerable source for adsorption of radionuclides in the performance assessment. However, since the amounts of these fracture filling materials in most cases are rather low (indicated by the estimated thickness of these layers, cf. Chapter 4), their relative importance in comparison to the rock matrix in the long term scale is more doubtful.

Table 3-6. Measured BET surface area (m^2/g) for the fractions 0.063–0.125 mm and 2–4 mm.

Rock type (SKB code)	2–4 mm size fraction				0.063–0.125 mm size fraction			
	Average ± σ	Median	Min–Max	N	Average ± σ	Median	Min–Max	N
501030	0.048±0.032	0.043	0.0007–0.10	17	0.57±0.27	0.53	0.14–0.93	16
501033	0.032±0.025	0.030	0.0088–0.059	4	0.44±0.05	0.44	0.39–0.49	4
501036	0.036±0.028	0.029	0.0024–0.098	20	0.48±0.30	0.35	0.088–1.1	20
501044	0.062		0.058–0.066	2	1.12		1.11–1.12	2
501046	0.043±0.017	0.040	0.018–0.071	10	0.38±0.12	0.36	0.22–0.58	10
501056	0.033±0.022	0.039	0.0001–0.066	14	0.25±0.14	0.27	0.04–0.44	15
505102	0.079		0.072–0.087	2	0.78		0.77–0.80	2
511058	0.094±0.064	0.079	0.015–0.21	8	0.69±0.69	0.35	0.25–1.8	8

Table 3-7. Measured BET surface area (m^2/g) for the fractions <0.125 mm and 2–4 mm.

Description, cf. Table 2-4 and Table 2-5 for gelogical description	2–4 mm size fraction				<0.125 mm size fraction			
	Average ± σ	Median	Min–Max	N	Average ± σ	Median	Min–Max	N
Fracture type A	16			1	15±9	15.0	2.8–24	5
Fracture type B	2.6±1.3	3.0	1.2–3.7	3	6.5±2.1	7.3	3.4–8.1	4
Fracture type C	7.5±9.9	1.9	1.8–19.0	3	13±11	7.9	2.6–34	6
Fracture type D	-	-	-	0	-	-	-	0
Fracture type E	-	-	-	0	2.2	-	2.0–2.5	2
Fracture type FA	-	-	-	0	24	-	23.5–24.8	2
Fracture type G	-	-	-	0	-	-	-	0
Fracture type H	-	-	-	0	-	-	-	0
Fracture type I	-	-	-	0	-	-	-	0
Deformation zone unit 1A	9.8	-		1	24.1		24.1–24.2	2
Deformation zone unit 2	-	-		0	7.9		7.88–7.89	2
Deformation zone unit 3A	1.8	-	1.4–2.2	2	13.0		12.7–13.4	1
Deformation zone unit 4B	6.0	-	5.7–6.3	2	15±8	10.1	10–24	3
Deformation zone unit 5A	0.10	-	0.09–0.10	2		0.60	0.58–0.62	2

A) fine fraction analyzed from fraction 0.063–0.125 mm

B) fine fraction analyzed from 2 samples of fraction 0.063–0.125 mm, 1 sample from <0.125 mm

BET surface area vs particle size

One main purpose of the BET surface area measurements of the crushed rock samples was to estimate the amounts of surfaces created during the crushing process; surfaces that therefore cannot be regarded as representative for intact rock. Such surfaces will give increased amounts of surfaces in the batch sorption experiments which are nonrepresentative for intact rock and an overestimation of the sorption capacity can therefore be expected.

In the laboratory strategy document /Widestrand et al. 2003/ for the batch sorption experiment, it is stipulated that:

- If it can be established that the largest size fraction (2–4 mm) has a surface area of >75% compared to the smallest size fraction (0.063–0.125 mm), it means that only a negligible increase of the total amount of surfaces of the rock material is obtained during the crushing and that the major part of the surfaces in the crushed material is representative for the intact rock. The tracer distribution coefficient should then be independent of the size fraction and, in order to avoid diffusion impact, the smallest size fraction is used and the obtained tracer distribution coefficient (R_d) could thus directly be input as the K_d for the rock material.

- In the case where the BET-measurements show that the surface area of the largest size fraction (2–4 mm) has a surface area of up to 75% compared to the smallest size fraction (0.063–0.125 mm), it is concluded that a significant part of the material in the smaller fraction is caused by the crushing of the rock material and is therefore not representative for the intact rock. For the results of the batch experiments, it is therefore assumed that the sorption obtained is a sum of the:
  - Interaction with the inner surfaces (representative for the intact rock)
  - Interaction with the outer surfaces (non-representative for the intact rock)

In order to differentiate between these two processes, three different size fractions were proposed to be used for the batch sorption experiment (0.063–0.125 mm, 0.25–0.5 mm, 1–2 mm) and extrapolation of the results were to be performed according to:

$$R_\mathrm{d} = K_\mathrm{d} + \frac{6K_\mathrm{a}}{d_\mathrm{p}\,\rho}$$

(Eq 3-8)

which is analogous to the concept of distinction of inner and outer surfaces in the BET surface area measurements, cf. Equation 3-7. As can be seen in Figures 3-15 and 3-16, it is obvious that a significant increase of the total surface amount is obtained with decreased particle size. Except for the fracture type F material, the increase from the largest size fraction to the smallest size fraction is much higher than 25%, i.e. the limit for when the extrapolation concept should be used according to the laboratory strategy set up by /Widestrand et al. 2003/. It is indicated that the increase is more pronounced for the crushed fresh rock material than for fracture material and/or altered rock material. The increase is however generally lower than what should be expected for ideally spherical shaped particles since a strict geometrical model would yield an increase of the specific surface area by a factor of 32 from the 2–4 mm size fraction to the 0.063–125 mm size fraction. This deviation could be regarded as an indication of the presence of a significant part of the surfaces in the larger size fraction being "inner surfaces". An alternative explanation could be that the surface roughness is not constant as a function of the particle size.

When considering the comparatively high number of samples investigated of the unaltered rock, e.g. 501036, a rather high variation is nevertheless observed. This observation is valid both for the measured values within one size fraction as well as for the ratios between the two measured size fractions. Provided that the BET surface measurement procedure gives reliable values, this could be an indication of a considerable heterogeneity even within what is identified as a single rock type. The large BET-surface area measured for the deformation zone units could indicate that an influence of alteration on the BET surface area occurs even on levels when the alteration is hardly visibly observable.

A comparative measurement campaign was performed in which crushed material in the size fractions 0.063–0.125 mm, 2–4 mm and intact drill core samples with a diameter of 50 mm were measured for its BET surface area. The results (Figure 3-16) show that a reasonable agreement (given the uncertainties) is obtained for the large size fraction, the intact drill core and a size fraction extrapolation of inner and outer BET surface area (cf. Equation 3-7). One may from this finding postulate
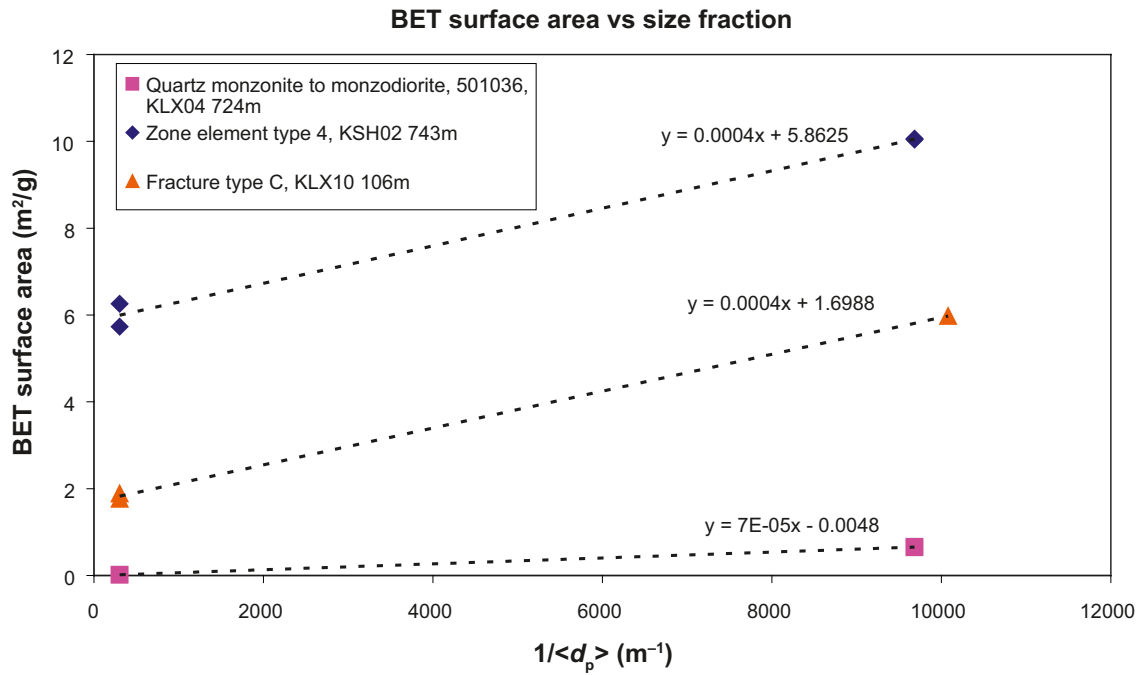
Figure 3-15. *Examples of results of BET surface area measurements as a function of the inverse of the particle size of the rock material used.*
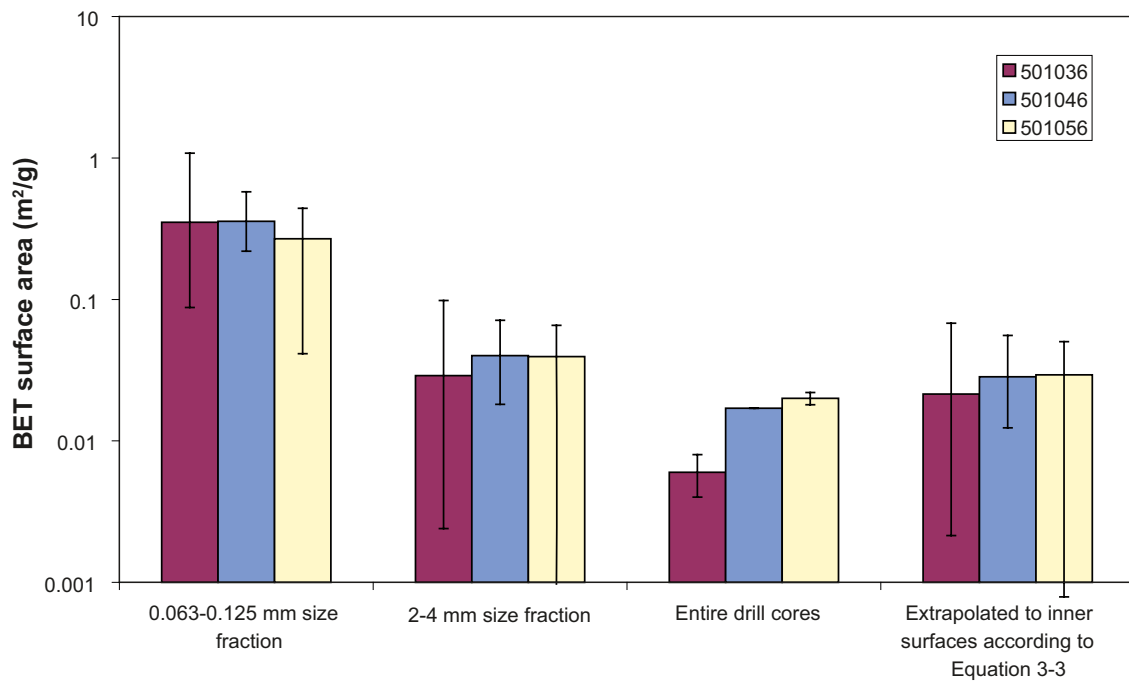
Figure 3-16. *Comparison between the results of the total number of BET surface area measurements of the 501036, 501046 and 501056 rock types. The presented values refer to the median values and the error bars refer to the uncertainty represented by the minimum and maximum values obtained for all the measurements.*

a conceptual model for the interaction of the intact rock in which the matrix diffusion in the intact rock mainly takes part in a network of pores surrounding mineral grains in the size of 2–4 mm with increased surface roughness compared to a spherical shape. If applying such a concept, one would preferably use the batch sorption experiment results from the largest size fraction and input the measured tracer distribution coefficient directly as the K_d. This means that for the larger size fractions, the $6K_a/d_p\rho$ term of Equation 3-8 can be neglected and the equation can thus be written as:

$$R_d \approx K_d \qquad\qquad\qquad\qquad\qquad\qquad\qquad\qquad\qquad \text{(Eq 3-9)}$$

3.5.2 Cation Exchange Capacity

The method applied for the measurement of CEC of the rock material is the ISO 13536 which consists of:

1. A saturation of the cation exchange sites with Ba^{2+} from a 1 M $BaCl_2$ solution buffered to pH 8.1.

2. An optional step in which the amount of leached cations from the saturation step is specified and measured.

3. A desorption step in which the solid phase is contacted to a 0.02 M $MgSO_4$ solution, in which the adsorbed Ba^{2+} is expected to exchange with Mg^{2+} followed by a precipitation of the very insoluble $BaSO_4$ (s). The concentration of Mg^{2+} is thereafter measured and the decrease of the concentration is thus a measure of the capacity of the solid material to adsorb cations, i.e. the cation exchange capacity (CEC).

4. Optionally, the amount of desorbed cations in step 2 can be compared to the concentration in the naturally abundant groundwater. The ratio of these two measures can be regarded as a sorption distribution coefficient K_d (m^3/kg), a quantity which normally is obtained by batch sorption experiments, cf. Section 3.5.3.

However, one should be aware of that for some of the materials included in this report, the demand of 5–10 g of material could, due to material shortage, not be fulfilled. This resulted in a less sensitive measurement and, consequently, larger uncertainties for the results. Furthermore, the material shortage did not allow triplicate samples; therefore all results reported are based on single samples.

The CEC measurements were in the original laboratory strategy document identified as a rather important parameter for obtaining a general sorption capacity of the rock material and therefore acting as a bridge between the batch sorption methods and a related method obtainable in a standardized form (ISO 13536). However, it was soon realised that the CEC methods were mainly aimed for soil investigations and therefore not likely to be sensitive enough for rock material with much lower CEC than soil. The CEC method was instead decided to be a comparative method only applied on a very limited numbers of rock materials.

The results of the CEC are given in Table 3-8. There are comparatively high uncertainties associated with the method; mainly due to the fact that only a very small part of the Mg^{2+} is adsorbed in step #3 which makes it difficult to verify a small concentration decrease from a blank solution (> 5% uncertainty in Mg^{2+} concentration determination is reported, Analytica 2008). For this reason, no CEC can be statistically verified for the majority of the fresh rock types where detection limits instead are reported.

As expected, a higher CEC can be observed for the fracture material compared to the samples consisting of fresh rock; a difference of a factor >10 is indicated. This is also valid for the fault rock material and the sealed fracture material which have higher CEC than the fresh unaltered rock. This difference is, however, smaller than the corresponding difference in BET surface area, where corresponding differences of a factor >100 could be observed. A general comparison of the CEC to the BET surface area is presented in Figure 3-17. The relationship between these two parameters is far from straight linear; however, the obvious conclusion that larger amounts of surface areas increase the capacity of binding cations is supported.

The amounts of desorbed cations from the saturation process in the CEC measurements are also given in Table 3-8, For the majority of the samples, the desorbed amount of the dominating cations (i.e. Na^+, K^+, Mg^{2+} and Ca^{2+}) was found to be below the detection limit, which could be expected due to the

Table 3-8. CEC characteristics of different Laxemar rock materials.

Rock material	Size fraction (mm)	Position (borehole, depth)	CEC[A] (cmole/kg)	Desorbed amount of cations[B] (cmole/kg)
Rock types				
501056	0.063–0.0125	KLX02, 217.00	<2.5	21
	1–2	KLX02, 217.00	<1.0	8.4
501046	0.063–0.0125	KLX03, 522.61	2.1±1.4	
	1–2	KLX03, 522.61	0.9±0.7	
501030	0.063–0.0125	KLX02, 682.70	2.3±1.4	14
	1–2	KLX02, 682.70	1.0±0.6	
501036	0.063–0.0125	KLX04, 489.85	2.2±0.9	0.9
	0.063–0.0125	KLX05, 482.30	2.3±1.8	3.4
	1–2	KLX04, 489.85	1.0±0.7	
Fracture materials				
Fracture type A	<0.125	KLX13, 373.35	40±13	69
Fracture type C	<0.125	KLX10, 106.38	12±2	24
		KLX13, 554.89	24±4	28
	1–2	KLX10, 106.38	3.9±1.1	4.7
		KLX13, 554.89	15±1	20
Deformation zone units				
Type 2	<0.125	KLX03, 732.59	13±2	23

A) Uncertainties and detection limits are based on the estimation that the Mg^{2+} quantification is associated with a 5% uncertainty.
B) Values are only given for the samples where the desorbed amount of Ca^{2+} (the cation that occupies the major cation exchange sites) has been reported to be above the detection limit.
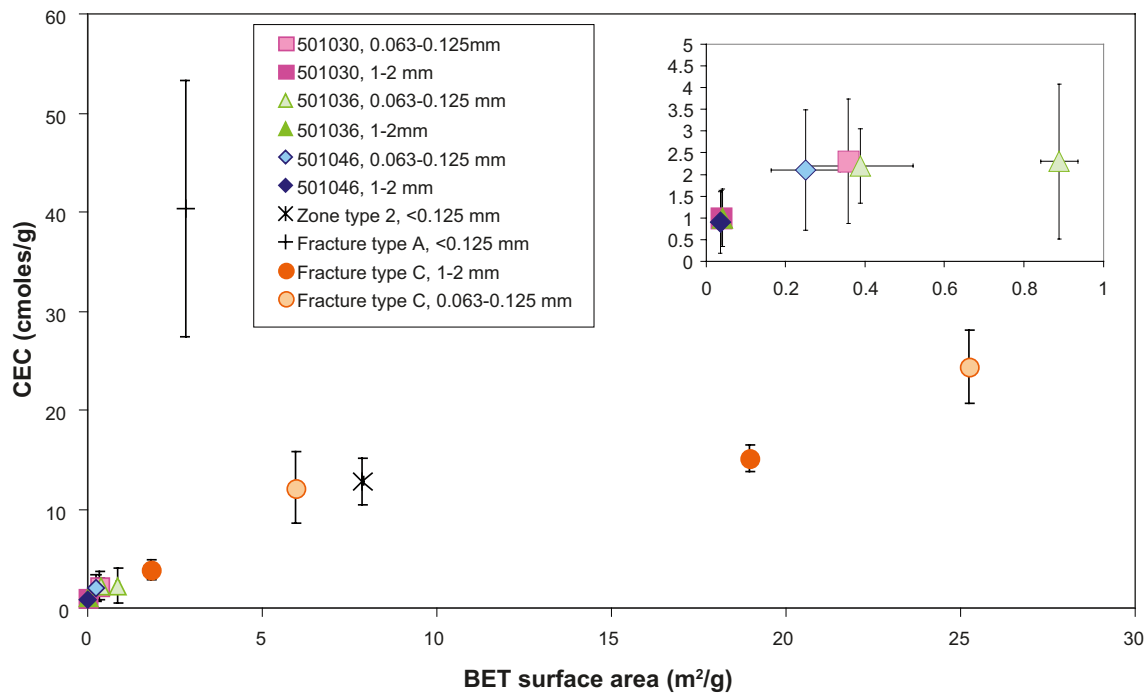
Figure 3-17. *Results of the CEC measurements as a function of their measured BET surface area (expansion of the lower parts in upper right).*

relatively low CEC. However, for the rock materials where the dominating cation Ca^{2+} could be quantified, a summation of the desorbed cations has been performed and is presented in the table. Under ideal conditions, these measurements should be identical. Generally, the amount of desorbed cations is somewhat higher than the measured CEC for reasons that are not known. A possible explanation is that e.g. traces of calcite could be dissolved during the saturation process, i.e. implying that parts of the Ca^{2+} in the adsorption solution has not been desorbed by the cation exchange leaching process.

Measurements of e.g. the Cs desorbed during the saturation step of the CEC measurement provides the total amount of Cs adsorbed by cation exchanged in the rock material. Knowing this concentration in combination with the concentration of Cs in the aqueous phase, allows an approximate estimate of the sorption coefficient (K_d) for the material to be calculated. This coefficient should under ideal conditions be identical to the sorption coefficient determined by batch sorption experiment technique (dealt with under section 3.5.3). Comparisons have thus been made of this type of K_d relative to the batch sorption K_d for all materials which were exposed for CEC measurements. In these calculations, it was consequently assumed that all cation exchanged Cs was desorbed during the Ba saturation step and that this rock material was (before sampling) in contact with a pore water with the same composition as the saline Laxemar groundwater.

The results of these calculations are presented in Figure 3-18. As can be seen, there is a poor correlation between the results of the two methods which suggests an unsuspected source of error in the mass balance. Approximately half of the samples give higher K_d for the CEC desorption method and half of the samples give higher K_d for the traditional batch adsorption method; deviations over two orders of magnitudes can be observed. The extremely deviating samples are the ones where high K_d have been measured in the adsorption experiment and one can speculate on the possibility that the 1 M $BaCl_2$ desorption solution is not enough to desorb all Cs from the rock material. Another possible uncertainty is that a generalised water composition is used for the calculation of the CEC desorption method; it is possible that the groundwater that naturally is in equilibrium with that particular rock material has a different Cs concentration than what was used in the calculations.
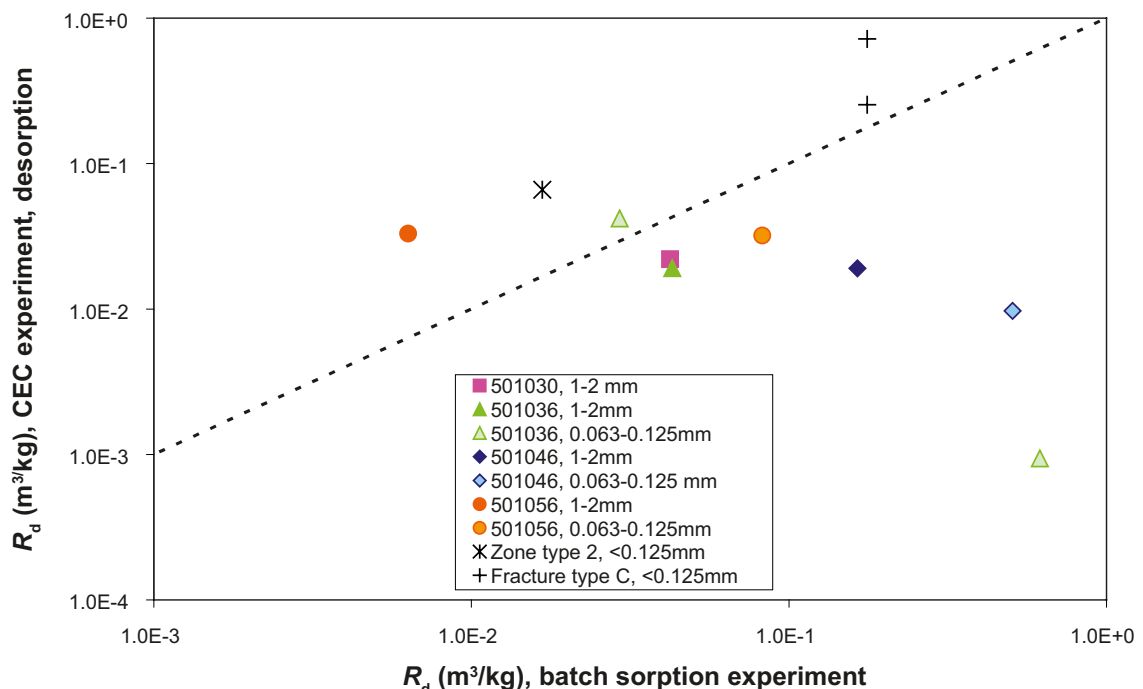
Figure 3-18. Comparison of sorption coefficient (R_d) for Cs measured using the Batch sorption method and estimation made on the measured amount of cation exchanged Cs in combination with the groundwater concentration.

3.5.3 Batch sorption data

As mentioned earlier, the evaluation method that was originally proposed /Widestrand et al. 2003/ for the interpretation of the batch sorption experimental results to sorption parameters consisted of Equation 3-8. A graph of R_d versus $1/d_p$ gives an intercept corresponding to the K_d value, and a slope corresponding to $6K_a/\rho$. This concept of evaluation implies the following assumptions:

- The outer-surface area normalised sorption partitioning ratio (i.e. K_a) is constant over the particle size distribution. Using the idealized conditions proposed in this report, this corresponds to a spherical shape of the particles.

- The size distributions within each particle diameter interval can be represented by the mean of that interval.

Preliminary evaluations according to this concept indicated general difficulties implied with this method. Primarily, the agreement of the results to the model was in most cases poor, which gave considerable uncertainties when extrapolating the K_d value from the intercept. Including the uncertainty in the intercept estimations resulted in several cases in uncertainty intervals involving negative values; i.e. indicating that no inner surface sorption could be confirmed and validated using this concept.

Parallel to these observations, it was found that the results of the BET measurement of intact drill cores (cf. Section 3.5.1) gave results corresponding to the larger size fractions of the crushed material (i.e. 2–4 mm), possibly even with indication of lower surface area of the intact drill cores compared to the 2–4 mm size fraction. The same relation applied to the extrapolations of the different particle sizes (Equation 3.3) where the intercept (corresponding to the inner surface) becomes similar to the BET surface value obtained for the 2–4 mm size fraction.

Summing up all these facts, a conceptual model for the tracer interaction with crystalline rock is postulated (used also in the Forsmark report /Byegård et al. 2009/), consisting of:

- An intact rock consisting of the pore volume distributed in a network surrounding grains of rock material of 2–4 mm size, i.e. the grain boundary porosity.

- Matrix diffusion being a process in which diffusion of the tracer takes place mainly in the grain boundary porosity and to a minor degree into the grains.

- The crushing/sieving process giving:
  - o Larger size fractions, e.g. 2–4 mm and 1–2 mm size fraction, which mainly have undergone cleavage in the naturally occurring grain boundary porosity and, therefore, no formation of extra BET-surface (compared to the intact rock) is obtained.
  - o Crushed rock in the <1mm size fractions which, to a large degree, have undergone cleavage through the natural mineral grains. An increase in the BET surface area compared to intact rock is therefore obtained for these size fractions.

Studying the visualization of the porosity distribution using the PMMA technique for the 501036 rock type (Figure 3-19), one can identify the porosity distributed in a grid system i.e. grain boundary porosity which would correspond to the proposed conceptual model.

Following this conceptual model, the sorption data used in this retardation model are:

- For the matrix rock material which has undergone a heavy crushing procedure before the sieving, the retardation data will consist of the tracer distribution coefficient (R_d, m³/kg) determined for the largest size fraction (1–2 mm) with the longest contact time, 180 days, which will be directly used as the K_d, m³/kg. Consequently, no evaluation or data delivery of the K_a parameter (cf. Equation 3-8) will be performed and the contribution of retardation caused by surface sorption (cf. Equation 3-1) is neglected.

- For the rock material that is associated with fractures (coatings and/or fracture fillings) sampling has been performed using much milder methods compared to the matrix rock, e.g. by mild scraping or by just collecting loose material. It is therefore not expected that creation of new surfaces will be performed to the same extent as in the crushing process for the matrix rock. Therefore, the tracer distribution coefficient (R_d, m³/kg) determined for the smallest size fraction (0.063–0.125 mm or the <0.125 mm) with the longest contact time, 180 days, will be directly used as the K_d, m³/kg.
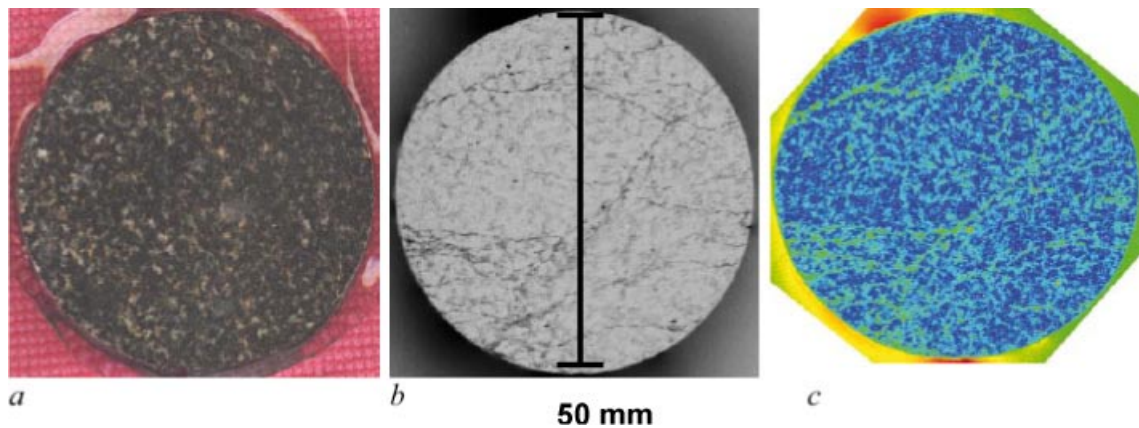
Figure 3-19. *Photograph (left), autoradiograph of PMMA saturated rock and evaluated digitalised porosity distribution of a 501036 rock sample, KSH01 714.89 m.*

Since there is no established method available for the validation of the underlying assumptions of this conceptual model, one has to be aware of the conceptual uncertainty in the sorption coefficients given in the retardation model tables in this report. This conceptual uncertainty is difficult to give in quantitative numbers but, nevertheless, has to be acknowledged. A reasonable assumption is that the sorption coefficients for strongly sorbing species are underestimated by this method; this because a penetrative equilibrium is not likely to have been obtained within the relatively short time perspectives applied.

On the other hand, it is acknowledged that the results for the BET surface area measurement for intact rock (cf. Figure 3-16) give some indications of that even the 2–4 mm size fraction includes surfaces that are created during the crushing. Using the proposed conceptual model, i.e. that the tracer distribution ratios (R_d) measured for the 1–2 mm size fractions could be directly used as the K_d, could thus be suspected to cause an overestimation of the sorption capacity of the rock.

Sorption results

The results for the sorption coefficients selected from the large database, with application of the conceptual model described in the previous sections are presented in Tables 3-9 to 3-15. Sorption coefficients are thus presented for the different groups of geological material, according to the:

- major rock types
- fracture types
- deformation zone units

Some general comments can be made from the results:

1. Concerning the Sr tracer, the sorption loss from the aqueous phase can only (for a few number of exceptions) be statistically verified for the fresh groundwater. Based on the variation observed for the blank samples, one can roughly estimate that a 10% concentration decrease in the water phase is generally the lowest sorption that can be detected using this method. Given that a 2 g to 8 ml ratio has been used in the experiments, the detection limit for the R_d can be calculated to $5 \cdot 10^{-4}$ m³/kg. This number has, however, varied during the experiment programme; the stability of the blank signal seems to have varied which has caused both higher and lower detection limits. One should, however, consider R_d values in the range of $1 \cdot 10^{-3}$ m³/kg and lower as potential indicators that no sorption has taken place. For the other groundwater types, the high salinity causes a high competition for the adsorption sites, giving very low adsorption. This can be seen in the minimum values, which range into the negative part, indicating that any possible sorption is lower than the variation of the measurements of the blank solution.

2. Besides Sr, the Ra and Cs tracers are highly influenced by the water compositions; as expected with high influence of cation exchange the sorption decreases with increasing salinity.

3. The trivalent actinide/lanthanide is adsorbed to a very high degree; even in the blank sample with groundwater without any geological material present, a severe adsorptive loss of the tracer can be observed, i.e. adsorption on test tube walls. Thorough investigations of these samples have, however, shown that in samples with rock material present, the amount of tracer associated with the test tube walls are negligible compared to the adsorption on the rock material.

4. The trivalent actinide/lanthanide, redox sensitive elements U and Np, as well as Ni are not very much influenced by the salinity. This is in agreement with that the major sorption mechanism for these tracers is supposed to be surface complexation instead of cation exchange. Potentially, the higher concentration of HCO_3^- in the fresh groundwater may have caused aqueous carbonate complexation of Ln-Ac(III) which could explain an indication of lower sorption of this tracer in the fresh groundwater.

5. The sorption of the redox sensitive elements Np and U is comparatively low; indicating a presence of the Np(V) and U(VI) species, respectively (Figure 3-20). This indicates that the laboratory conditions used were not sufficient to achieve the reducing conditions in which the strongly sorbing tetravalent species of these elements dominates, e.g. /Carbol and Engkvist 1997/. However, for some of the measurements, a pronounced increase of the sorption can be found for the smallest size fraction, an increase that is far much higher than what should be expected from the BET surface area measurements. A possible explanation to this is that minerals having reducing capacity have been enriched in the smaller size fraction during the crushing/sieving process.

6. The time dependence of the losses of tracer in the aqueous phase could potentially be regarded as a result of the diffusion rate of the solute into the inner surfaces of the crushed particles. An attempt to calculate the losses of the tracer Cs^+ in the aqueous phase as a function of time by a model consisting of diffusion into spheres /Crank 1975/ is illustrated in Figure 3-21. The result shows that use of the laboratory experiment determined retardation parameters for sorption and diffusivity (the 501056 average values for the K_d and F_f, respectively) gives a reasonable model fit to the experimental results of the time dependence of the sorption in the largest size fractions. This can be regarded as an additional indication of that the retardation properties (diffusivities and sorption) of the larger size particles are very similar to that of the intact rock and that a reasonable penetrative equilibrium has been reached after 180 d of contact time, at least for the Cs tracer. However, the result that the extent of sorption after 1 day is only approximately 30% of that obtained after 180 days seems to indicate that a large proportion of the sorptive surface area of the 1–2 mm size fraction is only accessible by diffusion (i.e. it cannot be considered to be located on external surfaces of the particles). This finding is therefore somewhat contradictory to the postulated assumption under section 3.5.1 that the porosity should mainly consist of grain boundary porosity between larger grains of mm-size. Provided that the sorption surfaces could be related to the porosity, the diffusion characteristics of the batch sorption result indicates that >70% of the porosity is to be considered as intra-granular porosity. One also has to consider that alternative processes (e.g. weathering of the geological material, chemical kinetic effects) may influence the time dependence of the sorption process: i.e. diffusion may not be the only process causing the time dependence.

Table 3-9. Sorption coefficients for 501036 fresh rock type, i.e. the tracer distribution coefficient measured in the 1–2 mm size fraction after 180 days of contact time.

Rock type (SKB code)	Tracer		K_d (m³/kg) Groundwater type				
			Marine	Type V	Saline	Fresh	Brine
501036	**Cs**	**Average**		6.1E-2	2.4E-2	1.5E-1	4.9E-3
Quartz monzo-diorite		σ		1.1E-2	1.8E-2	1.3E-1	4.4E-4
		Median		6.2E-2	1.6E-2	1.4E-1	4.7E-3
		Min-Max		(4.8-7.1)E-2	(7.7-44)E-3	(3.1-30)E-2	(4.6-5.4)E-3
		# samples		3	7	6	3
	Sr	**Average**		3.1E-3	2.9E-3	2.5E-2	-4.1E-4
		σ		1.1E-3	1.7E-3	7.2E-3	4.9E-4
		Median		2.6E-3	3.6E-3	2.6E-2	-6.4E-4
		Min-Max		(2.3-4.3)E-3	(-4.9-45)E-4	(1.7-3.6)E-2	(-7.4-1.5)E-4
		# samples		3	7	6	3
	Ln-Ac (III)	**Average**		1.2E+0	1.4E+0	1.7E-1	4.1E-1
		σ		2.3E-1	7.6E-1	6.6E-2	7.2E-2
		Median		1.1E+0	1.1E+0	1.8E-1	4.5E-1
		Min-Max		(1.0-1.4)E+0	(3.3-26)E-1	(8.4-25)E-2	(3.3-4.6)E-1
		# samples		3	7	6	3
	Ra	**Average**			7.7E-3	2.4E-1	
		σ			3.9E-4	9.3E-3	
		Median			7.8E-3	2.4E-1	
		Min-Max			(7.3-8.1)E-3	(2.3-2.5)E-1	
		# samples			3	3	
	Ni	**Average**			8.4E-2	3.5E-1	
		σ			7.3E-3	3.0E-2	
		Median			8.3E-2	3.4E-1	
		Min-Max			(7.7-9.1)E-2	(3.2-3.8)E-1	
		# samples			3	3	
	Np	**Average**			3.8E-3	5.5E-3	
		σ			2.4E-4	7.8E-4	
		Median			3.7E-3	6.0E-3	
		Min-Max			(3.7-4.1)E-3	(4.6-6.0)E-3	
		# samples			3	3	
	U	**Average**			1.2E-2	5.0E-3	
		σ			1.6E-3	7.8E-4	
		Median			1.2E-2	5.4E-3	
		Min-Max			(1.1-1.4)E-2	(4.1-5.5)E-3	
		# samples			3	3	

Table 3-10. Sorption coefficients for 501046 fresh rock type, i.e. the tracer distribution coefficient measured in the 1–2 mm size fraction after 180 days of contact time.

Rock type (SKB code)	Tracer		Marine	Type V	Saline	Fresh	Brine
					K_d (m³/kg) Groundwater type		
501046, Ävrö quartz-monzo-diorite	Cs	Average		3.3E-2	2.9E-2	1.6E-1	
		σ		3.3E-3	2.7E-3	3.1E-3	
		Median		3.3E-2	2.9E-2	1.6E-1	
		Min-Max		(3.0-3.7)E-2	(2.6-3.2)E-2	(1.6-1.7)E-1	
		# samples		3	3	3	
	Sr	Average		3.7E-3	2.6E-3	1.9E-2	
		σ		8.6E-4	7.0E-4	1.6E-3	
		Median		3.4E-3	2.5E-3	1.9E-02	
		Min-Max		(3.0-4.7)E-3	(1.9-3.3)E-3	(1.7-2.0)E-2	
		# samples		3	3	3	
	Ln-Ac (III)	Average		1.1E+0	1.5E+0	1.5E-1	
		σ		4.7E-1	3.1E-1	6.0E-3	
		Median		1.3E+0	1.4E+0	1.4E-1	
		Min-Max		(5.2-14)E-1	(1.3-1.9)E+0	(1.4-1.5)E-1	
		# samples		3	3	3	
	Ra	Average		4.0E-2	8.1E-3	1.6E-1	
		σ		5.3E-3	1.9E-3	2.4E-2	
		Median		3.8E-2	7.7E-3	1.5E-1	
		Min-Max		(3.7-4.7)E-2	(6.5-10)E-3	(1.4-1.9)E-1	
		# samples		3	3	3	
	Ni	Average		5.7E-2	6.6E-2	3.7E-1	
		σ		1.8E-3	4.2E-3	6.6E-2	
		Median		5.7E-2	6.6E-2	4.0E-1	
		Min-Max		(5.5-5.9)E-2	(6.1-6.9)E-2	(2.9-4.1)E-1	
		# samples		3	3	3	
	Np	Average		-1.7E-4	3.8E-3	3.3E-3	
		σ		2.4E-4	2.4E-4	2.4E-5	
		Median		-1.8E-4	3.7E-3	3.3E-3	
		Min-Max		(-40-8.2)E-5	(3.7-4.1)E-3	(3.3-3.4)E-3	
		# samples		3	3	3	
	U	Average		3.5E-3	4.0E-3	2.9E-3	
		σ		2.9E-4	2.3E-4	4.3E-5	
		Median		3.5E-3	3.9E-3	2.9E-3	
		Min-Max		(3.3-3.8)E-3	(3.8-4.3)E-3	(2.8-2.9)E-3	
		# samples		3	3	3	

Table 3-11. Sorption coefficients for 501030, 501056 and 511058 fresh rock type, i.e. the tracer distribution coefficient measured in the 1–2 mm size fraction after 180 days of contact time.

Rock type (SKB code)	Tracer		K_d (m³/kg) Groundwater type				
			Marine	Type V	Saline	Fresh	Brine
501030, Fine-grained dioritoid	Cs	Average			3.4E-2	2.5E-1	
		σ			1.6E-2	9.8E-3	
		Median			4.2E-2	2.5E-1	
		Min-Max			(1.0-4.3)E-2	(2.5-2.6)E-1	
		# samples			4	3	
	Sr	Average			3.0E-3	3.0E-2	
		σ			2.2E-3	9.4E-3	
		Median			4.0E-3	3.4E-2	
		Min-Max			(-3.2-43)E-4	(1.9-3.6)E-2	
		# samples			4	3	
	Ln-Ac (III)	Average			8.3E-1	1.2E-1	
		σ			4.6E-1	1.7E-2	
		Median			1.4E-1	1.2E-1	
		Min-Max			(8.3-28)E-2	(1.1-1.4)E-1	
		# samples			4	3	
501056, Ävrö grano-diorite	Cs	Average	1.3E-2	2.5E-2	5.5E-3	5.3E-2	5.9E-3
		σ	1.4E-3	1.6E-3	1.1E-3	3.9E-2	4.4E-3
		Median	1.3E-2	2.6E-2	5.7E-3	3.5E-2	5.1E-3
		Min	(1.1-1.3)E-2	(2.3-2.6)E-2	(4.0-6.8)E-3	(2.2-12)E-2	(2.0-13)E-3
		# samples	3	3	6	9	6
	Sr	Average	3.3E-3	3.7E-3	3.9E-4	1.3E-2	1.5E-3
		σ	7.0E-4	2.6E-4	7.2E-4	8.9E-3	2.0E-3
		Median	3.3E-3	3.5E-3	3.1E-4	8.2E-3	1.1E-3
		Min	(2.6-4.0)E-3	(3.5-4.0)E-3	(-5.5-1.7)E-4	(7.0-28)E-3	(-1.9-50)E-4
		# samples	3	3	6	8	6
	Ln-Ac (III)	Average	1.0E+0	1.1E+0	3.4E-1	2.2E-1	3.4E-1
		σ	2.5E-1	1.9E-1	1.1E-1	3.6E-2	3.1E-1
		Median	9.5E-1	1.1E+00	3.1E-1	2.2E-1	3.0E-1
		Min-Max	(8.5-13)E-1	(8.8-12)E-1	(1.9-4.8)E-1	(1.5-2.8)E-1	(5.5-74)E-2
		# samples	3	3	6	9	6
511058, Granite	Cs	Average			1.4E-2	9.8E-2	
		σ			5.3E-4	9.3E-3	
		Median			1.3E-2	9.7E-2	
		Min-Max			(1.3-1.4)E-2	(9.0-11)E-2	
		# samples			3	3	
	Sr	Average			3.2E-3	2.3E-2	
		σ			2.6E-4	1.7E-3	
		Median			3.2E-3	2.3E-2	
		Min-Max			(3.0-3.5)E-3	(2.1-2.4)E-2	
		# samples			3	3	
	Ln-Ac (III)	Average			8.2E-1	1.1E-1	
		σ			1.6E-1	2.3E-2	
		Median			7.7E-1	1.2E-1	
		Min-Max			(6.9-10)E-1	(8.3-13)E-2	
		# samples			3	3	

Table 3-12. Sorption coefficients for fracture material, i.e. the tracer distribution coefficient measured in the <0.125 mm size fraction after 180 days of contact time.

Location used	Fracture type		Tracer		K_d (m³/kg) Groundwater type Saline	Fresh	Brine
KLX03A 457.4	**A**	**<0.125 mm**	**Cs**	**Average**		3.2E+0	
				Min-max		(3.1-3.3)E+0	
				# samples		2	
			Sr	**Average**		1.6E-1	
				Min-max		(1.6-1.7)E-1	
				# samples		2	
			Ln-Ac (III)	**Average**	6.6E+0	8.8E-1	
				σ		1.6E-1	
				Min-max	(5.6-7.6)E+0		
				# samples	2	1	
KLX04A, 951.3	**B**	**<0.125 mm**	**Cs**	**Average**	2.9E-2	2.6E-1	1.6E-02
KLX11A, 509.3				σ	2.0E-2	7.2E-3	8.8E-05
				median	2.9E-2	2.6E-1	1.6E-02
				Min-max	(1.1-4.8)E-2	(2.6-2.7)E-1	(1.6-1.6)E-02
				# samples	6	3	3
			Sr	**Average**	9.6E-4	1.1E-1	1.7E-4
				σ	8.8E-4	7.8E-2	4.9E-5
				median	8.8E-4	7.7E-2	2.0E-4
				Min-max	(1.4-20)E-4	(6.2-20)E-2	(1.2-2.1)E-4
				# samples	6	3	3
			Ln-Ac (III)	**Average**	1.3E+0	3.4E-1	1.3E-1
				σ	5.4E-1	1.3E-1	7.5E-3
				median	1.2E+0	3.9E-1	1.3E-1
				Min-max	(5.0-19)E-1	(1.9-4.3)E-1	(1.2-1.4)E-1
				# samples	6	3	3
KSH02, 578.2	**C**	**<0.125 mm**	**Cs**	**Average**	1.9E-1	3.5E-1	1.1E-2
KLX04A, 874.5				σ	1.8E-1	5.0E-2	
KLX07A, 620.9				**median**	1.8E-1	3.4E-1	
				Min-max	(2.4-39)E-2	(3.0-4.1)E-1	(1.1-1.2)E-2
				# samples	6	5	2
			Sr	**Average**	1.7E-3	3.8E-1	7.4E-4
				σ	6.2E-5	1.5E-1	
				median	1.6E-3	3.9E-1	
				Min-max	(1.6-1.7)E-3	(1.6-5.5)E-1	(6.2-8.7)E-4
				# samples	3	5	2
			Ln-Ac (III)	**Average**	9.3E-1	3.8E-1	5.6E-1
				σ	9.6E-1	4.3E-1	
				median	7.6E-1	7.5E-2	
				Min-max	(0.5-22)E-1	(6.1-87)E-2	(4.4-6.7)E-1
				# samples	6	5	2
	D		**No data**				
	E		**No data**				
KLX03A 278.3	**F**	**<0.125 mm**	**Cs**	**Average**	3.0E+0	3.2E+0	
				σ	1.5E+0	4.7E-1	
				# samples	1	1	
			Sr	**Average**	3.0E-3	1.6E-1	
				σ	9.7E-4	2.2E-2	
				# samples	1	1	
			Ln-Ac (III)	**Average**	9.3E+0	1.2E+0	
				σ	1.9E+0	2.2E-1	
				# samples	1	1	
	G		**No data**				
	H		**No data**				
	I		**No data**				

Table 3-13. Sorption coefficients for deformation zone units, i.e. the tracer distribution coefficient measured in the 0.063–0.125 mm size fraction (unless other specification) after 180 days of contact time.

Zone category / sample location	Tracer		K_d (m³/kg) Groundwater type			
			Type V	Saline	Fresh	Brine
Deformation zone unit type 1, Fault gouge	Cs	Average		6.0E-1	5.1E+0	
		σ		2.7E-2		
		Median		5.9E-1		
KLX06A, 384.0 m (size fraction <0.125 mm)		Min-max		(5.8-6.3)E-1	(4.8-5.5)E+0	
		# samples		3	2	
	Sr	Average		1.8E-3	1.4E-1	
		σ		5.3E-5		
		Median		1.8E-3		
		Min-max		(1.7-1.8)E-3	(9.6-19)E-2	
		# samples		3	2	
	Ln-Ac (III)	Average		2.6E+0	2.5E+0	
		σ		1.7E+0		
		Median		1.7E+0		
		Min-max		(1.5-4.5)E+0	(2.3-2.7)E+0	
		# samples		3	2	
Deformation zone unit type 3, Porous episy-enitic wall rock	Cs	Average		1.2E-1	6.9E-1	
		σ		3.2E-2	1.3E-1	
		Median		1.3E-1	6.5E-1	
		Min-max		(9.1-15)E-2	(5.8-8.3)E-1	
KSH03A , 164.8 m		# samples		3	3	
	Sr	Average		3.9E-3	6.5E-2	
		σ		1.0E-3	1.4E-3	
		Median		3.5E-3	6.5E-2	
		Min-max		(3.1-5.0)E-3	(6.4-6.7)E-2	
		# samples		3	3	
	Ln-Ac (III)	Average		1.3E+0	5.2E-1	
		σ		1.1E+0	9.5E-2	
		Median		8.5E-1	5.3E-1	
		Min-max		(5.4-25)E-1	(4.2-6.1)E-1	
		# samples		3	3	
Deformation zone unit type 5, Strongly oxidized wall rock	Cs	Average	1.1E-2	1.7E-3		4.9E-4
		σ	1.0E-3	1.3E-4		1.6E-4
		Median	1.1E-2	1.7E-3		5.6E-4
		Min-max	(1.0-1.2)E-2	(1.6-1.9)E-3		(3.1-6.0)E-4
KLX02, 936.1 m		# samples	3	3		3
	Sr	Average	4.0E-3	-3.3E-5		-5.3E-5
		σ	5.3E-4	6.2E-4		2.7E-4
		Median	4.0E-3	-9.8E-5		-5.2E-5
		Min-max	(3.4-4.5)E-3	(-6.1-6.1)E-4		(-3.2-2.2)E-4
		# samples	3	3		3
	Ln-Ac (III)	Average	1.7E+0	1.7E-1		2.6E-1
		σ	3.7E-1	3.0E-2		1.6E-2
		Median	1.9E+0	1.7E-1		2.7E-1
		Min-max	(1.3-1.9)E+0	(1.4-2.0)E-1		(2.5-2.7)E-1
		# samples	3	3		3

Table 3-14. Sorption coefficients for deformation zone units type 2, i.e. the tracer distribution coefficient measured in the <0.125 mm size fraction.

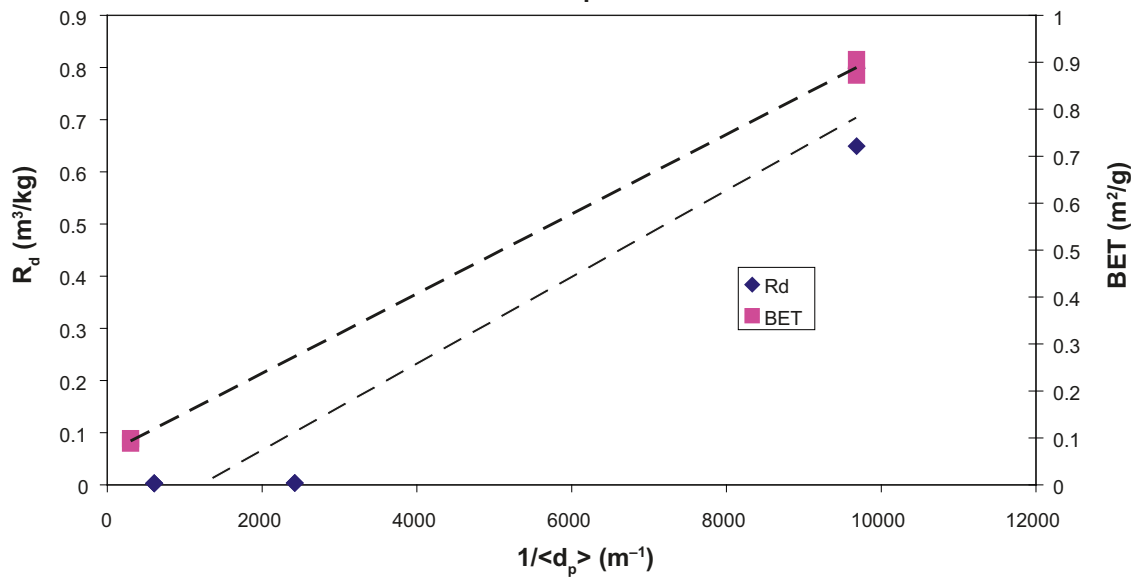| Def. zone unit / sample location	Tracer		K_d (m³/kg) Groundwater type	
			Saline	Fresh
Deformation zone unit type 2, Chlorite	**Cs**	**Average**	1.7E-2	4.0E-1
		σ	1.4E-3	8.2E-2
		# samples	1	1
KLX03A , 732.6 m	**Sr**	**Average**	5.1E-3	3.8E-2
		σ	2.3E-3	4.6E-3
		# samples	1	1
	Ln-Ac (III)	**Average**	9.5E+0	1.2E+0
		σ	2.7E+0	3.4E-1
		# samples	1	1
	Ra	**Average**	2.9E-2	1.7E+0
		σ	2.9E-3	2.0E-1
		# samples	1	1
	Ni	**Average**	1.2E+0	1.0E+0
		σ	5.2E-1	4.8E-1
		# samples	1	1
	Np	**Average**	4.7E-2	2.1E-1
		σ	7.2E-3	7.8E-3
		# samples	1	1
	U	**Average**	3.5E+0	4.0E-2
		σ	2.7E-1	1.8E-3
		# samples	1	1

Table 3-15. Sorption coefficients for deformation zone units type 4, i.e. the tracer distribution coefficient measured in the <0.125 mm size fraction after 180 days of contact time.

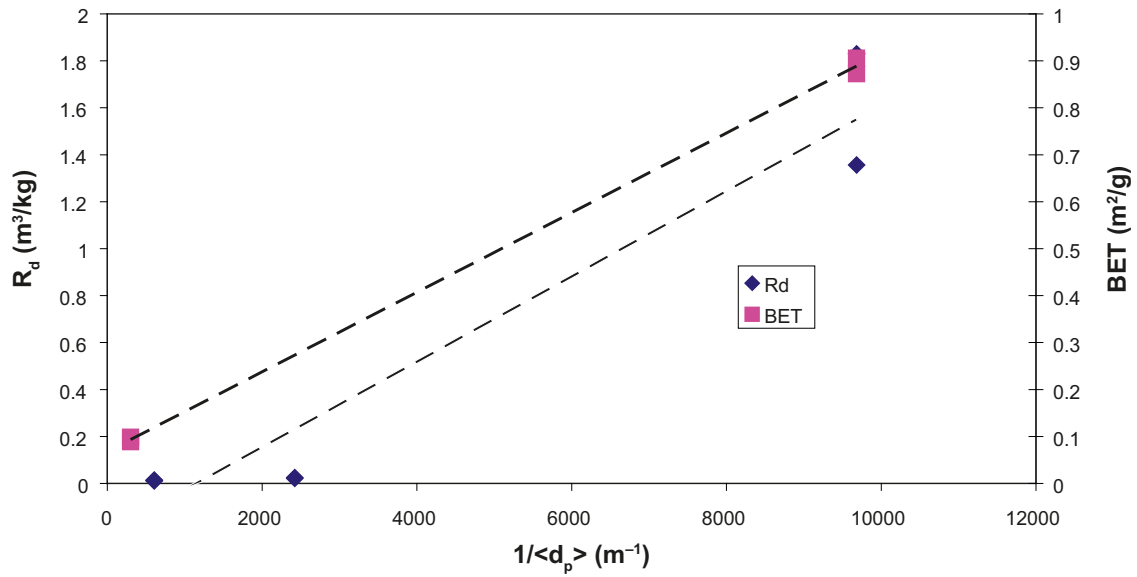| Def. zone unit / sample location	Tracer		K_d (m³/kg) Groundwater type	
			Saline	Fresh
Deformation zone unit type, Type 4, Cataclasite (with mylonitic banding).	**Cs**	**Average**	8.5E-2	7.6E-1
		σ	7.6E-3	1.9E-1
		# samples	1	1
	Sr	**Average**	1.0E-2	3.3E-2
KSH02, 397.4 m		σ	3.7E-3	4.0E-3
		# samples	1	1
	Ln-Ac (III)	**Average**	5.6E+0	4.4E-1
		σ	1.0E+0	8.1E-2
		# samples	1	1
	Ra	**Average**	1.9E-1	1.9E+0
		σ	2.1E-2	1.1E+0
		# samples	1	1
	Ni	**Average**	5.2E-1	9.0E-1
		σ	1.1E-1	5.1E-1
		# samples	1	1
	Np	**Average**	8.1E-2	2.3E-1
		σ	1.2E-2	8.5E-3
		# samples	1	1
	U	**Average**	5.8E+0	5.9E-2
		σ	4.4E-1	2.6E-3
		# samples	1	1

Figure 3-20. *Sorption of Np (upper) and U (lower) as function of the inverse of the particle size of the crushed rock material. The results of the corresponding BET surface area measurements are also presented in the figure.*
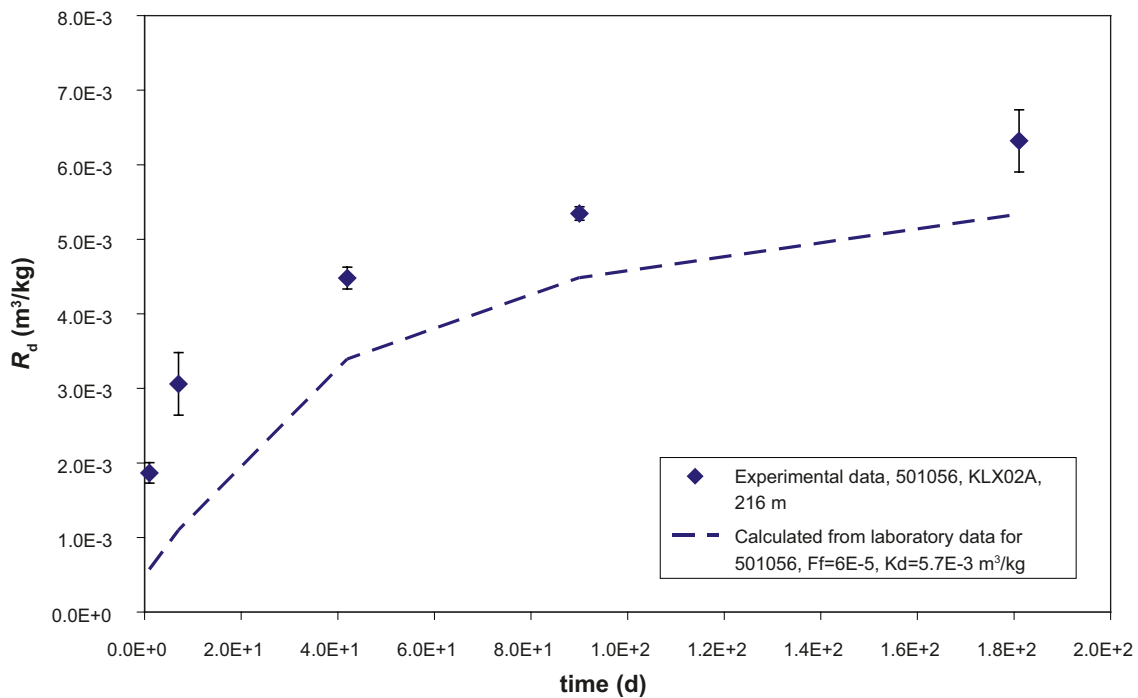
Figure 3-21. *Sorption (i.e. the tracer distribution ratio, Rd) of Cs as a function of contact time, given for the rock type 501056. Experimental results are given in comparison to a prediction using a model consisting of diffusion in a sphere /Crank 1975/ together with the average values of the diffusivity of the K_d and the D_e (=$F_f D_w$) determined for the 501056 rock type.*

3.6 Confirmation studies

The retardation data used in this model can be criticized due to the fact that the major mechanisms for radionuclide retardation (i.e. diffusion into the rock matrix and adsorption) are not studied interactively and are mainly addressed using disturbed rock material. At least for confirmation purposes, it would be advantageous to be able to see if the retardation parameters determined on a very small scale can be used to correctly predict radionuclide retardation on a larger scale.

Although not being part of the strategy /Widestrand et al. 2003/ proposed for determining retardation parameters, two sets of experiments will be presented in which the retardation will be addressed to intact drill cores:

- Radionuclide adsorption on intact drill cores. (Byegård et al. in prep.)

- Adsorption of Cs using electromigration in order to reduce the time for reaching a diffusion equilibrium; methods, data and evaluation procedures according to /André et al. 2008ab/.

- It should be emphasized that the studies presented under this section is intended only for confirmation purposes and are not addressed during the retardation data summary in Chapter 4.

3.6.1 Adsorption studies using intact drill cores
Diffusion and sorption on intact drill core samples

In these experiments the diffusion cells used for the through-diffusion experiments were spiked with a radionuclide cocktail on one side of the cell. The loss of tracer in the injection cell of the diffusion cell was thereafter studied as a function of time. According to the sorption concept used, the rate of losses should be dependent on the diffusivity as well as the sorption coefficient. A prediction of the expected rate of loss of tracer in the injection cell was made (based on the analytical solution for diffusion in a sheet /Crank 1975/), based on the:

- Diffusivity, based on the formation factor determined for that particular diffusion cell using HTO as tracer combined with the tabulated water diffusivity of the tracer.

- K_d values determined for that particular rock type.

83

Two sets of comparisons are presented in this report, one is for the Cs adsorption on the 501036 rock type and the other is for Cs adsorption on the 501056 rock type. Both examples refer to the use of saline Laxemar groundwater as the aqueous phase. The results, Figure 3-22 show an underestimation of the sorption rate for the prediction using the laboratory retardation data (i.e. K_d and F_f) compared to the experimentally obtained results. For that reason, an attempt was made to perform calculations in which either the K_d or the F_f has been varied in order to obtain the best fit to the experimental results. The results show that:

- For the 501036 rock type, the best fit is obtained either by increasing the laboratory determined K_d of $1.6 \cdot 10^{-2}$ m³/kg to $4.7 \cdot 10^{-1}$ m³/kg or by increasing the laboratory determined F_f of $1.8 \cdot 10^{-5}$ to $5.2 \cdot 10^{-4}$, i.e. in both cases an increase by a factor of approximately 30.

- For the 501056 rock type, the best fit is obtained either by increasing the laboratory determined K_d of $5.7 \cdot 10^{-3}$ m³/kg to $2.2 \cdot 10^{-2}$ m³/kg or by increasing the laboratory determined F_f of $3.2 \cdot 10^{-4}$ to $1.2 \cdot 10^{-3}$, i.e. in both cases an increase by a factor of approximately 4.

Considering the variations and the uncertainties associated to the diffusivity and sorption data, the results from the 501056 case indicate no severe deviation from conceptual sorption model. However, for the results of the 501036 case, the differences of up to a factor 30 between the batch sorption /through-diffusion data and the calibrated data could be indicative of conceptual mismatches. A possible explanation to the differences could be that the sorption of Cs due to the low diffusivity to a vast majority takes place at the low penetration depth of the rock sample. Using a homogenous diffusion-sorption model one can estimate the average penetration depth to less than 0.4 mm, which would indicate that basically no or very little interaction takes place behind the first crystal layer of the rock. It is therefore possible that sampling disturbances during the sawing of the drill core sample causes increased surface areas as well as increased numbers of micro fractures at these low sample depths which can increase the sorption as well as the diffusion.

3.6.2 Electromigration sorption studies

Comparative studies on adsorption on crushed rock material in different size fractions in combination with adsorption studies on intact drill core have been performed by /André et al. 2008ab/. In these experiments, the adsorption on intact drill core was done by applying an electrical field which speeded up the migration rate of the sorbing tracer, Cs, in the experiment, i.e. diffusive equilibrium was expected to be reached in a much shorter time.

Parallel to this, BET surface area measurements were performed using both the crushed material in different size fractions as well as intact drill cores.

The results (Figure 3-23) show that the BET surface area actually decrease with a factor of 15 going from crushed 1–2 mm size fraction to intact drill core samples. This decrease is even higher than what is proposed from the conceptual model, described in Section 3.5.1, indicating a potential conclusion that addressing results of the 1–2 mm size fraction as representative of intact rock could be an overestimation of the sorption capacity. Regarding the sorption results of Cs in the same series of experiment, it is found that the decrease in sorption between the largest size fraction and the intact rock is not as high as the difference in corresponding BET surface area results; a factor of 5 is indicated. This decrease in K_d is not fully understood and must probably be further investigated. A similar exercise performed for the Forsmark case /Byegård et al. 2009/ gave less than a factor 2 deviation between the BET on intact drill core and 1–2 mm size fraction; combined with a corresponding difference in K_d of a factor 7. Hence the trend does not seem to be fully consistent. However, the general assumption that crushed rock gives extra surfaces that are non-representative for intact rock is not contradicted by the results.

For the data presentation in Chapter 4, it has been decided to maintain the results obtained for the 1–2 mm size fraction. However, if future similar experiments can confirm the trend that crushed material even in the 1–2 mm size fraction overestimates the sorptivity of intact rock, one should address the question of a necessary reduction of the K_d for intact rock.
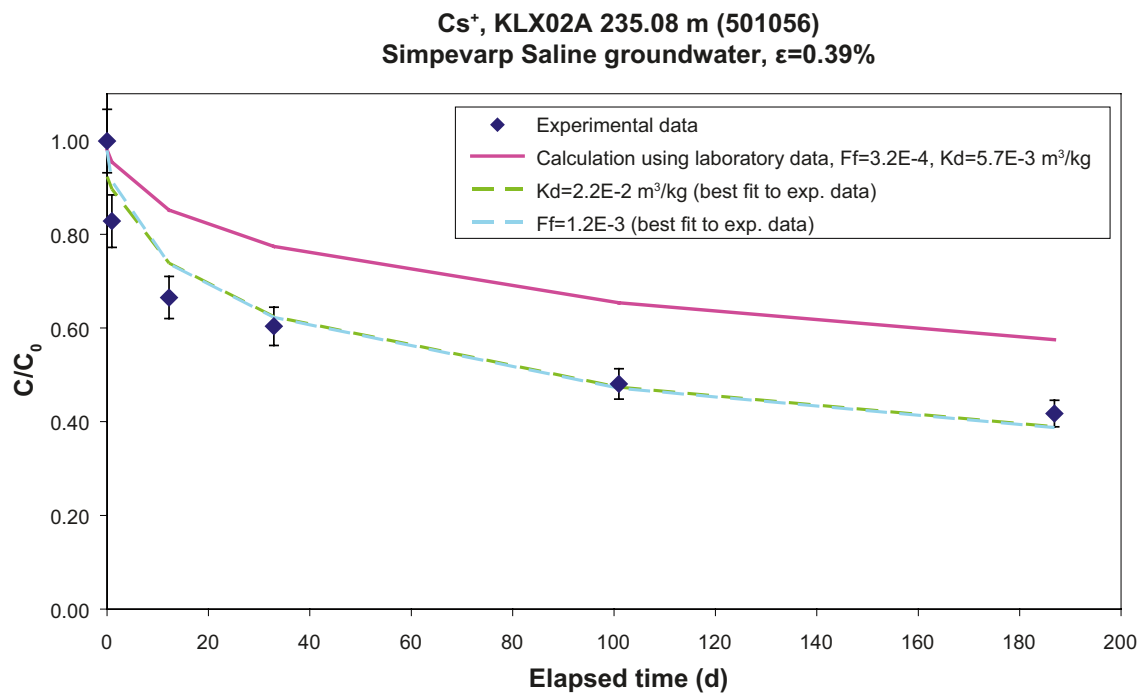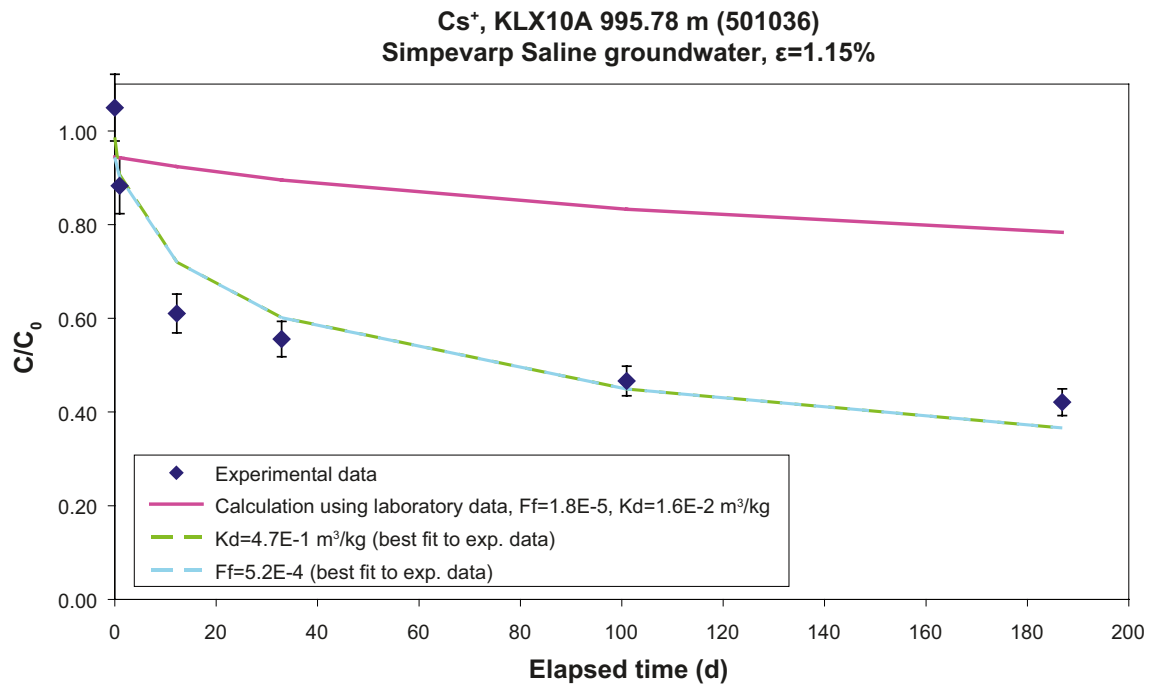
Figure 3-22. *Results of the adsorption experiments using intact rock pieces, see text for details .The C/C$_0$ refers to the part of the added tracer remaining in the aqueous phase; i.e. the figure illustrates the depletion of the aqueous tracer concentration with time. Comparative results are also given for calculation using the laboratory data (solid lines), as well as for the cases in which the K$_d$ and the F$_f$, respectively, has been varied in order to obtain the best fit to the experimental results (dashed lines).*
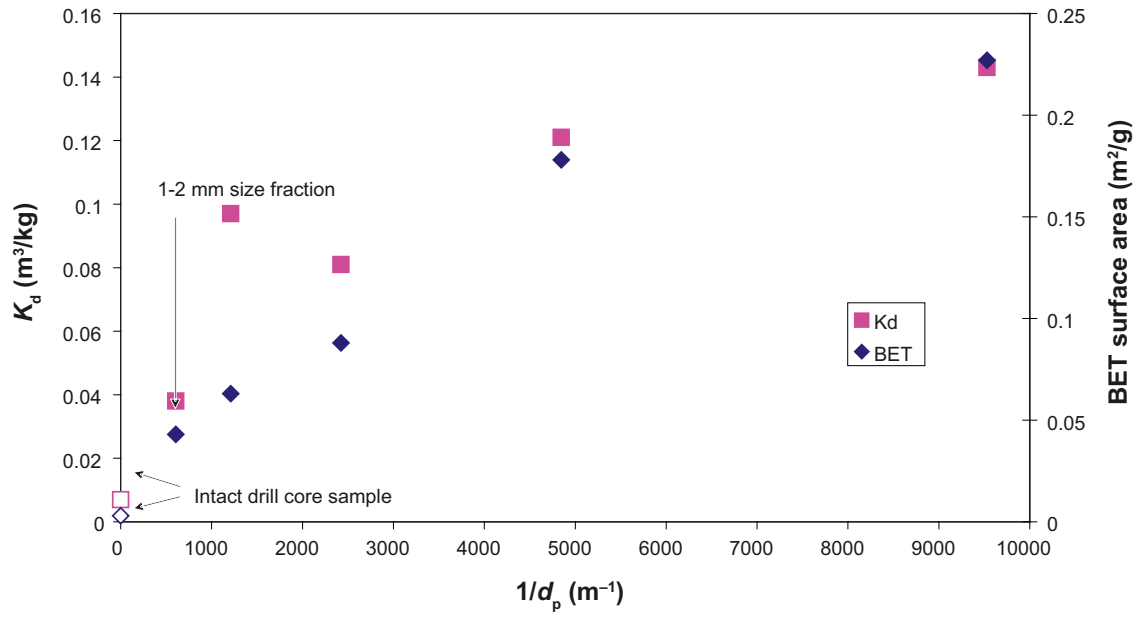
Figure 3-23. *Results of the batch experiments of Cs on crushed material given in comparison with the electromigration-induced sorption studies using intact drill core. The results of the corresponding BET surface area measurements are given in the same figure. All results of the crushed rocks are given with filled markers (diamonds for K_d, squares for BET) while non-filled markers are used for the intact drill core samples.*

4 Retardation model

In accordance with the general concept for a site descriptive retardation model proposed by /Widestrand et al. 2003/, the model should consist of tables in which the geological description is combined with the selected transport parameters for each unit (rock mass or fracture types or deformation zone units, i.e. the different geological units where retardation of radionuclides can take place) are given.

4.1 Methodology

The developed retardation model description consists of three sections, one for the major rock types, and one for the fracture types and deformation zone units, respectively. In the first section, the retardation characteristics of the major rock types, i.e. rock matrix interaction parameters, are described. The second section provides a description of the retardation in the water-conducting fractures and in the third section retardation parameter description for the deformation zone units are described.

For the numerical values presented in the retardation model tables, they are referred to the data part of this report (Chapter 3) where the different experimental details and discussions concerning the uncertainty are given.

4.1.1 Selection and presentation of retardation data

According to the retardation concept applied in the present work (cf. Section 1.2 and Chapter 3), the retardation of radionuclides in the rock matrix can be described using the parameters listed below.

- *Rock matrix porosity, θ_m (-):* The results from the water saturation porosity measurements on site-specific rock materials have been selected in this work (cf. Table 3-1).

- *Rock matrix formation factor, F_f (-):* This parameter is used to multiply literature values of the radionuclide-specific free diffusivities in water (D_w (m^2/s); a tabulation is given by, e.g. by /Ohlsson and Neretnieks 1997/) to obtain the effective diffusivities, D_e (m^2/s), for the different radionuclides. Values given in the retardation model tables refer to the values obtained by the through-diffusion method using tritiated water which is motivated by the use of the identical physical process in these studies. However, the considerably lower formation factors (leading to a generally lower diffusivity of the radionuclides) obtained from the in situ electrical resistivity measurements should be considered, since they could indicate that measurements on sampled rock material could have been exposed to stress release and/or mechanical damage causing a general overestimation of the formation factors. Since this hypothesis has not been fully confirmed, it is in this stage only referred to a possible factor (the observed difference between formation factor determined by in situ resistivity and determined by through diffusion experiment, determined to 19±17 in Section 3.4.3) to reduce the formation factors presented in the retardation model tables because of potential influence of stress release and/or mechanical damage for the laboratory samples. It should also be emphasized that the retardation model tables are mainly aimed for identifying relative differences in retardation properties of the different rock types.

Further discussions of how to address the in situ electrical resistivity measurements are found in Appendix C in /Crawford and Sidborn 2008/.

- *Rock matrix sorption coefficient, K_d (m^3/kg):* Values presented in the retardation model tables are based on the following assumptions (more thoroughly motivated in Chapter 3)
  - o For the samples representing matrix rock which has undergone sawing, crushing and sieving, the results from the 1–2 mm size fraction with the 0.5 years contact time has been selected, i.e. choosing the tracer distribution ratio directly as the K_d.
  - o For the samples representing fracture coating and/or fracture filling, the samples have been collected in their natural form (no crushing process) and the results from smallest size fraction (<0.125 mm or 0.063–0.125 mm) with 0.5 years contact time has been selected. Also for this case, the tracer distribution ratio has directly been adopted as the K_d.

The same selection concept has been applied in the presentation of the other parameters closely related to the sorption, i.e. the specific surface area measurements (BET) and the Cation Exchange Capacity (CEC).

For simplicity of the overview of the tables, presentation of sorption coefficients from a tracer point of view has been restricted to Cs^+ (ion exchange sorbing tracer) and a trivalent lanthanide actinide (more specifically, Am(III) or Eu(III), expected to be influenced by surface complexation). Furthermore, only results for the use of a saline groundwater composition are included in the tables; one exception has been made for a case where the Cs sorption coefficient was only available for fresh groundwater. For sorption coefficients for other tracers and/or other groundwater compositions, the reader is directed to Tables 3-9 to 3-15.

The uncertainties presented in the retardation tables are given according to the strategy outlined in Section 3.2.

4.1.2 Rock types

For the presentation of retardation data of the matrix rock, the data is presented according to their respective rock type. Alternative concepts used for sub-division within the Laxemar site investigation (e.g. rock domain concept, fracture domain concept, hydraulic rock domain concept) are not used for the retardation model presentation. The motivation for this is mainly the strategy set for the retardation model /Widestrand et al. 2003/ which stipulates a mineralogical approach on the retardation description. Furthermore, the attempt to represent porosity using the alternative concepts (cf. Section 3.3.4) gave no indication of less variation within the sub-divided groups using any of the alternatives.

For the rock mass, the following retardation parameters are included in the tables:

*   Porosity.
*   Formation factor (to be used in calculations of the diffusivities of the different radionuclides, as described in Chapter 3).
*   Specific surface area (BET).
*   Cation exchange capacity (CEC).
*   Sorption distribution coefficients, K_d (m³/kg).

4.1.3 Fracture types and deformation zone units

Retardation capacity in the vicinity of fractures and in deformations zones are of particular interest since the water transport occurs here. Even though diffusion of any potentially escaped radionuclide in to the microfractures and/or the grain boundary porosity of the rock followed by adsorption has often been considered as the major retardation mechanism, one must be aware of that the fractures are the starting place for the retardation processes. The finding of strongly increased specific surface area for the fracture material may also give a substantial impact of the importance of the fracture material to the total retardation of radionuclides.

In the retardation modelling, the following parameters of obvious importance of the retardation process will be given for the different fracture types and deformation zone units, identification according to Table 2-4 and Table 2-5, respectively:

*   Thickness of the fracture coatings.
*   Porosity.
*   Formation factor (to be used in calculations of the diffusivities of the different radionuclides).
*   Specific surface area (BET).
*   Cation exchange capacity (CEC).
*   Sorption distribution coefficients, K_d (m³/kg).
*   Mineral contents.

For the fracture types the following data on each particular type will also be given:

- Abundance (percentage) of the fracture type, i.e. a quantification of how large portion of the entire fracture class of open fractures for which the given description is valid.

- Abundance (percentage) of the transmissive fracture type, i.e. a quantification of how large portion of the entire fracture class of transmissive fractures for which the given description is valid.

- Wall rock alteration depth.

The description of the retardation properties of the fractures and deformation zone units are made on a stand-alone basis and addressing of their respective location in Rock domains, Fracture domains and Hydraulic domains is not performed. The rationale for this is based on the results given in Section 2.2.1 where any significant difference in distribution of fracture types is found neither for the Rock domains nor for the Fracture domain concepts.

4.2 Retardation model

4.2.1 Rock types

The retardation properties for the different rock types involved in the Laxemar site description are summarized in Table 4-1. In the table, results are presented for all rock types that are present in the RSMA01, RSMD01 and RSMM01 rock domains, respectively, with an occurrence of more than 2%.

Summary of retardation properties of the rock types

The data presented below for the different rock types indicate that there are generally no significant differences in the retardation properties between the rock types. Furthermore, when also considering the variation reported for the parameter values (cf. data tables in Chapter 3) there are very few indications of significant differences between the different rock types. The minor differences that can be observed are e.g. that:

- 501030 and 501036 have low porosities and 501046 the highest porosity

- 501046 has a higher formation factor than the other rock types. As is earlier pointed out, the data is based on a large deep sample group (KSH01 891.69-891.94 m), i.e. 8 out of 9 samples in the group represent the same location. Consequently, the coverage for 501046 at Laxemar is very poor.

- 501056 has the lowest sorption coefficient for Cs, Sr and Ln-Ac than the other rock types in saline water. However, no rock type shows a clear difference in sorption strength for the fresh groundwater type. It should be noted that the data compared originates from a few sample positions only per rock type (measured in triplicates). The ratio between the most strongly sorbing rock type and the weakest sorbing rock type for a given tracer range from about 4 to 8 in saline water and 2 to 5 in fresh water for Cs, Sr and Ln-Ac. The impact of water chemistry is summarised in section 3.5.3.

- The CEC values seem to be very close to each other. It should be noted that the uncertainty in the CEC-values are roughly ±50% since the CEC is closely above the detection limit for crushed rock. Thus, any correlation with BET or sorption coefficients is hidden by the uncertainty in CEC.

It should also be noted that the shift of focus area during the investigation process has lead to an uneven distribution of samples with regards to the focus area of today. Approximately half of all samples are from Simpevarp and the other half has an overweight of samples in RSMA01 and fewer samples in RSMD01. However, only small differences are found in porosity between the two sites as is shown in Section 3.3.2 and Table 3-3.

Table 4-1. Suggested transport parameters for the rock types (more than 2% occurrence), expressed with rock codes within the dominant rock domains RSMA01, RSMD01, RSMM01 and RFMBA03.

	501030, Fine-grained dioritoid	501033, Diorite / Gabbro	501036, Quartz monzodiorite	501046, Ävrö Quartz monzodiorite	501056, Ävrö Granodiorite	501058, Granite	505102, Fine-grained diorite-gabbro	511058, Fine-grained granite
Porosity (vol%)	0.23±0.26	0.06	0.19±0.19	0.35±0.14	0.32±0.15	0.61	0.16±0.06	0.27±0.19
Formation factor	(6.6±11)E-05	-	(1.1±1.2)E-04	(4.1±1.6)E-04	(1.5±1.7)E-04	-	9.8E-05	(4.5±1.5)E-05
BET (m²/g)	0.048±0.032	0.032±0.025	0.036±0.028	0.043±0.017	0.033±0.022	-	0.079	0.094±0.064
CEC (cmoles/kg)	1.0±0.6	-	1.0±0.7	0.9±0.7	<1.0	-	-	-
K_d (m³/kg) (here only exemplified by the Kd for Cs in saline Simpevarp groundwater, full coverage of sorption data cf. Tables 3-9 to 3-11)	3.4±1.6E-2	-	(2.4±1.8)E-2	(2.9±0.3)E-2	(5.5±1.1)E-3		-	(1.4±0.1)E-2

4.3 Fracture types

Retardation parameters for the identified fracture types are given in Tables 4-2 to 4-10.

Three imports of data, due to shortage of experimentally measured data for the actual fracture types of the Laxemar area, have been performed for the retardation properties of the fracture types:

- Fracture group D (Laumontite) has been given retardation data according to the data for the Laumontite fractures studied in the Forsmark area /Byegård et al. 2009/. The two types of Laumontite fractures have by the authors been considered as similar enough to allow this import.

- The data for the porosity of the fracture coating of Fracture type E (Chlorite and Calcite) are based on the elaborate investigation of a similar fracture in the LTDE-SD experiment performed at the Äspö Hard Rock Laboratory /Widestrand et al. 2009, in prep/. The porosity of the thin fracture coating was in this investigation determined by PMMA technique as exemplified in Figure 3-7.

- The retardation properties of the chlorite fracture coating in Fracture type G has been imported from the investigation of the corresponding chlorite deformation zone unit, cf. Section 4.4. This seems motivated since these two features are considered to consist of the same mineralogy; the only major difference is the thickness of the chlorite layers.

Table 4-2. Retardation model for Fracture group A.

	Fracture coating
	Calcite + Chlorite + Pyrite and/or Chalcopyrite ± other
Thickness	0.2–1 mm
Porosity	n/a
Formation factor	n/a
BET surface area (m^2/g)	15±9
CEC (cmoles/kg)*	40±13
Sorption properties, K_d (m^3/kg),	Cs: 3.0 (fresh groundwater) Ln-Ac (III): 7.0 (saline Simpevarp groundwater)
Percentage of all open fractures	7%
Percentage of transmissive fractures	10%
Wall rock alteration	≤ 10 mm

* <0.125 mm fraction. BET value for this fraction = 2.8 m^2/g

Table 4-3. Retardation model for Fracture group B.

	Fracture coating
	Epidote and/or Prehnite and/or Adularia ± chlorite ± quartz ± calcite
Thickness	0.5–1 mm
Porosity	n/a
Formation factor	n/a
BET surface area (m^2/g)	6±2
CEC (cmoles/kg)	n/a
Sorption properties, K_d (m^3/kg), saline Simpevarp ground-water	Cs: (3±2)E-2 Ln-Ac (III): 1.3±0.5
Percentage of all open fractures	8%
Percentage of transmissive fractures	5%
Wall rock alteration	~ 20 mm

Table 4-4. Retardation model for Fracture group C.

	Fracture coating *Hematite* ± other
Thickness	0.5–5 mm
Porosity	n/a
Formation factor	n/a
BET surface area (m²/g)	13±11
CEC (cmoles/kg)	12–24
Sorption properties, K_d (m³/kg), saline Simpevarp ground-water	Cs: (1.9±1.8)E-1 Ln-Ac (III): (9.3±9.6)E-1
Percentage of all open fractures	10%
Percentage of transmissive fractures	9%
Wall rock alteration	≤ 50 mm

Table 4-5. Retardation model for Fracture group D.

	Fracture coating *Laumontite* ± calcite ± chlorite
Thickness	0.2–2 mm
Porosity	n/a
Formation factor	n/a
BET surface area (m²/g)*	0.42±0.02
CEC (cmoles/kg)*	18±5
Sorption properties*, K_d (m³/kg), saline groundwater	Cs: 1.6E-2 Ln-Ac(III): 1.2
Percentage of all open fractures	0.3%
Percentage of transmissive fractures	0.3%
Wall rock alteration	≤ 20 mm

*Based on results obtained in Forsmark retardation model 2.3 /Byegård et al. 2009/.

Table 4-6. Retardation model for Fracture group E.

	Fracture coating *Chlorite + Calcite* ± oxidized walls ± saussuritized walls
Thickness	0.2–0.5 mm
Porosity	3–5%*
Formation factor	n/a
BET surface area (m²/g)	2.2
CEC (cmoles/kg)	n/a
Sorption properties	n/a
Percentage of all open fractures	23%
Percentage of transmissive fractures	20%
Wall rock alteration	≤ 10 mm

* Based on results from the SKB LTDE-SD experiments /Widestrand et al. 2009, in prep./.

Table 4-7. Retardation model for Fracture group F.

	Fracture coating
	Clay ± other
Thickness	0.2–5 mm
Porosity	n/a
Formation factor	n/a
BET surface area (m^2/g)	24
CEC (cmoles/kg)	n/a
Sorption properties, K_d (m^3/kg), saline Simpevarp groundwater	Cs: 3.0 Ln-Ac (III): 9.3
Percentage of all open fractures	21%
Percentage of transmissive fractures	27%
Wall rock alteration	≤ 50 mm

Table 4-8. Retardation model for Fracture group G.

	Fracture coating
	Chlorite +/- other
Thickness	~ 0.2 mm
Porosity	0.9
Formation factor	n/a
BET surface area (m^2/g)*	7.9
CEC (cmoles/kg)*	13±2
Sorption properties, K_d (m^3/kg), saline groundwater*	1.7E-2
Percentage of all open fractures	11%
Percentage of transmissive fractures	7%
Wall rock alteration	≤ 50 mm

* Data from deformation zone unit 2. Fracture group G is supposed to have virtually the same retardation properties as the deformation zone unit 2 (cf. Table 4-11).

Table 4-9. Retardation model for Fracture type H.

	Fracture coating
	No mineral
Thickness	n/a
Porosity	*
Formation factor	*
BET surface area (m^2/g)	*
CEC (cmoles/kg)	*
Sorption properties*	*
Percentage of all open fractures	3%
Percentage of transmissive fractures	4%
Wall rock alteration	≤ 10 mm

* The retardation properties are referred to the properties of the non-altered rock types.

Table 4-10. Retardation model for Fracture type I.

	Fracture coating
	Calcite +/- other
Thickness	~0.2 mm
Porosity	n/a
Formation factor	n/a
BET surface area (m²/g)	n/a
CEC (cmoles/kg)	n/a
Sorption properties	n/a
Percentage of all open fractures	11
Percentage of transmissive fractures	13%
Altered rock surrounding the fracture?	≤ 10 mm

Summary of retardation properties of fractures

For the different fracture types for which retardation models have been set up, a thin layer of fracture coating (0.1–5 mm) has been identified for all of them except the G and H types. Due to their limited thickness and to the fact that they sometimes were not consolidated, porosity and/or diffusivity determinations were not possible to perform. There are data from the LTDE-SD project /Widestrand et al. 2009, in prep/ for Type E that shows an increased porosity in chlorite-calcite layers of 3–5% and the PMMA-measurements also show increased porosity in fracture coatings /Penttinen et al. 2006/. Thus, it is likely that these layers are characterized by a higher porosity and therefore a higher diffusivity (i.e. formation factor). Altogether, it therefore seems motivated in a realistic time perspective for modelling to consider the entire fracture coatings/fillings to be in immediate contact with flowing water and that the retardation caused by the interaction of these materials could be treated as a surface effect.

The measured BET surface areas of the fracture materials are significantly higher than the corresponding BET surface areas of samples from the rock mass. They vary from 2 m²/g to 24 m²/g, which is in the order of 100–300 times higher than the corresponding range for the rock types. This finding indicates that fractures with their content of material with high specific surfaces constitute a considerable source for adsorption of any dispersed radionuclide. The finding is supported by the 10 to 40 times higher CEC-values for Fracture type A and C compared to the CEC values of the rock types.

However, the large difference found for the BET values between fracture material and intact rock is not accompanied by a similar trend for the K_d values. For this case the differences are much more moderate, e.g. the sorption of Cs is a factor of 1–100 higher than the corresponding value for adsorption of Cs on intact 501046. Compared to the 100–300 times higher BET values it is an indication that the high measured BET surface areas for fracture material cannot be directly interpreted as a corresponding sorption capacity of the fracture material. Since Cs is considered to adsorb mainly by cation exchange, it is not so unexpected that the increase in available surface area does not necessarily give higher sorption coefficients. For example, any presence of iron oxides gives high values BET surface area but is not expected to give selective cation exchange sites. Furthermore, increased BET surface area caused by presence of small clay particles is not expected to cause a very significant increase in sorption for radionuclides that adsorb by surface complexation, e.g. trivalent actinides/lanthanides and Ni.

4.4 Deformation zone units

During and after the effort to parameterize and give retardation properties to deformation zone units, some conclusions and simplifications were made:

- Deformation zones at Laxemar display a wide spectrum of brittle, brittle-ductile and hydrothermal alteration, together with parts of unaltered bedrock. Consequently, it is not possible to give specific retardation properties for every single deformation zone because of their internal complexity (e.g. along borehole sections) in addition to the variations between the zones. A concept of how to deterministically describe retardation properties for a deformation zone is exemplified in Section 2.2.2; otherwise, only an identification of important deformation zone units (Table 2-5) together with their respective retardation properties are presented in this section.

- Even though deformation zones are complex, varying in composition and even contain undeformed rock, five categories of altered bedrock have been possible to distinguish as recurrent units within deformation zones (or close to deformation zones). Retardation parameters for these units are given below (Table 4-11 to 4-15).

Table 4-11. Retardation model for deformation zone unit 1 – Fault rock/gouge (strongly tectonized and partly incohesive material).

Mineral content	Altered rock fragment, mineralogy partially dependant on host rock. Generally, chlorite, saussurite and clay together with rock fragments
Porosity (vol%)*	3%
Formation factor	Not available
BET (m²/g)	24.1
Sorption coefficient, Kd (m³/kg) saline Simpevarp groundwater	Cs: (6.0±0.3)E-1 Ln-Ac (III): 2.6±1.7

* determined by C^{14}PMMA, cf. Table 3-4.

Table 4-12. Retardation model for deformation zone unit 2 – Chlorite (primarily close to mafic rock types).

Mineral content	Chlorite ± corrensite
Porosity (vol%)*	12%
Formation factor	Not available
BET (m²/g)	8
Sorption coefficient, Kd (m³/kg) saline Simpevarp groundwater	Cs: 1.7E-2 Ln-Ac (III): 9.5
CEC** (cmoles/kg)	13±2

* determined by C^{14}PMMA, cf. Table 3-4. **CEC was measured only for this deformation zone unit type.

Table 4-13. Retardation model for deformation zone unit 3 – Porous episyenitic wall rock.

Mineral content	Prehnite, adularia, quartz, calcite ± laumontite, epidote, hematite Quartz dissolution sometimes occur
Porosity (vol%)	6
Formation factor*	1.1E-03
BET (m²/g)	13
Sorption coefficient, Kd (m³/kg) saline Simpevarp groundwater	Cs: (1.2±0.3)E-1 Ln-Ac (III): 1.3±1.1

* Outside deformation zone but defined as crushed zone in Boremap.

Table 4-14. Retardation model for deformation zone unit 4 – Cataclasite (with mylonitic banding).

Mineral content	Epidote, adularia, quartz, hematite ± laumontite although there are strong variations in mineralogy.
Porosity (vol%)	3±2
Formation factor	7.6E-03
BET (m²/g)	15±8
Sorption coefficient, Kd (m³/kg) saline Simpevarp groundwater	Cs: 8.5E-2 Ln-Ac (III): 5.6

Table 4-15. Retardation model for deformation zone unit 5 – oxidized (medium to strong alteration) wall rock.

Mineral content	Hydrothermally altered host rock, mineralogy due to initial rock type. Red staining from small hematite grains, K-feldspar, saussurite, plagioclase, quartz, chlorite is common in granitic variants
Porosity (vol%)	0.7±0.4
Formation factor	(1.5±1.3)E-04
BET (m²/g)	0.6
Sorption coefficient, Kd (m³/kg) saline Simpevarp groundwater	Cs: (1.7±0.13)E-3 Ln-Ac (III): (1.7±0.3)E-1

Summary of retardation properties of deformation zone units

The deformation zone units for which retardation properties have been tabulated are all comparatively heterogeneous in their structure. The porosities are considerably higher than for intact rock (average porosities of 3–12% except for the oxidized wall rock which is only slightly more porous (0.75%) than the intact rock types).

The high porosities should consequently be accompanied by an increased diffusivity (formation factor). This is confirmed by the observed formation factor range of the porous episyenitic wall rock and cataclasite of $1.1 \cdot 10^{-3}$ to $7.6 \cdot 10^{-3}$. The formation factor increase is in accordance with what would be expected from an Archies law relationship for which a 10 times increase in porosity would yield about 40 times increase in formation factor. The observed increase is in the range 30–100 times larger than the rock types.

When considering the measured sorption parameters (BET-surface areas and sorption coefficient) it is indicated that the deformation zone units have sorption properties that vary compared to the ones for intact rock. It should however be acknowledged that the indications are based on a few number of samples. The BET-surface areas range from 0.6 to 24.1 which is about 20 to several hundred times larger than those of the intact rock types. A more moderate sorption increase is indicated for cataclasite and porous episyenitic wall rock (about 3–4 times increase when Cs is compared to 501046 in fresh and saline waters) and Fault rock/gouge (roughly at maximum 20 times increase for Cs when compared to 501046 in fresh and saline waters). On the other hand, oxidized wall rock indicates about 20 times weaker sorption of Cs compared to 501046 in saline water, even though its BET surface is larger than that of 501046. Consequently, this indicates that the high measured surface areas of the deformation zone unit materials cannot be directly interpreted as a corresponding sorption capacity; probably for the same reasons as discussed in Section 4.3.

The sorption data for the deformation zone units are based on very few samples and are therefore uncertain. However, porosity and formation factors are clearly increased for the deformation zone units compared to the host rock. Consequently, from the data we can suspect that these deformation zone units might provide a relatively greater degree of retardation for a given flow magnitude and interfacial surface area for mass transfer to the rock matrix.

4.5   Application of the retardation model

The quantitative descriptions of the identified rock material, including the available retardation parameters, are presented in this chapter, Table 4-1 for the dominant rock types, Tables 4-2 to 4-10 for the different fracture types and the deformation zone units in Tables 4-11 to 4-15. The fracture types and deformation zone units can be used as a basis for modelling radionuclide transport along flow paths in the fractured medium. It is possible to parameterize the open fracture types found within the transition zones and core in a deformation zone using the retardation parameters for the different fracture types presented in Table 4-2 to 4-10. Statistics of fracture frequency and the relative fracture type distribution within (as well as outside) identified deformation zone are presented in Section 2.2.1. However, this is a general fracture type distribution based on data from all deformation zones at Laxemar. In the specific case, i.e. parameterization of a particular deformation zone the methodology presented in Section 2.2.2 (cf. Figure 2-19) can be applied.

Combined with the variation/uncertainty of the different numerical values (presented in Chapter 3 as the average values, standard deviation, maximum, minimum, median values of the measurements) a distribution is given that can be used as a basis for stochastic parameterisation of transport models. However, for some of the geological features, the numbers of samples were too low to allow a full statistical representation.

Due to the need of an early start of the time-consuming laboratory measurements (diffusion and batch sorption experiment) a relatively large number of the rock samples had to be obtained from the Simpevarp area (e.g. 48% of porosity samples and 47% of the diffusion samples). This gave a somewhat biased representation of the samples used in the laboratory programme. Furthermore, with regards to the Laxemar area, the first part of the investigation was placed in the northern and central parts of the area (i.e. KLX02 and KLX04). Although complementary sampling was performed in the southern area (KLX03 and KLX05) there is an overrepresentation of laboratory samples from this area compared to the presently presumed target area (SW area). However, the vast majority of the different rock types, fracture types and altered rocks that are found in the SW area of Laxemar are represented in the sample collection described in this report, although the statistical basis of samples collected in the target area is limited (e.g. 21 samples in RSMD01). For porosity it has been shown that very similar values are obtained at the Simpevarp and Laxemar areas according to Table 3-3. Thus, this indicated that the formation factor also would be similar between the sites.

This report should be regarded as a proposal of how to formulate a descriptive and qualitative retardation model based on the available database. Recommendations on the selection of data are given, however with an acknowledgement of the qualitative uncertainty as well as the numerical uncertainty for the retardation parameters. This implies that the model does not provide exact and detailed guidelines on how to "dress" the geological model with transport parameters using the retardation model tables, but, nevertheless, it provides the authors' opinion of what is the best representation that can be done with the data available. The retardation model should be viewed as a presentation of the interpreted site-specific information on retardation parameters, intended to provide a basis for the formulation of alternative parameterisations and/or necessary simplifications within the Safety Assessment modelling.

5   References

Andersson J, Ström A, Svemar C, Almén K-E, Ericsson, L O, 2000. What requirements does the KBS-3 repository make on the host rock? Geoscientific suitability indicators and criteria for siting and site evaluation. SKB TR-00-12, Svensk Kärnbränslehantering AB.

Andersson P, Byegård J, Dershowitz B, Doe T, Hermanson J, Meier P, Tullborg E-L, Winberg A (ed.), 2002. Final report of the TRUE Block Scale projekt 1. Characterisation and model development. SKB TR-02-13, Svensk Kärnbränslehantering AB.

André M, Neretnieks I, Malmström, M E, 2008a. Measuring sorption coefficients and BET surface areas on intact drillcore and crushed granite samples, Radiochim. Acta 96, 1-5 (2008).

André M, Malmström, M E, Neretnieks I, 2008b. Determination of sorption properties of intact rock samples: New methods based on electromigration, J. Contam. Hydrology (2008), doi: 10.1016/j.jconhyd.2008.09.006.

Berglund S, Selroos J-O, 2004. Transport properties site descriptive model – Guidelines for evaluation and modelling. SKB R-03-09, Svensk Kärnbränslehantering AB.

Birgersson L, Neretnieks I, 1990. Diffusion in the matrix of granitic rock. Field test in the Stripa mine. Water Resources Research 26 p 2833–2841.

Brunauer S, Emmett P.H. Teller E. 1938. Adsorption of gases in multimolecular layers. J Amer Chem Soc 60: 309–319.

Byegård J, Gustavsson E, Tullborg E-L, 2006. Bedrock transport properties. Data evaluation and retardation model. Preliminary site description Laxemar subarea – version 1.2. SKB R-06-27, Svensk Kärnbränslehantering AB.

Byegård J, Selnert E, Tullborg E-L, 2009. Bedrock transport properties. Data evaluation and retardation model. Site descriptive modelling. SDM-Site Forsmark. SKB R-08-98, Svensk Kärnbränslehantering AB.

Byegård J, Selnert E, Andersson P, in prep. Diffusion and sorption experiments using drill core samples – a test of the general applicability of the site specific laboratory retardation data, SKB R-report.

Caine J S, Evans J P, Forster C B, 1996. Fault zone architecture and permeability structure. Geology, 24, 11, 1025–1028.

Carbol P, Engkvist I, 1997. Compilation of radionuclide sorption coefficients for performance assessment, SKB R-97-13, Svensk Kärnbränslehantering AB.

Crank J, 1975. The mathematics of diffusion, 2nd ed. Oxford University Press, New York.

Crawford J, Sidborn M, 2008. Bedrock transport properties, Laxemar Site descriptive modelling, SDM-Site Laxemar, SKB R-08-94, Svensk Kärnbränslehantering AB.

Drake H, Sandström B, Tullborg E-L, 2006. Mineralogy and geochemistry of rocks and fracture fillings from Forsmark and Oskarshamn: Compilation of data for SR-Can. SKB R-06-109, Svensk Kärnbränslehantering AB.

Drake H, Tullborg E-L, Annersten H, 2008. Red-staining of the wall rock and its influence on the reducing capacity around water conducting fractures. Applied Geochemistry, vol.23, 7, 1898–1920.

Drake H, Tullborg E-L, 2009. Fracture mineralogy of the Laxemar site. Final report. SKB R-08-99, Svensk Kärnbränslehantering AB.

Eklund S, Mattsson K-J, 2008. Oskarshamn site investigation. Quantitative mapping of fracture minerals in Laxemar. SKB P-08-38, Svensk Kärnbränslehantering AB.

Jakobsson A-M 1999. Measurement and modelling using surface complexation of cation (II to IV) sorption onto mineral oxides, Thesis, Chalmers University of Technology, Department of Nuclear Chemistry, Göteborg, Sweden.

Laaksoharju M, Smellie J, Tullborg E-T, Wallin B, Drake H, Gimeno M, Hallbeck L, Molinero J, Waber N, 2009. Bedrock hydrogeochemistry Laxemar. Site descriptive modelling. SDM-Site Laxemar. SKB R-08-93, Svensk Kärnbränslehantering AB.

La Pointe P, Fox A, Hermanson J, Öhman J, 2008. Geological discrete fracture network model for the Laxemar site. Site Descriptive Modelling. SDM-Site Laxemar. SKB R-08-55, Svensk Kärnbränslehantering AB.

Löfgren M, Neretnieks I, 2005a. Formation factor logging in-situ and in the laboratory by electrical methods in KSH01A and KSH02. Measurements and evaluation of methodology. Oskarshamn site investigation. SKB P-05-27, Svensk Kärnbränslehantering AB.

Löfgren M, Neretnieks I, 2005b. Formation factor logging in-situ by electrical methods in KLX03 and KLX04. Oskarshamn site investigation. SKB P-05-105, Svensk Kärnbränslehantering AB.

Löfgren M, Pettersson M, 2006. Formation factor logging in situ by electrical methods in KLX05 and KLX06. Oskarshamn site investigation. SKB P-06-143, Svensk Kärnbränslehantering AB.

Löfgren M, 2007. Formation factor logging in situ by electrical methods in KLX07A, KLX08, KLX10 and KLX12A. Oskarshamn site investigation. SKB P-06-288, Svensk Kärnbränslehantering AB.

Löfgren M, Sidborn M, 2009. Statistical analysis of results from the quantitative mapping of fracture minerals in Laxemar. Svensk Kärnbränslehantering AB, in prep.

Mills R, Lobo V M M, 1989. Self-diffusion in electrolyte solutions, a critical examination of data compiled from the literature. ELSEVIER, Amsterdam . Oxford – New York – Tokyo.

Munier R, Stanfors R, Milnes A G, Hermanson J, Triumf C A, 2003. Geological Site Descriptive Model. A strategy for the development during site investigations. SKB R-03-07, Svensk Kärnbränslehantering AB.

Ohlsson Y, Neretnieks I, 1997. Diffusion data in granite – Recommended values. SKB TR-97-20, Svensk Kärnbränslehantering AB.

Parkhomenko E I, 1967. Electrical properties of rocks. Moscow, Institute of Physics of the Earth, Academy of the Sciences of the USSR, 277 p.

Penttinen L, Siitari-Kauppi M, Ikonen J, 2006. Determination of porosity and micro facturing using the 14C-PMMA technique in samples taken from Oskarshamn area. Oskarshamn site investigation. SKB P-06-62, Svensk Kärnbränslehantering AB.

Rhén I, Forsmark T, Hartley L, Jackson P, Roberts D, Swan D, Gylling B, 2008. Hydrogeological conceptualisation and parameterisation. Site descriptive modelling. SDM-Site Laxemar. SKB R-08-78, Svensk Kärnbränslehantering AB.

Selnert E, Byegård J, Widestrand H, 2009. Laboratory measurements within the site investigation programme for the transport properties of the rock. Final report. Oskarshamn site investigation, SKB P-07-179, Svensk Kärnbränslehantering AB.

Sibson R H, 1977. Fault rocks and fault mechanisms, Journal of the Geological Society of London 133, 191–213.

Skagius K, Neretnieks I, 1986. Diffusivity measurements and electrical resistivity measurements in rock samples under mechanical stress. Water Resources Research 22 (4), p 570–580.

SS EN 1936:1999. Natural stone test methods – Determination of real density and apparent density, and of total and open porosity.

Thunehed H, 2005a. Resistivity measurements on samples from KLX02. Oskarshamn site investigation. SKB P-05-19, Svensk Kärnbränslehantering AB.

Thunehed H, 2005b. Resistivity measurements and determination of formation factors on samples from KLX04 and KSH02. Oskarshamn site investigation. SKB P-05-75, Svensk Kärnbränslehantering AB.

Thunehed H, 2007a. Resistivity measurements on samples from KSH01, KSH02, KLX02, KLX04 and KLX11A. Oskarshamn site investigation. SKB P-06-289, Svensk Kärnbränslehantering AB.

Thunehed H, 2007b. Complementary resistivity measurements on samples from KLX03, KLX04, KLX05, KLX10, KLX12A and KLX13A. Oskarshamn site investigation. SKB P-07-203, Svensk Kärnbränslehantering AB.

Viola G, Venvik Ganerød G, 2007. Oskarshamn site investigation. Structural analysis of brittle deformation zones in the Simpevarp-Laxemar area, Oskarshamn, southeast Sweden. SKB P-07-41, Svensk Kärnbränslehantering AB.

Wahlgren C-H, Hermanson J, Forsberg O, Curtis P, Triumf C-A, Drake H, Tullborg E-L, 2006. Geological description of rock domains and deformation zones in the Simpevarp and Laxemar subareas. Preliminary site description Laxemar subarea - version 1.2. SKB R-05-69, Svensk Kärnbränslehantering AB.

Wahlgren C-H, Curtis P, Hermanson J, Forssberg O, Öhman J, Fox A, La Pointe P, Drake H, Triumf C-A, Mattsson H, Thunehed H, Juhlin C, 2008. Geology Laxemar. Site descriptive modelling. SDM-Site Laxemar. SKB R-08-54, Svensk Kärnbränslehantering AB.

Widestrand H, Byegård J, Ohlsson Y, Tullborg E-L, 2003. Strategy for the use of laboratory methods in the site investigations programme for the transport properties of the rock. SKB R-03-20, Svensk Kärnbränslehantering AB.

Widestrand H, Byegård J, Selnert E, Skålberg M, Gustafsson E, 2009. Long Term Sorption Diffusion Experiment (LTDE-SD), Supporting laboratory program – Sorption diffusion experiments and rock material characterisation, SKB R-09-XX, in prep.

Porosity data

Table A1-1. Results of the different approaches of sub-division of the porosity data, cf. Section 3.2.4.

|	Average	σ	σ/(*N*¼)	Median	Min	Max	Number
Rock Types (Deformation zones included)							
All	2.8E-1	2.5E-1	1.4E-2	2.2E-1	0.0E+0	1.6E+0	324
501030	2.2E-1	2.5E-1	2.5E-2	1.3E-1	0.0E+0	1.5E+0	94
501033	5.9E-2				5.4E-2	6.4E-2	2
501036	2.7E-1	3.0E-1	3.6E-2	1.6E-1	0.0E+0	1.6E+0	71
501046	4.0E-1	2.6E-1	4.5E-2	4.0E-1	5.1E-2	1.5E+0	34
501056	3.4E-1	1.7E-1	1.9E-2	3.2E-1	1.3E-1	9.9E-1	77
501058	6.6E-1	2.5E-1	1.4E-1	7.6E-1	3.8E-1	8.4E-1	3
501061	2.0E-2						1
505102	2.6E-1	3.0E-1	8.7E-2	1.9E-1	3.4E-2	1.1E+0	12
511058	2.5E-1	1.9E-1	3.4E-2	2.3E-1	5.0E-2	1.2E+0	30
Rock Types (Deformation zones excluded)							
All	2.5E-1	2.1E-1	1.3E-2	2.1E-1	0.0E+0	1.5E+0	262
501030	2.3E-1	2.6E-1	3.0E-2	1.5E-1	0.0E+0	1.5E+0	76
501033	5.9E-2				5.4E-2	6.4E-2	2
501036	1.9E-1	1.9E-1	2.5E-2	1.3E-1	0.0E+0	1.3E+0	61
501046	3.5E-1	1.4E-1	2.7E-2	4.0E-1	5.1E-2	6.0E-1	28
501056	3.2E-1	1.5E-1	2.0E-2	2.9E-1	1.3E-1	9.9E-1	58
501058	6.1E-1	3.3E-1	2.3E-1	6.1E-1	3.8E-1	8.4E-1	2
501061	2.0E-2						1
505102	1.6E-1	6.3E-2	2.2E-2	1.9E-1	3.4E-2	2.2E-1	8
511058	2.7E-1	1.9E-1	3.8E-2	2.4E-1	7.0E-2	1.2E+0	26
Rock Domains (Deformation zones included)							
All	2.9E-1	2.5E-1	1.4E-2	2.2E-1	0.0E+0	1.6E+0	315
RSMA01	3.1E-1	2.3E-1	2.2E-2	2.5E-1	5.1E-2	1.5E+0	105
RSMB01	2.3E-1	2.2E-1	2.2E-2	1.9E-1	0.0E+0	1.3E+0	100
RSMC01	3.4E-1	2.6E-1	3.8E-2	3.0E-1	2.0E-2	1.6E+0	47
RSMD01	3.1E-1	3.6E-1	7.0E-2	1.6E-1	0.0E+0	1.3E+0	27
RSMM01	2.2E-1	1.2E-1	3.3E-2	2.2E-1	5.1E-2	4.3E-1	13
RSMBA03	3.4E-1	3.4E-1	7.0E-2	2.7E-1	4.0E-2	1.5E+0	23
Rock Domains (Deformation zones excluded)							
All	2.6E-1	2.1E-1	1.3E-2	2.1E-1	0.0E+0	1.5E+0	253
RSMM01	2.2E-1	1.2E-1	3.3E-2	2.2E-1	5.1E-2	4.3E-1	13
RSMA01	2.7E-1	1.5E-1	1.6E-2	2.3E-1	5.1E-2	9.9E-1	88
RSMC01	2.9E-1	1.7E-1	2.6E-2	2.9E-1	2.0E-2	6.0E-1	40
RSMB01	2.3E-1	2.2E-1	2.3E-2	1.9E-1	0.0E+0	1.3E+0	88
RSMBA03	7.2E-1	6.8E-1	3.9E-1	4.2E-1	2.4E-1	1.5E+0	3
RSMD01	2.2E-1	3.0E-1	6.7E-2	1.4E-1	0.0E+0	1.3E+0	21
Fracture Domains							
All	2.6E-1	1.9E-1	1.7E-2	2.2E-1	0.0E+0	1.3E+0	122
FSM_NE005	2.2E-1	1.3E-1	4.7E-2	2.0E-1	5.4E-2	4.1E-1	8
FSM_N	4.3E-1	2.2E-1	7.3E-2	3.9E-1	2.4E-1	9.9E-1	9
FSM_C	2.7E-1	1.9E-1	4.0E-2	2.2E-1	5.1E-2	8.0E-1	21
FSM_EW007	2.5E-1	1.3E-1	1.6E-2	2.2E-1	5.1E-2	8.4E-1	65
FSM_W	2.0E-1	2.9E-1	6.8E-2	1.4E-1	0.0E+0	1.3E+0	19
Hydraulic rock domains							
All	2.6E-1	1.9E-1	1.7E-2	2.2E-1	0.0E+0	1.3E+0	118
HRD_C	2.6E-1	1.7E-1	3.2E-2	2.2E-1	5.1E-2	8.0E-1	29
HRD_N	4.3E-1	2.2E-1	7.3E-2	3.9E-1	2.4E-1	9.9E-1	9
HRD_EW007	2.5E-1	1.3E-1	1.6E-2	2.2E-1	5.1E-2	8.4E-1	65
HRD_W	2.0E-1	3.3E-1	8.6E-2	8.6E-2	0.0E+0	1.3E+0	15
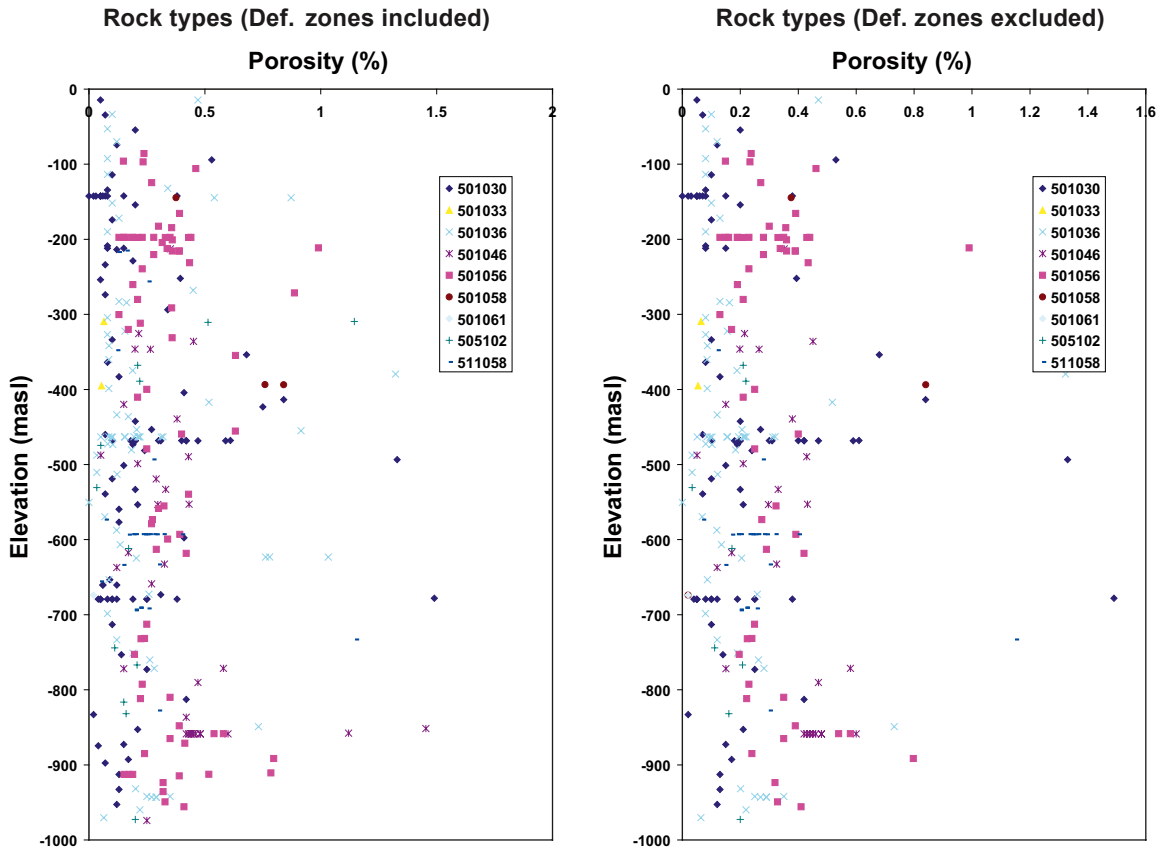
Figure A1-1. *Illustration of porosity vs elevation, data sorted according to Rock types. Data are given with deformation zone samples included (left) and also given with deformation zones samples excluded (right).*
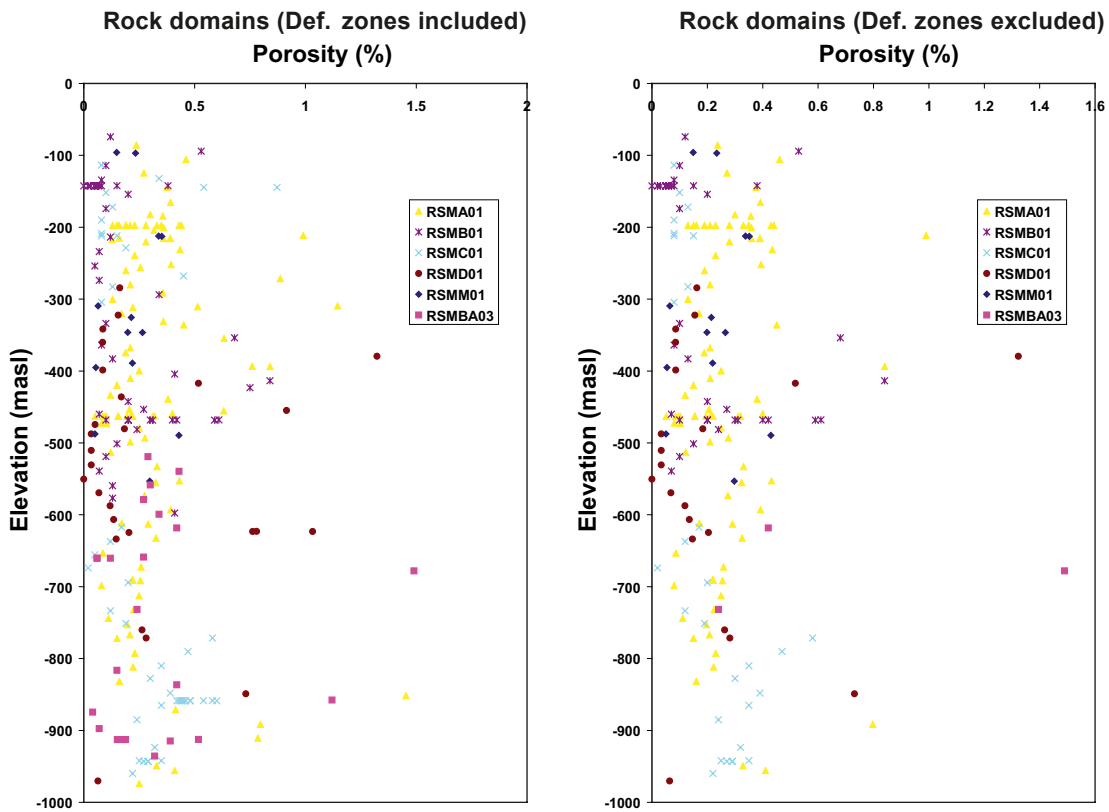

Figure A1-2. *Illustration of porosity vs elevation, data sorted according to Rock domains. Data are given with deformation zone samples included (left) and also given with deformation zones samples excluded (right).*
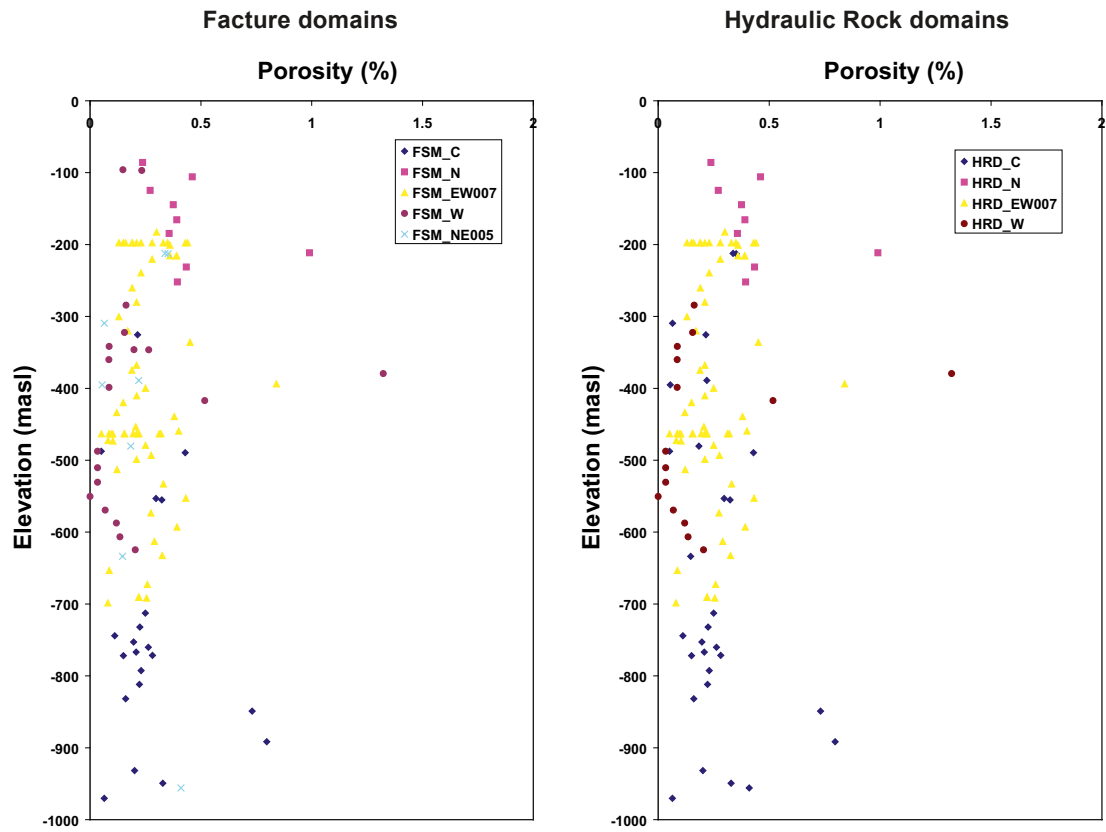
Figure A1-3. *Illustration of porosity vs elevation, data sorted according to Fracture domains (left) and Hydraulic rock domains (right). Since the concepts of Fracture domains and Hydraulic rock domains implicitly excludes deformation zones, no representation of the data when deformation zone data is excluded is necessary for these two concepts.*

Procedure for calculation of frequency distribution for the fracture types

In the analysis of the dataset, fractures with coatings consisting of a mineral assembly as defined in Table 2.4 were selected and extracted according to the sequence described below.

The following notations are used:

+ = the mineral must be present

and/or = one or several of the minerals must be present

± = the minerals may or may not be present

The sequence for calculation of the fracture distribution was:

1. Search and count all fractures of type C (i.e. find all fractures that contains hematite ± any mineral)
   1.1. Remove the identified C fractures from the data set

2. Search and count the remaining data set for all fractures of type F (i.e. find all fractures that contains clay ± any mineral)
   2.1. Remove the identified F fractures from the data set

3. Search and count all fractures of type A (i.e. find all fractures that contains chlorite + calcite + pyrite/chalcopyrite ± any mineral)
   3.1. Remove the identified A fractures from the data set

4. Search and count the remaining data set for all fractures of type B (i.e. find all fractures that contains epidote and/or prehnite and/or adularia ± chlorite ± calcite ± quartz)
   4.1. Remove the identified B fractures from the data set

5. Search and count all fractures of type D (i.e. find all fractures that contains laumontite ± calcite ± chlorite)
   5.1. Remove the identified D fractures from the data set

6. Search and count the remaining data set for all fractures of type E (i.e. find all fractures that contains chlorite + calcite ± oxidized walls ± saussuritized walls)
   6.1. Remove the identified E fractures from the data set

7. Search and count all fractures of type I (i.e. find all fractures that contains calcite ± any mineral)
   7.1. Remove the identified I fractures from the data set

8. Search and count the remaining data set for all fractures of type G (i.e. find all fractures that contains chlorite ± any mineral)
   8.1. Remove the identified G fractures from the data set

9. Search and count the remaining data set for all fractures of type H (i.e. find all fractures that contains no minerals ± oxidized walls ± saussuritized walls ± epidotized walls)
   9.1. Remove the identified H fractures from the data set

10. The remaining fractures in the dataset are summarized as a control of the amount of unidentified fractures. This "Rest" group is included in the fracture type distribution figures.

The total extraction order of the fracture types was: C, F, A, B, D, E, I, G and H.